NOTICE

The quality of this microform is heavily dependent upon the quality of the original thesis submitted for microfilming. Every effort has been made to ensure the highest quality of reproduction possible.

If pages are missing, contact the university which granted the degree.

Some pages may have indistinct print especially if the original pages were typed with a poor typewriter ribbon or if the university sent us an inferior photocopy.

Reproduction in full or in part of this microform is governed by the Canadian Copyright Act, R.S.C. 1970, c. C-30, and subsequent amendments.

AVIS

La qualité de cette microforme dépend grandement de la qualité de la thèse soumise au microfilmage. Nous avons tout fait pour assurer une qualité supérieure de reproduction.

S'il manque des pages, veuillez communiquer avec l'université qui a conféré le grade.

La qualité d'impression de certaines pages peut laisser à désirer, surtout si les pages originales ont été dactylographiées à l'aide d'un ruban usé ou si l'université nous a fait parvenir une photocopie de qualité inférieure.

La reproduction, même partielle, de cette microforme est soumise à la Loi canadienne sur le droit d'auteur, SRC 1970, c. C-30, et ses amendements subséquents.

EVALUATION OF A MOCK CIRCULATION MODEL THROUGH TIME-SERIES ANALYSIS

Andrew R. Hicks

A thesis submitted to the School of Graduate Studies and Research in partial fulfilment of the requirement for the degree of
Master of Applied Science
in the
Department of Chemical Engineering
University of Ottawa

ISBN 0-315-60038-1

UNIVERSITÉ D'OTTAWA
UNIVERSITY OF OTTAWA

Acknowledgements

The work of this thesis has been made possible by the support of many people who warrant mention. Firstly, to Wilbert Keon for his dedication to cardiac research and the establishment of the Heart Institute Research Centre. Secondly, to Don Olsen, Paul Diegel and others in Salt Lake City who offered much help during the summer of 1988 and beyond. Thirdly, to David Maclean for the seeds he planted in my brain concerning non-linear regression analysis and to Michael Margerum for his early help. Fourthly, to Bill Adams and George Adams for their helpful comments and direction in focusing the thesis. And finally, to my wife, Christine, who besides wanting her name in the thesis has been a pillar of patience and support during the good, the not so good and the horrible days of any thesis project.

EVALUATION OF A MOCK CIRCULATION MODEL THROUGH TIME-SERIES ANALYSIS

Abstract

The Donovan Mock Circulation Unit (MCU) provides an *in vitro* representation of the human circulatory system. As a test bed, it can be used for laboratory or *in vitro* evaluation of both the total artificial heart (TAH) and electric ventricular assist device (EVAD) prior to *in vivo* use of the devices in both animals and humans. A mathematical model of the Donovan MCU, derived from fundamental principles of fluid dynamics is utilized to represent this system. For the model to provide useful predictions, it must be well-fitted to both the data from the MCU and the physiological data from the human circulation. In addition, it must provide a reliable means for evaluation of the system parameters of resistance, compliance and inertance.

A new solution to a lumped-parameter model of the human circulation is developed using discontinuous line segments to approximate the complicated aortic flow profile. Aortic pressure and flow data for the human circulation are taken from the literature and are collected as a time-series from the mock circulation unit. The model is fitted to this data using non-linear regression analysis. Residual plots and autocorrelation functions for the data sets suggest that the model should be fitted using a first-order moving average process and tests for lack-of-fit indicate that the model is adequate. Parameter estimates are within acceptable physiological limits. Approximate inference bands for the model predictions are presented for both the human physiological data and the MCU data.

EVALUATION OF A MOCK CIRCULATION MODEL THROUGH TIME-SERIES ANALYSIS

List of Figures

List of Tables

Nomenclature

Symbol	Quantity	Units (if applicable)
V	Volume	litres
C	Compliance	litres/mmHg
I	Inertance	mmHg seconds^2/litres
P	Pressure	mmHg
Q	Flow	litres/min
t	Time	seconds, minutes
R	Resistance	mmHg seconds/litres
η	Viscosity	
r	Radius	
L	Length	
Y	Response Variable	
f,g	Function	
x	Independent Variable	
β,θ	Parameter	
Z	Random Disturbance	
E	Expected Value	
$V(),\sigma^2,s^2$	Variance	
Cov( )	Covariance	
p( )	Probability	
s( )	Sum of Squares function for Parameters Vector	
N	Number of Data Points	
M	Number of Replicates	
P	Number of Parameters	

$\underline{X}$	N x P matrix of Regressor Variables
se	Standard Error
γ	Probability Level
$\Gamma(\ )$	Gradient Function
e ( )	Residual Function
u,i,n,j	Position or Run Number
J( )	Jacobian Function
H( )	Hessian Function
F	Fisher Distribution
ε	Residual
ω	Fit Parameter
K	Lag
r	Residual Autocorrelation Function
P_a	Mean Venous Pressure or Filling Pressure
$\alpha(\ )$	Unit Step Function
m_i	Slope of Line Segment i
b_i	Intercept of Line Segment i
D_i	Time of Discontinuity of Line Segment i
t_a	Cardiac Cycle Time
g,h	Roots of s^2+Bs+D
T	Student's Statistic

Superscripts

°	Gradient
–	Mean
^	Least Squares Estimate

Subscripts

–	Matrix
0	Zero Time

Note on Units:

Flow in litres/minute and pressure in mmHg are used in this thesis to conform with current practice in the cardiac and biomedical engineering field.

1 - INTRODUCTION

Heart disease in Canada affects one of the largest patient populations in this country. The failure of the heart to function properly is the most common disorder in our society causing suffering, loss of health and premature death. It affects approximately three million Canadians and is responsible for fifty thousand deaths annually at a cost to the health care system upwards of $3.7 billion each year excluding the costs of lost productivity (1).

The sudden or progressive failure of the heart causes the death of many people whose health is otherwise sound. As a result, it has been recognized that members of this patient population could benefit from some form of circulatory assist device, which would be permanently implanted and assist the diseased or failing natural heart. The use of a mechanical device could, therefore, extend human life, aid in improving a patient's quality of life and enhance the probability of adding years of productivity.

Recent advancements in heart transplant technology have neither reduced nor eliminated the need for mechanical circulatory support. The demand for donor hearts continues to exceed the supply, where for each available donor heart, there are somewhere between 20 and 35 patients waiting (1). The heart, as a potential organ for replacement, is attractive due to its dominant mechanical function of pumping the blood. In an age where medical and engineering science is advancing, the ability to replace bodily structures is more likely to succeed where the main function is primarily mechanical and not one complicated by numerous and complex biochemical reactions. As a result, a prosthetic heart assist device is

recognized as a highly suitable application of engineering and medical technology.

There are many types of heart assist devices which are currently being used clinically, including the total artificial heart (TAH) and the ventricular assist device (VAD). The TAH is designed to fully support the circulation when biventricular failure of the natural heart results in complete incapacity of maintaining minimum cardiac function. Consisting of two separate ventricles, it is attached to the natural atria upon removal of the two natural ventricles and is, typically, driven by percutaneous, pneumatic drive-lines. It is mainly used as a temporary bridge to transplant when a donor heart cannot be located in time to save a patient's life. The main disadvantages of the TAH are its size, the percutaneous drive-lines required to sustain it and the associated risk of infection.

The VAD is designed to supplement the circulation when the ability of the natural heart to pump is compromised. It consists of a single ventricle and can be attached either in series or in parallel to the natural ventricles. The devices being used clinically are, typically, driven by a percutaneous, pneumatic drive system. The VAD is also used as a temporary bridge to transplant but can also provide a period of rest for the natural heart whereby recovery of the natural heart is sometimes possible. One of the disadvantages of the VAD is the lack of space in the thoracic cavity to accommodate it which typically results in percutaneous cannulae and the device being worn externally to the body or implantation in the abdomen.

The clinical use of both the TAH and VAD for short term implants as a bridge to transplant has met satisfactory success. Long term

implantation of either device has been less successful mainly due to infectious complications arising from the percutaneous leads. As the availability of donor organs is likely to remain lower than the demand for them, assist devices that eliminate the percutaneous drive lines would be a significant improvement.

Estimates of the number of patients in Canada that could benefit from an assist device are in the order of several thousand each year. However, the use of such a device is not unqualified. Minimum constraints must be attained in order to ensure that patient comfort, mobility and, hence, quality of life are realized to acceptable standards. To date, the major constraint of existing devices is the degree of mobility a patient can attain in performing the activities of daily life, mainly due to the bulky and heavy, pneumatic drive systems required to support them. A totally implantable electric device, with an intracorporeal pumping device, controller, and energy storage mechanism with a transcutaneous energy transmission system and an extracorporeal, high energy density power source would provide the patient with the mobility to pursue normal activities for considerable periods of time each day.

Supporting the systemic side of the circulation, the left heart works at higher pressures during its operation to maintain a given cardiac output as a result of the larger volume and resistance of the systemic arterial and venous networks. The right heart supports the pulmonary circulation and works at a lower pressure due to the relatively lower volume and resistance of the pulmonary bed. The power output of the left heart is greater than the right heart power output and is more likely to require assistance as its ability to pump is compromised through heart disease. A ventricular assist device (VAD) is generally used to support the left heart.

The totally implantable electric ventricular assist device (EVAD) being developed at the University of Ottawa Heart Institute in conjunction with the University of Utah Institute for Biomedical Engineering is being designed to assist the left heart in its function of pumping the blood.

1.1 - Description of the EVAD project

The totally implantable EVAD is comprised of a number of sub-components, each of which must perform to specific design specifications in order to meet the program goals. The major components of the system are the blood pump or artificial ventricle, the energy converter and controller, the volume displacement chamber, the physiological controller and sensors, the energy management circuitry, the internal energy storage system, the transcutaneous energy transfer and telemetry (TET) system and the external energy storage system. Figure 1.1 indicates the system components in their anticipated implanted positions. Figure 1.2 indicates the data and energy flow for the system.

The blood pump consists of a polyurethane housing containing a system of flexible diaphragms, a hydraulic inflow port and blood inflow and outflow ports each with a one-way valve. The diaphragm system is a flexible, four-layer Biomer sheath that physically separates the blood from the hydraulic fluid. The inflow and outflow ports in conjunction with the valves ensure a unidirectional flow of blood into and out of the ventricle. The hydraulic inflow port, located at the base of the ventricle, enables hydraulic fluid to enter to ventricle behind the diaphragm to cause pumping. At the beginning of diastole, blood enters the housing through an

Figure 1.1 - The Implantable Electric Ventricular Assist Device

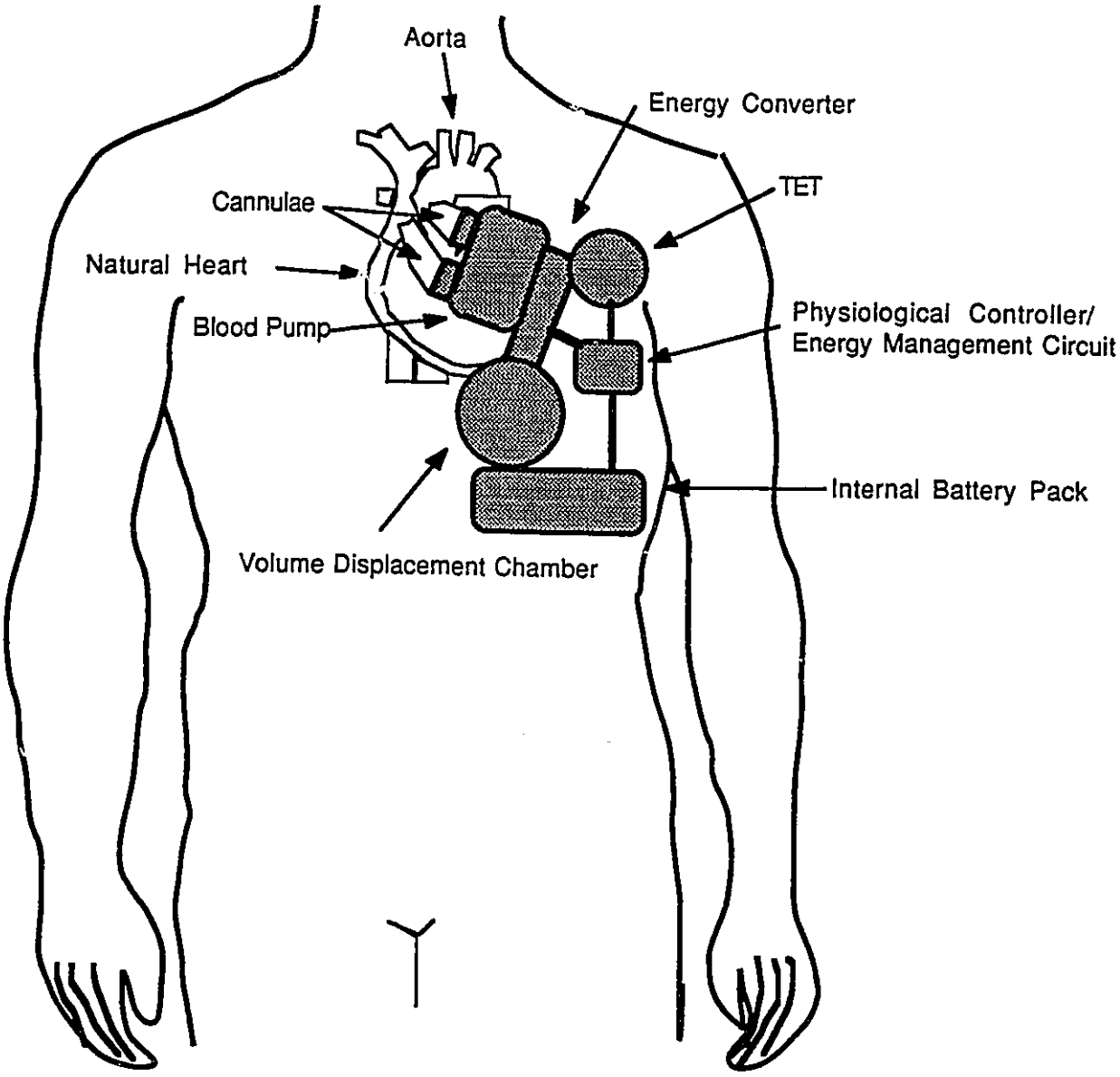

Figure 1.2- Energy and Data Flow between System Components of the EVAD

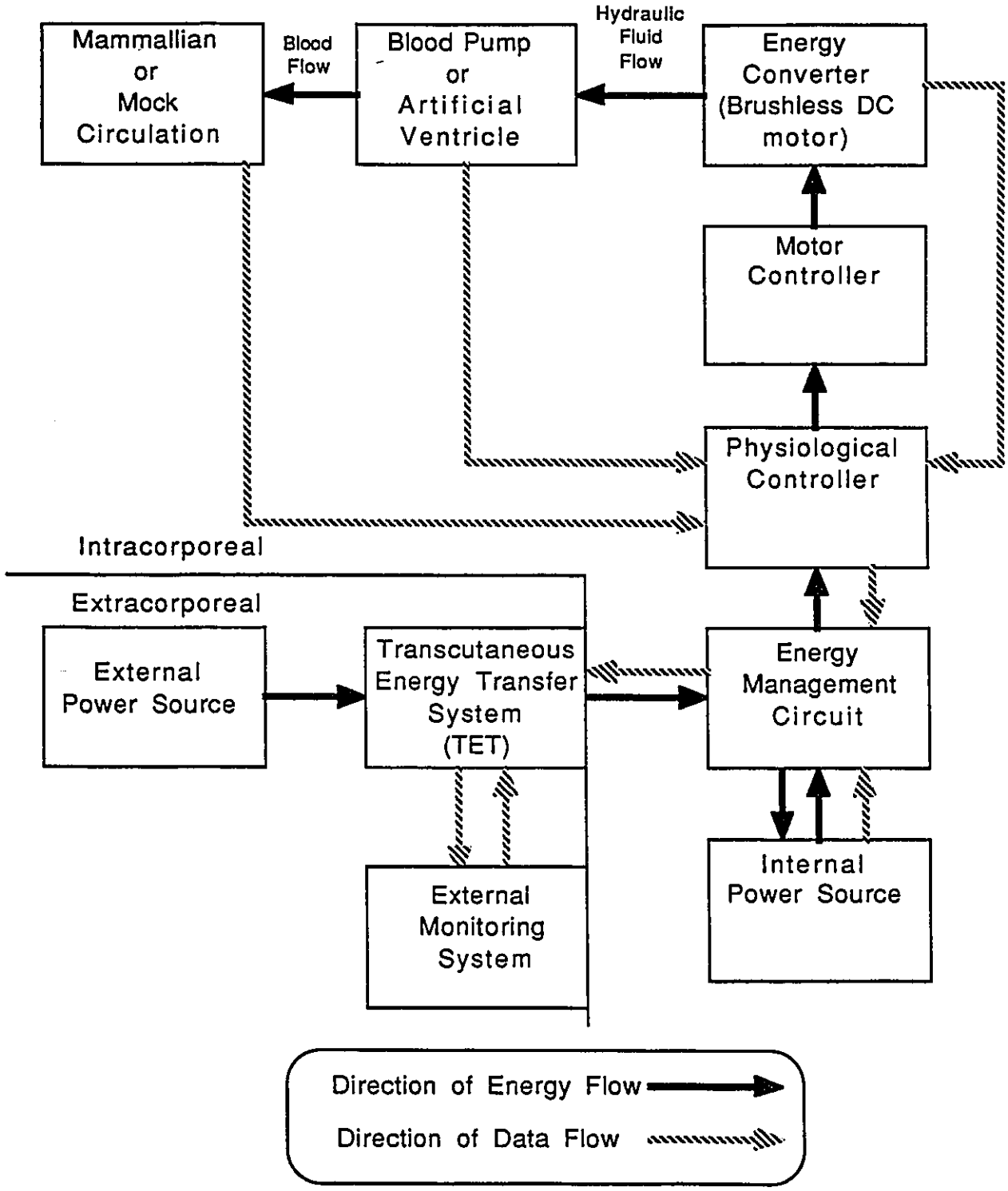

inflow port physically connected to the blood return system of the circulation. The one-way valve opens passively, in response to the pressure difference between the fluid outside the housing relative to the pressure of fluid inside the housing. It is this pressure difference that permits filling to occur. At this time, the flexible diaphragm would be approaching its pre-systolic position during filling against an internal screen at the base of the ventricle. Hydraulic fluid would be leaving the ventricle through the hydraulic inflow port during this stage. This action of filling completes the diastolic phase of the cardiac cycle. At the beginning of systole, the ventricle is full of blood, the diaphragm is flat against the internal screen, the outflow port valve is closed and the inflow port valve is open. As hydraulic fluid enters the ventricle through the hydraulic inflow port, the diaphragm is pushed away from the screen. This increases the pressure inside the ventricle causing the inflow valve to close, the outflow valve to open and blood to move out of the ventricle through the outflow port. The diaphragm will continue to move away from the screen as hydraulic fluid is entering the ventricle until it reaches its fully extended position or the hydraulic fluid ceases to move. At the end of systole, the inflow valve will remain closed, the outflow valve will be open, the diaphragm will be fully extended against the inside of the housing and a maximum volume of hydraulic fluid will be inside the ventricle. As diastole begins, hydraulic fluid will once again begin to move out of the ventricle, the outflow valve will close and the process begins itself again. This outline describes the normal passive full-fill, full-eject mode of operation of the blood pump. Other variations would include active-fill, partial-fill and partial ejection modes. Passive-fill occurs when ventricle filling is accomplished by the natural, positive pressure

gradient between the venous system and the ventricle interior. Active-fill involves lowering the intraventricular pressure through the expenditure of energy when hydraulic fluid is quickly removed from the ventricle by the energy converter. The level of ventricular filling with passive or active fill is dependent on the pressure gradient and the time of filling. Passive-fill occurs at a lower pressure gradient and usually results in partial filling of the ventricle. Active-fill occurs more quickly and normally completely fills the ventricle.

The energy converter in the EVAD is designed to convert electrical energy to mechanical energy to pump hydraulic fluid and thus, operate the blood pump. In order to sustain the pumping of blood, the hydraulic fluid must alternately move in and out of the hydraulic inflow port of the ventricle as described for the normal cardiac cycle. For a long-term implantable device, reliability is a key factor in the design of an energy converter. The number of moving parts within a system can severely affect the reliability of the component and hence, the overall reliability of the system. For this reason, the project has sought to minimize the number of moving parts within the energy converter in order to maximize reliability. This is achieved with the current design by the use of a low density silicone oil as a hydraulic fluid in conjunction with a brushless DC motor reversing turbine pump and volume displacement chamber. This system contains a single moving part besides bearings - the rotor of the brushless DC motor coupled to the blades of a turbine. During the cardiac cycle, the motor is alternately run in opposite directions, moving hydraulic fluid to the ventricle to cause systole and away from the ventricle to the volume displacement chamber during diastole. The volume

displacement chamber is a small pouch of sufficient capacity to temporarily hold hydraulic fluid during diastole.

The energy converter is controlled electronically with associated motor control circuitry. Power for the controller and energy converter is obtained from either the internal power source or from the external power source. The mode of operation of the energy converter is determined through input from the physiological controller through the motor controller.

The physiological controller has the functions of detecting operational or physiological conditions in the device or body, interpreting the conditions and responding to them through signal output to the motor controller. Pressure and flow conditions and possibly other parameters within both the device and circulation will be measured.

The energy management circuitry determines whether the power required to operate the energy converter should be received from the internal or external power source as well as monitoring control over the operation of the power sources (for example, monitoring charging, state-of-charge and capacity of battery). Energy is transferred into the body, across the intact skin, by the transcutaneous energy transfer system (TET). In the event that the external power source is disconnected, the energy management circuit will take energy from the internal power source to drive the energy converter. At the same time, it must monitor the amount of energy remaining in that power supply. If the energy is being received from the external power source, the energy management circuitry will channel to the energy converter the amount of energy required to maintain the circulation. When power required by the energy converter is in excess of the load requirements, the excess power from

the TET is directed to the internal power supply (a battery) for storage (battery charging). When power in excess of the capacity of the TET is required by the energy converter, it is obtained from the internal battery.

The physiological controller and motor control and energy management circuitry receive power from either the internal energy storage system or from the external energy storage system. The internal system is intended to provide backup power for the energy converter in the event of the disconnection of the external power supply. This could happen either voluntarily in order to give the patient the opportunity to move around in a completely untethered mode or accidentally whereby the circulation could be maintained for a short period of time. This power supply would be an advanced rechargeable electrochemical system with high cycle life, energy and power density and favourable charging and discharging characteristics. It would be designed to provide the patient with approximately one hour per day of energy away from the external supply. The external supply would provide the power required for continuous operation of the device for the remaining twenty-three hours of each day in addition to the energy required to recharge the internal system. This power supply could take a number of forms including rechargeable battery, fuel cell or standard 120 V AC power.

Energy from the external power supply is transferred into the body through the transcutaneous energy transfer system (TET). The system consists of control circuitry and Litz wire coils, one of which is implanted just beneath the skin and the other which is worn above the other extracorporeally. Direct current (DC) power from the external energy source undergoes a DC to radio frequency alternating current (RFAC) conversion. It is then transmitted into the body by the external coil as

RFAC. The internal coil receives the RFAC energy, where it undergoes RFAC to DC transformation. As DC power, it is directed to the internal energy management circuitry.

1.2 - Mock Circulation Research

The development of an electric ventricular assist device (EVAD) requires extensive testing and evaluation of prototype devices prior to implantation in both animal models and humans (2-6). To aid in the design process, extensive *in vitro* testing of the device is necessary on a mock circulatory system that reflects the important characteristics of the natural mammalian circulation. A mock circulation unit is usually a hydraulic analog of the natural circulation, that is, a series of pressure chambers and tubes designed to represent pressure and flow characteristics of the natural circulation. Testing is required for both development of the device and for demonstrating reliability of the system or its components. A mock circulation unit used in the development of an EVAD is used in a large variety of testing procedures and protocols. To this end, a mock circulation unit must satisfy its own levels of reliability and performance. For short term experimentation, the unit must accurately reflect the responses of the natural circulation. For long term testing, it must demonstrate mechanical robustness and stability in its operation.

1.3 - Motivation and Considerations in Modelling Work

The energy management and control of an EVAD is a complicated and critical component in the overall function of supporting the circulation. The identification of a reliable system model and its associated parameters enables the effects of the input variables on the output variables to be determined. This will aid in developing an energy management and control scheme for the assist device where, for example, an instantaneous prediction of power demand could determine a discharge/charge regime for the internal batteries. The model can also be used in determining the adequacy of the MCU as an *in vitro* test bed. The quality of the model will determine the reliability and effectiveness of the predictions.

In order to evaluate the responses of a circulatory system hydraulic analog to experimental data, a mathematical model will be utilized. The circulatory systems of both test animals and humans are highly complex systems of highly variable geometries, pressures, flows and cycles involving thousands of variables and factors that affect properties, responses and control. It would be impossible to study all of them at the same time or simultaneously define the influence of one factor on a particular observation. The complexity is such that complete and rigorous attempts at developing mathematical solutions have proven to be difficult to use and interpret and, hence, of limited use in developmental engineering applications. This has precipitated the need for simplifying assumptions to maintain manageability (2,7-9) where the model eliminates most of the parameters and involves only a limited number of variables. Through these simplifications, however, the observed relationships no longer represent the complete system and, therefore, a

balance must be reached between the level of complexity and the efficiency of handling the model (2,10,11).

An accurate quantitative description of the physical state of the circulation can be achieved when assumptions are made concerning the behaviour and nature of the various subsystems of the circulation (2-10,12-15). Analogues of the circulatory system are models which replace the real body components of vessel walls and blood for example, with mechanical or electrical analogies, whose constitutive relationships are well understood. The other type of models are those which utilize a system of mathematical expressions to link and explain the behaviour of the individual components. The response of the real system is then compared to the solution of the mathematical expressions and potentially used to improve the model.

Models describing a system can be classified not only by their complexity but also by the purpose which they are designed to fulfil, ranging from engineering to teaching to mathematical analysis. The mathematical model can, likewise, be used for a number of purposes (7,16,17). These include the development of relations describing the behaviour of isolated organs, the development of expressions evaluating the behaviour of a particular parameter as a function of other parameters, the development of a model at a particular level of complexity of the whole circulatory system or a formulation of theories which describe the inter-relationships between system parameters. The mathematical model remains the only means of providing quantitative predictions of the behaviour of a particular system.

Mathematical models can be classified into two categories-those derived from theoretical relationships and those derived from

experimental measurements. The former is referred to as a mechanistic model and the latter is an empirical model.

An empirical model approach should be utilized when the system cannot be explained in terms of fundamental principles. This can be due either to the complexity of the system or to a lack of understanding of the fundamental engineering principles governing that particular system. A main limitation of the empirical model is the lack of certainty in extrapolation beyond the region of experimentation.

The mechanistic model is derived from fundamental principles of physics and chemistry. This can enable a greater understanding of the cause and effect relationships between variables as well as a greater level of certainty in extrapolation. Whenever possible, the mechanistic model should be sought as it provides a keener insight into the actual process being examined.

A model can also be classified as either deterministic or stochastic. A deterministic model is one which describes a system exactly. In practice, however, experimental techniques have limited accuracy and are affected by unknown, unexpected and unpredictable disturbances. In order to take into account the uncertainty associated with the experimental data, an additional term is added to the deterministic model, representing the random error associated with that data. This modification classifies the model as stochastic.

Mathematical models describing the circulatory system can be classified into four general levels of complexity and, therefore, of increasing difficulty of analysis (7). The simplest model is classified as the pure resistance model where blood flow is assumed to be continuous and its pulsatile nature is ignored. The second classification is the lumped-

parameter or Windkessel model. This model separates the circulatory subsystems into discrete elements of resistance, compliance and inertance according to the general divisional features of the natural circulation. The third classification involves distributed parameters of resistance, compliance and inertance effects where the pulsatile nature of pressure and flow are represented by a linear approximation. Parameters usually vary with respect to time. The fourth level is the non-linearly distributed representation of the system in a distributed, time-varying circulatory system.

In the selection of a model which could potentially be used as a control scheme for the VAD, consideration of the type of solution must be made. A model which can only be solved numerically involves a greater amount of computer time to obtain a response over one with an analytical solution. The final use of the model should influence the choice of the type of solution.

A model is either linear or non-linear in nature. A linear model is one in which each first partial derivative of the function with respect to each one of the parameters is not a function of that particular parameter. A non-linear model is the opposite, that is the first partial derivative is a function of that particular parameter. The human circulatory system is highly non-linear in nature which encourages its description with a non-linear model.

There are a number of statistical techniques available for model identification and parameter estimation for non-linear systems. In the case of a dynamic system, that is, one varying with respect to time, independence between successive samples is unlikely. For this reason, a branch of statistical analysis, time series analysis, is used to investigate

the significance of dependence between samples or the nature of the dependence itself.

2 - MODELLING THE CIRCULATORY SYSTEM

2.1 - History of Models of Human Blood Circulation

The beginning of man's efforts at modelling the human circulation was in 1628 by William Harvey when he recognized that blood flows continuously in a closed circuit (18). Since then, many attempts at developing precise mathematics describing the interrelations of blood forces on anatomical components have been performed.

In 1733, Stephen Hales attempted to apply principles of physics, developed by Isaac Newton, to the circulation. Hales recognized that the arterial tree smoothed out the pulsatile nature of blood flow from the left ventricle to a fairly steady level of flow (7,13). In his mathematical model, he represented the arterial part of the circulation as an elastic chamber. In 1775, the Swiss mathematician, Euler, developed a model describing viscous fluid flow in elastic arteries. Thomas Young, at the beginning of the 19th century, followed on the work of the hydrodynamics of an ideal fluid performed by Euler and Bernouilli. Young introduced the idea of travelling waves in arteries and the relationship between arterial elasticity and pulse wave velocity (13).

In 1899, Otto Frank proposed a "Windkessel" model of the circulation from ideas about the blood circulation (7,10,13). Figure 2.1 shows the Windkessel model of the circulation. This German word for air-chamber gives the model its name, consisting of an elastic reservoir representing the aorta and major arteries with an elastic air chamber with a linear pressure/volume relationship and a linear resistance element describing

Figure 2.1 - Windkessel Model of the Circulation

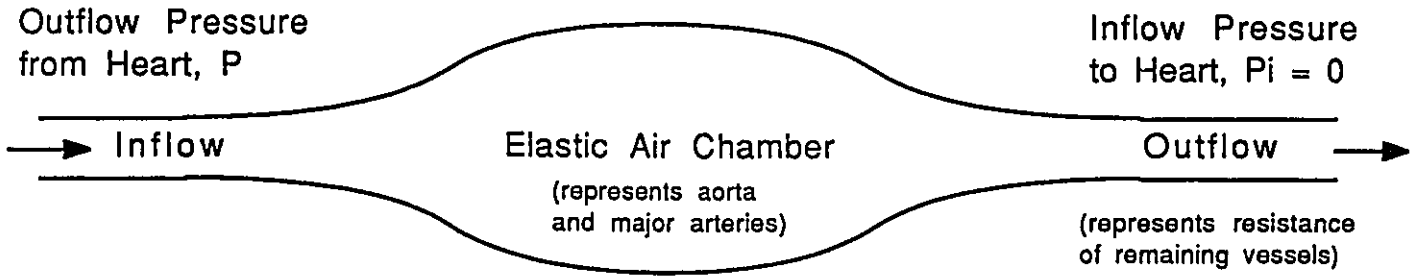

the remaining circulation elements. Inertial effects were considered to be minimal.

The Windkessel model assumes a linear relationship in the elastic chamber, between pressure, P, and volume, V, where,

$$V=CP \tag{2.1}$$

and C is a constant of proportionality. Fluid moves from the air chamber to a smaller vessel where Poiseuille flow is assumed. From this, it is assumed that the rate of change of internal volume is proportional to the driving pressure gradient or,

$$\frac{dV}{dt}=R(P_1-P_2). \tag{2.2}$$

By assuming the venous pressure, P_2, to be zero, R represents the resistance to fluid leaving the system and is inversely proportional to the rate of change of volume. Thus,

$$\frac{dV}{dt}=\frac{P}{R}. \tag{2.3}$$

During systole, the flow into the elastic chamber or fluid entering the system is Q_{in} or

$$Q_{in}=\frac{dV}{dt}=C\frac{dP}{dt}. \tag{2.4}$$

Mass Balance yields,

$$\frac{dV}{dt}=Q=C\frac{dP}{dt}+\frac{P}{R}, \tag{2.5}$$

which can be solved in terms of Pressure and Time with a suitable expression for Q.

Refinement of the Windkessel model was followed in the 1950's by J.R. Womersley and D.A. Macdonald by steady-state analysis of the arterial

pulse (13). Womersley showed that errors associated in using a linearized form of the Navier-Stokes equation to describe an arterial segment were small and that by breaking the arterial pulse down into individual component harmonics he developed a model based on longitudinal impedance. Through consideration of complex wave velocity, a pressure/flow relationship was developed in terms of the input impedance of a vascular bed. This followed from Fourier analysis of the time behaviour of pressure and flow.

Improvement on the elastic reservoir theory followed by representing the aortic arch and descending aorta as individual elastic chambers with an associated compliance, inertance and diameter dependent resistance between elements. The examination of time behaviour over the entire cardiac cycle is possible with this type of model. Another two reservoir model was developed in 1962 by Roston (13,19), where the ascending and descending aorta are represented as elastic reservoirs, each with its own compliant properties. The volume associated with each segment is dependent on a linear function of pressure. The two reservoirs are interconnected by an inelastic tube representing the aortic arch. No effect of inertia was examined with this particular model.

Extension of the various model forms proceeded through the 1960's by introduction of non-linear pressure/volume relationships in the elastic reservoir (13-19). Time-distributed parameters were also introduced.

The modelling, to this point, had focused on the mathematical descriptions of the vascular bed and the ventricle without verification of model adequacy when applied to real data. Lack of computer technology prohibited the solution of many of these equations.

The 1970's and 1980's saw the extension of the various models and modelling techniques developed previously. The emphasis has been to apply the model to specific areas of the circulation, to specific disease related states that affect the circulation or to specific device development projects (20-25). For example, the Pennsylvannia State University mock circulation loop was developed for their artificial heart program initiated in 1971 (2). The Novacor mock circulation loop and National Institute of Health mock circulation loop were developed for specific device development projects (26).

The final aim of model building is to implement the model on an analog or digital computer to study its behaviour. This can verify the theoretically derived model when a comparison is made between the real system and the model. The digital computer enables a more detailed study than the analog computer.

In the formulation of any mathematical model describing a complex system of parameters and dependent and independent variables, simplifying assumptions are made to enable the model's development. An understanding of the physiological system must be held before reasonable simplifying assumptions can be made.

A good mathematical model for the identification of parameters in the physiological, closed cardiovascular system has been based on the description of average, rather than instantaneous or dynamic behaviour of certain system variables. The knowledge gained from studying smaller subsystems of the overall system can provide insight into the localized behaviour thereby justifying simplifications. This approach allows simplification of the system to a manageable form while permitting an acceptable level of sophistication. A fine line exists between

oversimplification and sophistication and as Albert Einstein once said, "Make everything as simple as possible, but not simpler".

2.2 - Structure of the Circulatory System

The human circulation is a branching network of tubes consisting of an arterial and venous component. The systemic arterial system has two main functions - one, to accept the pulsatile flow of the blood from the left ventricle for distribution to the body, and two, to dampen the pulsatile effects of this flow (19,27). The venous component also has two main functions including delivering blood back to the heart and acting as a variable-volume reservoir for the blood.

In the ascending aorta, peak flow is achieved within the first third of systole and is decreased more slowly in the latter stages of systole. Systole typically represents 40% of the time of the entire cardiac cycle. Marginal regurgitation is seen immediately prior to aortic valve closure. Diastolic flow is close to zero.

The pressure wave in the ascending aorta is usually more rounded at peak systolic pressure tapering off slowly as the ventricle moves into diastole. Typical aortic pressure traces for the human are shown in Figure 2.2.

The effect of human age on the elasticity of arteries is also shown in Figure 2.2 where the aortic pressure profile for a 50 year old adult is shown compared to the profile for a 20 year old adult. As the human ages, the arteries lose their elasticity, resulting in a sharper systolic pressure peak due to the increased rigidity of the vessels.

Figure 2.2 - Typical Human Aortic Pressure Profiles

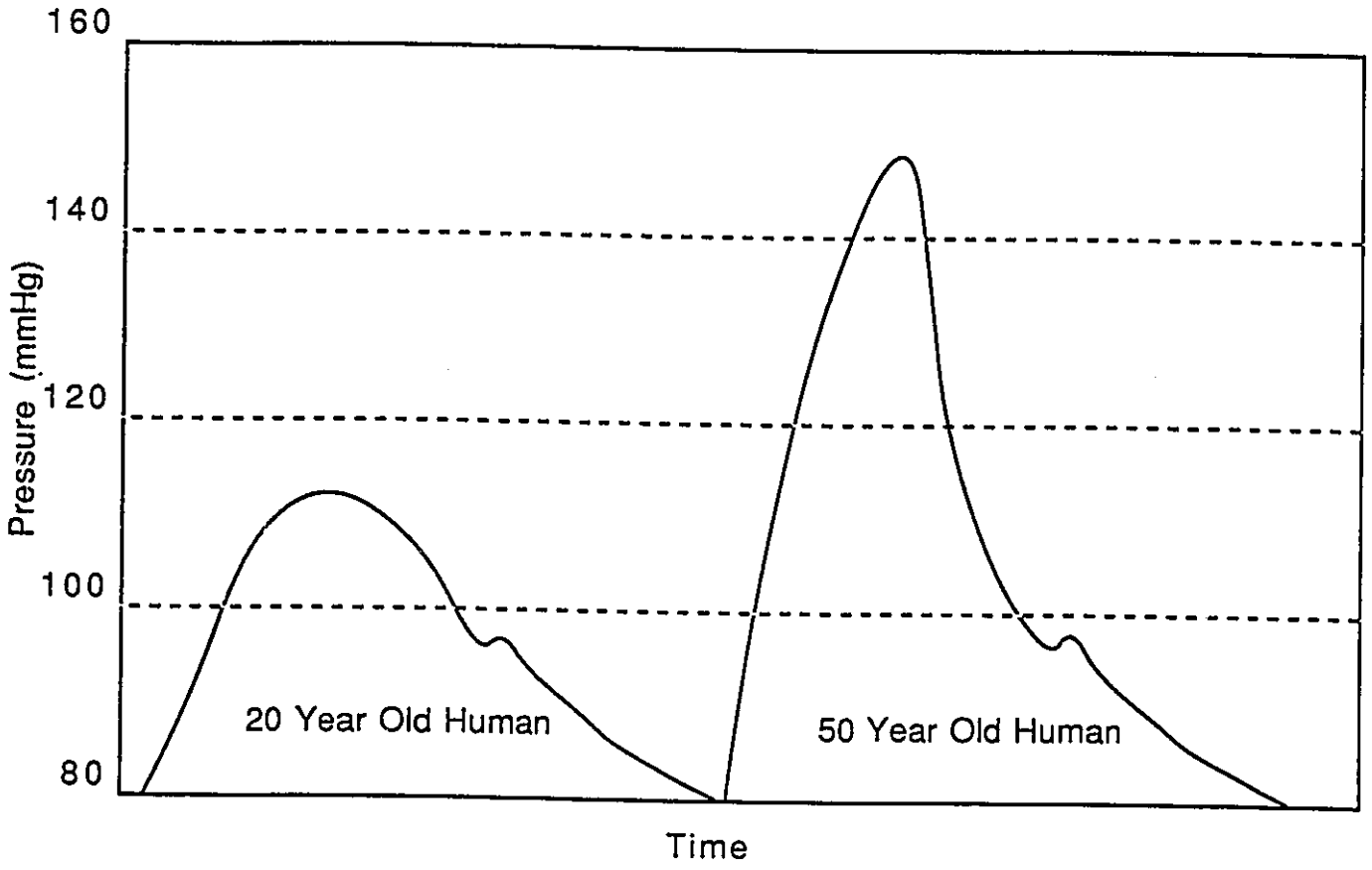

In large arteries, the maximal pressure (systolic) is approximately 120 mmHg and the minimal is about 80 mmHg (diastolic) in the healthy human. The arterial vessel walls are elastic, and the compliance is defined as

$$C = \frac{dV}{dP} \tag{2.6}$$

The greatest effect of compliance on aortic flow and pressure occurs in the great arteries, immediately downstream from the heart.

The resistance of the system occurs to the greatest extent in the arterioles where the pressure drops to 30 mmHg average as a result of the high degree of branching of the arteriole network. The resistance, R, in a round tube is,

$$R = \frac{8\eta L\pi}{r^4} \tag{2.7}$$

where η is the viscosity of the fluid, L is length of resistance and r is radius. The region where the greatest increase in resistance to flow is, therefore, where the greatest change in tube radius occurs. The venous blood pressure drops to 0-10 mmHg from the capillary level of approximately 20 mmHg (Figure 2.3). Resistance in the venous system is less significant as the vessels approaching the heart become larger in diameter.

The effect of time on compliance in the aorta or resistance the arterioles is minimal. That is, neither change dramatically in these regions over a single cardiac cycle enabling their approximation as average values.

The venous side of the circulation acts as a reservoir for the blood before it is returned to the heart. Compliance effects are minimal in this

region mainly due to the lower pressure and non-elastic structure of veins. Resistance effects are also less significant due to the larger diameter vessels. Fluid inertia and properties of the fluid including density and inertia affect its movement at this stage. The main property affecting the inertia is the density of the fluid.

2.3 - Non-Linear Regression Statistical Techniques

Parameter estimation in mock circulation can involve a variety of statistical techniques depending on the model used and the nature of the study. The literature indicates that previously developed MCU models have little or no statistical basis for parameter estimation. Rosenberg et al (2) solve the model utilized in this study on an analog computer and provide parameter estimates. No details about their method of obtaining the published response (Table 5.7) and parameters are given, nor are inference regions for these estimates outlined. Sandquist et al (7) develop a comprehensive model of the mammalian circulatory system incorporating both halves of the circulation and additional system parameters. Their model develops four equations in six variables with eight parameters making it possible to express a given variable as a function of any two other variables. Two dimensional graphs are constructed, holding two variables constant and observing the behaviour of the remaining two variables with assumed values of the parameters. No statistical arguments are presented for the choice of parameters and, therefore, no statements of model adequacy, parameter or response precision could be made. Arabia and Akutsu (3) develop an

Figure 2.3 - Blood Pressure in Different Regions of the Systemic Circulation

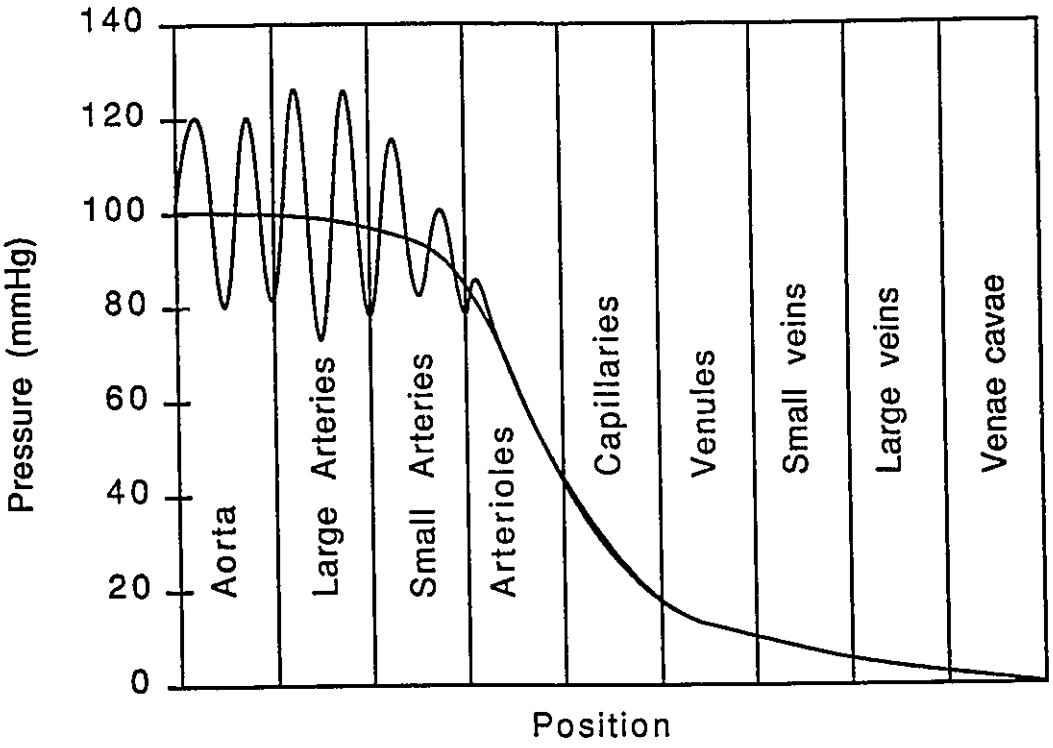

analytical model of the circulation and evaluate it in terms of previously reported values of empirically measured parameters. No attempt is made to improve upon these values. Martin et al (8) use a semi-analytical approach in the analysis of a lumped-parameter model of the cardiovascular system. A system of differential equations was numerically integrated and parameters were chosen from empirically measured values from a healthy human. Geselowitz et al (12) developed a model for the pressure and flow characteristics of an artificial ventricle. Parameters of resistance and compliance were estimated from empirical measurements. Ahmed and Giddons (28) employed autocorrelation functions to describe the velocity of blood through axisymmetric stenoses. This study fitted laser Doppler anemometer flow data to a model incorporating the effects of turbulence and axisymmetric stenoses.

A method of parameter estimation which is not statistically rigorous will not produce the best parameter estimates nor the best model predictions. In addition, statements concerning model adequacy or lack-of-fit, parameter precision and response prediction will not be reliable. In order for a modelling technique to be statistically sound, certain assumptions must be made. Some available techniques are reviewed and evaluated in terms of how closely they follow the necessary assumptions.

2.3.1 - Non-linear Least Squares

The modelling of the human circulation can involve using the method of least squares (19). The non-linear regression model can be written as

$$Y_n = f(\underline{x}_n, \underline{\theta}) + Z_n \qquad (2.8)$$

where f is the expectation function, n is the run number or position, Y is a response, $\underline{x}$ is a vector of independent variables, $\underline{\theta}$ is a vector of parameters and Z is a random variable or disturbance which perturbs the response.

For the model to be non-linear, at least one of the partial derivatives of the expectation function with respect to the parameters will be a function of one of the parameters or,

$$\frac{\delta f(\underline{x}_n,\underline{\theta})}{\delta \theta_i} = g(\theta) \qquad (2.9)$$

For least squares to be statistically sound, that is, providing parameter estimates with highest likelihood, the following assumptions must be true.

i) The operating variables, x_i, are fixed and known, that is,

$V(x_i)=0$ for i=1,2...k operating variables.

ii) The model is adequate or the response function contains only the correct operating variables accounting for them in the correct manner or,

$E(Z_n)=0$ for n=1,2,...N runs

iii) The variance of the residuals is constant at all run conditions, that is,

$V(Z_n)=\sigma^2$ for n=1,2,...N runs

iv) The residuals in different runs are not correlated and are distributed independently of one another, that is, the covariance,

$Cov(Z_u,Z_v)=0$ for u,v=1,2,...N runs and $u\neq v$

v) The residuals are distributed as a Gaussian distribution with mean, zero, and variance, σ^2, that is,

$$p(Z_n) = \frac{1}{\sqrt{2\pi\sigma^2}} \exp\left(-\frac{Z_n^2}{2\sigma^2}\right) \text{ for } n=1,2,...N \text{ runs}$$

Non-linear least squares involves finding the values of the parameters, $\underline{\theta} = (\theta_1,\theta_2,...\theta_p)^T$ which minimize the quantity,

$$s(\underline{\theta}) = \sum_{n=1}^{N} (Y_n - f(\underline{x}_n,\underline{\theta}))^2 \qquad (2.10)$$

where $(Y_n - f(\underline{x}_n,\underline{\theta}))$ is the residual at the n^{th} run.

Different forms for the residual can be developed using other techniques which must also avoid violation of the above assumptions. As a result of the parameter estimation procedures, it is important that a measured variable be used as a response when using least squares. A non-linear model is non-linear with respect to the parameters and, therefore, an iterative solution is required in order to minimize the sum of squares of residuals, $s(\underline{\theta})$, as the process involves the solution of a non-linear algebraic expression.

2.3.2 - Parameter Estimation and Precision

In the non-linear model, least squares estimates of the parameters are obtained iteratively as the expectation surface for the parameters is no longer planar as for the linear model. With a non-linear model, at least one of the normal equations will be a function of the parameters thus making the model non-linear. The solution to a non-linear algebraic equation requires an iterative numerical procedure. The expectation surface for the parameters can involve local minima in addition to the

global minima. Care must therefore be taken to avoid local minima usually achieved through a grid search. This technique involves varying the parameter estimates over a grid of values to obtain the location of the surface minima. The expectation surface may only exist for particular values of the parameters. The global grid search may also identify the limits of the parameter values across the surface.

For the linear model, information of the precision of parameter estimates is developed from the covariance matrix for the parameters, where,

$$V(\hat{\beta}) = (\underset{\sim}{X}^T\underset{\sim}{X})^{-1}\sigma^2 \qquad (2.11)$$

where $\underset{\sim}{X}$ is an N x P matrix of regressor variables and σ^2 is the variance of the response. From this matrix, information about the extent of linearity between parameter estimates can be obtained, expressed as the correlation between parameters. The correlation between two parameters is,

$$\text{correlation} = \frac{\text{Cov}(\hat{\beta}_u,\hat{\beta}_v)}{\sqrt{V(\hat{\beta}_u)V(\hat{\beta}_v)}}. \qquad (2.12)$$

A high correlation between parameters may indicate that the model is improperly parameterized.

The standard error for the parameter estimates can be estimated from,

$$se(\hat{\beta}_j) = s\sqrt{(\underset{\sim}{X}^T\underset{\sim}{X})^{-1}_{jj}} \qquad (2.13)$$

and a 100(1-γ)% inference region for the parameter estimates is,

$$(\hat{\beta}_j) \pm se(\hat{\beta}_j) \cdot T\left(N-P, \frac{\gamma}{2}\right) \qquad (2.14)$$

For a non-linear regression model, joint inference regions can be developed in two forms based on a linear approximation of the expectation function. Linear approximations are used to determine both increments in algorithms for obtaining least squares estimates and to determine approximate inference regions after convergence has been reached. A linear approximation of the expectation function is a quadratic approximation of the sum of squares function.

In the linear case, a 100(1-γ)% parameter inference region is,

$$(\underline{\beta} - \hat{\underline{\beta}})^T (\underline{X}^T \underline{X})^{-1} (\underline{\beta} - \hat{\underline{\beta}}) \leq Ps^2 F(P, N-P, \gamma) \qquad (2.15)$$

where $\underline{X}$ is a N x P matrix of regressor variables or the derivative matrix.

By analogy, in the non-linear case, a derivative matrix evaluated at $\hat{\underline{\theta}}$ results in approximate shape inference regions for the parameters in parameter space. The derivative of the sum of squares function with respect to the parameters is the gradient where,

$$\Gamma(\underline{\theta}) = \left\{ \frac{\delta s(\underline{\theta})}{\delta \theta_i} \right\} \qquad (2.16)$$

As,

$$s(\underline{\theta}) = (\underline{Y} - f(\underline{x}_n, \underline{\theta}))^T (\underline{Y} - f(\underline{x}_n, \underline{\theta})) \qquad (2.17)$$

$$= e^T(\underline{\theta}) e(\underline{\theta}) \qquad (2.18)$$

$$\Gamma(\underline{\theta}) = 2\left(\frac{\delta e(\underline{\theta})}{\delta \theta_i} \right)^T e(\underline{\theta}) \qquad (2.19)$$

$$= 2J^T(\underline{\theta}) e(\underline{\theta}) \qquad (2.20)$$

$$=2\sum_{u=1}^{N} e_u \frac{\delta e_u}{\delta \theta_j} \tag{2.21}$$

where $J(\underline{\theta})$ is the Jacobian,

$$J(\underline{\theta}) = \left\{ \frac{\delta e(\underline{\theta})}{\delta \theta_i} \right\} \tag{2.22}$$

The Hessian can, thus, be written as,

$$H(\underline{\theta}) = \left\{ \frac{\delta^2 s(\underline{\theta})}{\delta \theta_i \delta \theta_j} \right\} \tag{2.23}$$

$$=2\sum_{u=1}^{N} \left[e_u \frac{\delta^2 e_u}{\delta \theta_i \delta \theta_j} + \frac{\delta e_u}{\delta \theta_i} \frac{\delta e_u}{\delta e_j} \right] \tag{2.24}$$

$$=2\left[\underline{J}^T \underline{J} + \sum_{u=1}^{N} e_u G_u \right] \tag{2.25}$$

where G_u is the Hessian of e_u. If our model is good, we can assume that G_u is zero and, hence,

$$H(\underline{\theta}) \approx 2\underline{J}^T(\underline{\theta})\underline{J}(\underline{\theta}). \tag{2.26}$$

Thus, from expression (2.26) $\underline{X}^T\underline{X}$ is approximated as $\frac{H(\hat{\underline{\theta}})}{2}$. The validity of the approximation is as good as the derivative matrix, where the greater the extent of non-linearity at $\hat{\underline{\theta}}$, the poorer the approximation. An approximation of the gradient of the residual function with respect to the parameters can be obtained through a finite difference algorithm.

Also for the linear case, a likelihood contour exists for those values of $\underline{\theta}$ within a fixed distance of $\hat{\underline{\theta}}$ or at a level or value for which $s(\underline{\theta})$ is equal to a constant. An approximate confidence level is then associated with the contour where,

$$s(\underline{\theta}) \leq s(\hat{\underline{\theta}}) \left[1 + \frac{P}{N-P} F(P,N-P,\gamma) \right]. \qquad (2.27)$$

An evaluation of $s(\underline{\theta})$ over a grid of $\underline{\theta}$ values approximates the contour. For both the approximate shape and approximate probability level parameter inference region, graphical representation of a model with greater than two parameters is difficult to use or interpret.

2.3.3 - Tests for Model Adequacy

A model can be tested for lack-of-fit through both qualitative and quantitative analysis. Qualitative analysis is performed through residual plots which can reveal violations of the assumptions outlined in Section 2.3.1. Common plots include the residuals against time, the response variable, previous residuals or independent variables. The presence of outliers, time trends, heteroscedascity or other non-random behaviour may indicate that something is missing from the model. However, residual plots can be subjective and should be supplemented with a quantitative lack-of-fit test.

For the non-linear model, no rigorous lack-of-fit test exists and must, therefore, be based on a linear model. A quantitative lack-of-fit test involves an examination of replicates. The discrepancy between a data set and a fit curve arises from two sources - the experimental error and the inadequacy in the model being fitted. Model adequacy tests compare the error from the latter source to the former, to determine which is more significant. Experimental or "pure error" is estimated from replicate data points, that is data collected independently under similar conditions. Pure error variance, σ^2, is estimated from

$$\hat{\sigma}^2 = \sum_{u=1}^{M} \frac{(Y_u - \bar{Y})^2}{M-1} \qquad (2.28)$$

where, $$\bar{Y} = \sum_{u=1}^{M} \frac{Y_u}{M} \qquad (2.29)$$

is the sample mean response for that replicate set and M is the number of data points at operating condition u. For J replicate sets, the individual variance estimates can be pooled using

$$\hat{\sigma}_p^2 = \frac{\sum_{i=1}^{J} (M_i - 1)\sigma_i^2}{\sum_{i=1}^{J} (M_i - 1)} . \qquad (2.30)$$

The expression,

$$\sum_{u=1}^{N} (\bar{Y}_u - \hat{Y}_u)^2 \qquad (2.31)$$

is derived from the residual sum of squares function and arises from both experimental error and from model inadequacy. It can be shown that expression (2.31) is equal to

$$\sum_{u=1}^{N} e_u^2 - \hat{\sigma}_p^2 \sum_{i=1}^{J} (M_i - 1) \qquad (2.32)$$

having,

$$N - P - \sum_{i=1}^{J} (M_i - 1) \qquad (2.33)$$

degrees of freedom. The ratio of equation (2.32) with expression (2.33) degrees of freedom with the pure error variance (2.30) enables a

significance test to be performed when compared with the value of $F(\nu_1,\nu_2)$ at the desired probability level. If the calculated ratio is greater than the upper γ per cent value of $F(\nu_1,\nu_2)$ then the model shows lack-of-fit. The ratio compares the adequacy of fitting the data with an approximated variance to the model. A test ratio less than $F(\nu_1,\nu_2: \gamma)$ indicates that the model inadequacy is significantly less than the experimental error.

If the data contains no replicates, an external estimate of variance should be determined based on information derived from data similar to data being studied. In this case, the test ratio, W,

$$W = \frac{\sum_{u=1}^{N} \frac{e_u^2}{(N-P)}}{\hat{\sigma}_E^2}, \qquad (2.34)$$

where σ^2_E denotes an external estimate of pure error variance. The determination of external estimates of variance can be very difficult to obtain if the working system is unique for a particular series of experiments.

2.3.4 - Time Series Analysis

As the model involves the prediction of a pressure-time profile, the independence of the random disturbances must be checked in order to evaluate the validity of the assumption that they are randomly distributed (29,16). Correlation of the disturbances with respect to time can be identified by a time-series plot of the residuals with respect to time or by a lag plot where the residuals for the nth case are plotted against the

residual for the (n-k)th case, where k is the lag. From these plots, any tendencies for the residuals to remain either positive or negative in the first case or as a non-random distribution in the second, may indicate correlated disturbances (16).

Non-independent disturbances observed within a model must be accounted for within the model through alteration of the model to recognize the dependence. This dependence or autocorrelation can take several forms including a moving average or autoregressive models of variable order. Examples for a model of order p, are,

$$Z_n = \varepsilon_n + \omega_1\varepsilon_{n-1} + \omega_2\varepsilon_{n-2} +,.....,+ \omega_p\varepsilon_{n-p} \qquad (2.35)$$

and

$$Z_n = \varepsilon_n + \omega_1 Z_{n-1} + \omega_2 Z_{n-2} +,.....+ \omega_p Z_{n-p} \qquad (2.36)$$

respectively, where ε_n = 1,2,...N are independent random disturbances with zero mean and constant variances, Z_n is the n^{th} residual and $\omega_1,\omega_2,...\omega_p$ are additional parameters to be estimated.

In a regression situation, where the data is equally spaced over time, an appropriate form of the dependence of the disturbance can be determined by the residual autocorrelation function, r_K, where,

$$r_K = \sum_{n=K+1}^{N} \frac{\hat{Z}_n \hat{Z}_{n-K}}{N\sigma^2} \qquad (2.37)$$

where K=1,2... the lag, and σ^2 is the estimate of the variance of the sum of squares function. The residuals are assumed to have zero average and $\hat{Z}_n$ is the residual at n.

In practice, the residual autocorrelation function is calculated to K≈ N/5 where, if the residual autocorrelation function is consistently within

the range of $\pm 2/\sqrt{N}$, the limit where one would expect to find 95% of the correlations if the true correlation was zero, after a lag of 2 or 3, then the model may be assumed as a moving average process of order 1 or 2. If the residual autocorrelation function tends to decay to zero, then the process may be considered as an autoregressive process (16,29). On the basis of the autocorrelation plot, an estimate of the order of the process is made.

The main effect of accounting for the dependence of disturbances, is in reducing the residual variance and the correlation in residuals without greatly affecting the parameter estimates. It also has the effect of obtaining better estimates for the model parameters, due to smaller standard errors and because the method of least squares is applied without violating its assumptions of uncorrelated random errors.

2.3.5 - Precision of the Predicted Response

Inference regions for the precision of the predicted response are, again, based on a linearization of the expectation function. A $100(1-\gamma)\%$ confidence interval for E(y) is,

$$\hat{y}_k = \hat{y}_k \pm T_{v,\frac{\gamma}{2}} \sqrt{V(\hat{y}_k)} \qquad (2.38)$$

where,

$$V(\hat{y}_k) = x_k^T \left(\frac{H(\theta)}{2} \right)^{-1} x_k \sigma^2 \qquad (2.39)$$

$$\sigma^2 = \frac{s(\hat{\theta})}{N-P} \qquad (2.40)$$

$$x_k^T = (x_{k1}, x_{k2}, \ldots x_{kp}) \tag{2.41}$$

and

$$x_{kj} = \left[\frac{\delta f(\underline{x}, \underline{\theta})}{\delta \theta_j}\right]_{\theta = \hat{\theta}} \tag{2.42}$$

As with parameter precision, this confidence interval is only as good as the linear approximation of the variance.

3 - MODEL DEVELOPMENT

3.1 - Basis for Model Selection

Each level of increasing complexity of model can provide levels of insight into the nature of the circulation at varying degrees of predictability. For EVAD research, the lumped-parameter model may provide the best degree of accuracy for a specific degree of sophistication and manageability. For this reason, the model utilized in this study is a lumped-parameter model which can be solved analytically by an approximation of the normal physiological aortic flow characteristics. A lumped-parameter model is a model where the effects of the various parameters to be estimated are assumed to elicit their effects in discrete regions of the circulatory system.

The objective of the mathematical model is to provide an accurate quantitative description of the blood flow through the various sub-systems of the mock circulation loop as a simplified description of the natural circulation. Operation of the loop at steady-state conditions will provide a means of determining parameter values. Some of the assumptions utilized in developing the model are as follows (2,17,19,26):

i) The systemic circulation consists of an arterial and venous component as does the natural circulation.

ii) Chemical, biological and electrical effects which may affect the circulation are neglected. While the natural circulation is influenced by these effects, the level of influence is small when compared to the bulk characteristics of the circulation.

iii) The effect of time-distributed parameters over the cardiac cycle is small compared to the bulk characteristics of the circulation. Only the mean and steady-state values are assumed.

iv) The fluid flowing through the circulatory model is an isothermal, incompressible Newtonian fluid as at the operating pressures and temperatures of the system, the non-Newtonian characteristics are negligible. This assumption is made as the fluid is passing through an orifice greater than 100μm in diameter and can, therefore, be treated as a Newtonian fluid.

The model represents the human circulation as simplified by the mock circulation loop. The development of a ventricular assist device (VAD) requires extensive *in vitro* testing in order to evaluate various responses such as power required and efficiency of operation to supply a given cardiac output and pressure. The mock circulation unit must include those characteristics of the natural circulation which accurately reflect the natural physiological responses to various changes in operating conditions. This will aid in assuring that the *in vivo* operation of the VAD is closely linked to the true human body responses.

3.2 - Derivation of Model

Development of the model follows from principles of fluid dynamics and physiological characteristics of the natural circulation (2,30). The Mock Circulation Unit is shown in Figure 3.1. It is separated into two chambers representing the two main components of the systemic circulation, the arterial and venous sides. The former is the high pressure side while the latter is the low pressure side.

Figure 3.1 - Schematic Diagram of Mock Circulation Unit

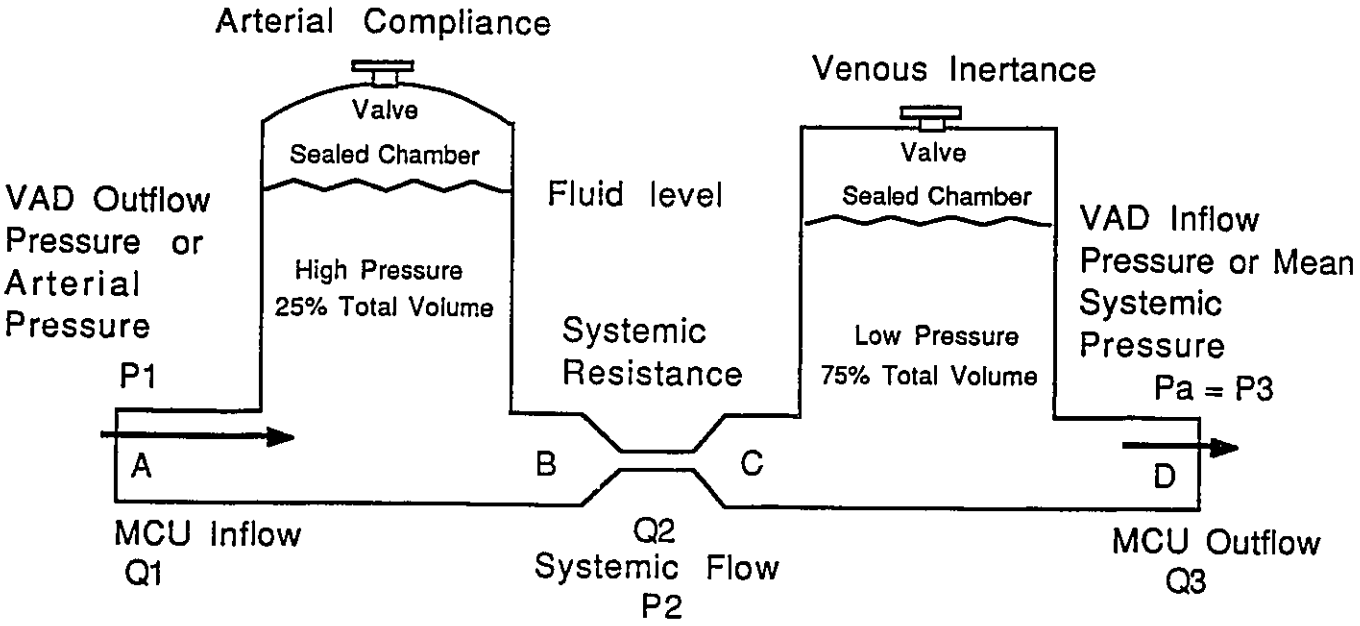

Parameters:	Independent Variables:
Resistance	Inflow Pressure
Compliance	Cardiac Cycle Time
Inertance	Cardiac Output

The parameters of arterial compliance, capillary resistance and venous inertance are assumed to be the dominant effects within discrete regions of the system. As in the natural aorta, the dominant force affecting pressure and flow is the compliance of the arterial walls. This is represented in the mock circulation unit by a volume of air above a fluid level on the high pressure side. The arterial chamber is sealed from the atmosphere which permits the volume of air to be compressed above the chamber during the systolic phase of pumping.

In the natural circulation, the blood vessels narrow as distance from the heart increases. The diameter ranges from centimetres in the aorta to micrometres in the capillaries to centimetres in the venous system. This narrowing increases the resistance to flow through the vessels making resistance the predominant effect in the capillary region as resistance is proportional to the fourth power of the diameter of the opening through which the fluid is passing. In the mock circulation unit, this effect is simulated by pumping fluid through a narrow orifice.

In the venous side of the circulation, the predominant effect is inertia on fluid flow. In this region, pressures are lower and the increasing diameter of the venous vessels has little effect on resistance to flow. As the mean flow rate throughout the system is constant and the volume of fluid in this region is large, whereas compliant and resistive effects are small, the inertia of the fluid becomes the predominant effect.

Assuming ideal fluid resistance, ideal fluid compliance and ideal fluid inertance to be:

$$\Delta P = RQ \qquad (3.1)$$

$$\Delta Q = C\frac{dP}{dt} \tag{3.2}$$

$$\Delta P = \phi\frac{dQ}{dt} \tag{3.3}$$

where, $R = \frac{8\eta L_R \pi}{A_R^2}$, $C = \frac{A_C^2}{k}$, and $\phi = \frac{\rho L_i}{A_i}$.

L_R is the length of resistance, η is the fluid viscosity, A_R is the cross-sectional area of resistance, A_C is area of compliance, k is a constant of proportionality, ρ is the fluid density and L_i and A_i are the length and area of inertance respectively.

A mass and energy balance across the sections of the MCU as in Figure 3.1, yields:

Continuity from A to B:

$$Q_1 - Q_2 = C\frac{dP_1}{dt} \tag{3.4}$$

Momentum between B and C:

$$P_1 - P_2 = RQ_2 \tag{3.5}$$

Momentum between C and D:

$$P_2 - P_3 = \phi\frac{dQ_2}{dt} \tag{3.6}$$

Combining (3.5) with (3.6)

$$P_1 - P_3 = \phi\frac{dQ_2}{dt} + RQ_2 \tag{3.7}$$

Differentiation of (3.4) with respect to time and combining with (3.7) yields:

$$P = \phi\frac{dQ}{dt} + RQ - \phi C\frac{d^2P}{dt^2} - RC\frac{dP}{dt} + P_a \qquad (3.8)$$

where the subscript on P_1 and Q_1 has been dropped, P_3 becomes P_a and P represents arterial pressure. The system is represented by independent variables, a response variable and parameters. The independent variables are P_a, the inflow pressure and Q, the aortic flow rate. An additional independent variable is t_a, the time of one cardiac cycle which is used in the evaluation of the boundary conditions. The response is P, the aortic pressure, and the parameters are R, resistance, C, compliance and ϕ, inertance. The addition of a random disturbance, ε_u, modifies the model to a stochastic form,

$$P = \phi\frac{dQ}{dt} + RQ - \phi C\frac{d^2P}{dt^2} - RC\frac{dP}{dt} + P_a + \varepsilon_u \qquad (3.9)$$

This model can, thus, be described as a non-linear, mechanistic, stochastic model.

A similar expression can be developed to represent the pulmonary side of the circulation and, therefore, the pulmonary arterial pressure, flow, compliance, resistance and inertance. The two sides are considered to differ only in the variables and parameters describing the specific side. Clinically, a VAD is usually configured to the left heart in order to supplement the systemic side of the circulation only and has little or no effect on the pulmonary circulation. For these reasons, this study deals only with parameter estimation of the systemic side of the circulation.

3.3 - Stages to Model Solution

Given that the atrial or filling pressure, P_a, is constant, a forcing function representing arterial flow, Q, can be developed. This forcing function utilizes the unit step function and discontinuous line segments where,

$$Q(t) = \sum_{i=1}^{n} \alpha(t-D_i)(m_i t - m_{i-1} t + b_i - b_{i-1}) \qquad (3.10)$$

$$\frac{dQ}{dt} = \sum_{i=1}^{n} \alpha(t-D_i)(m_i - m_{i-1}) \qquad (3.11)$$

where n is the number of line segments, $\alpha(T)$ is the unit step function evaluated at T ($\alpha(T)$ is zero for $T<0$ and one for $T \geq 0$), m_i is the slope of a particular line segment, b_i is the intercept of a particular segment and D_i is the time of discontinuity for a particular line segment. A rough example of a physiological flow profile represented in this form is indicated by Figure 3.2 with the values of the individual line segments indicated in Table 3.1.

The boundary conditions can be assumed to be:

i) The arterial pressure at the beginning of the cardiac cycle, t=0, is equal to the arterial pressure at the end of the cardiac cycle, $t=t_a$. That is, $P_{(t=0)} = P_{(t=ta)}$

ii) The pressure gradient at the beginning of the cardiac cycle is equal to that at the end of the cardiac cycle.

$$\left(\frac{dP}{dt}\right)_{t=ta} = \left(\frac{dP}{dt}\right)_{t=0} \qquad (3.12)$$

Figure 3.2 - Example of Forcing Function Approximation of Aortic Flow

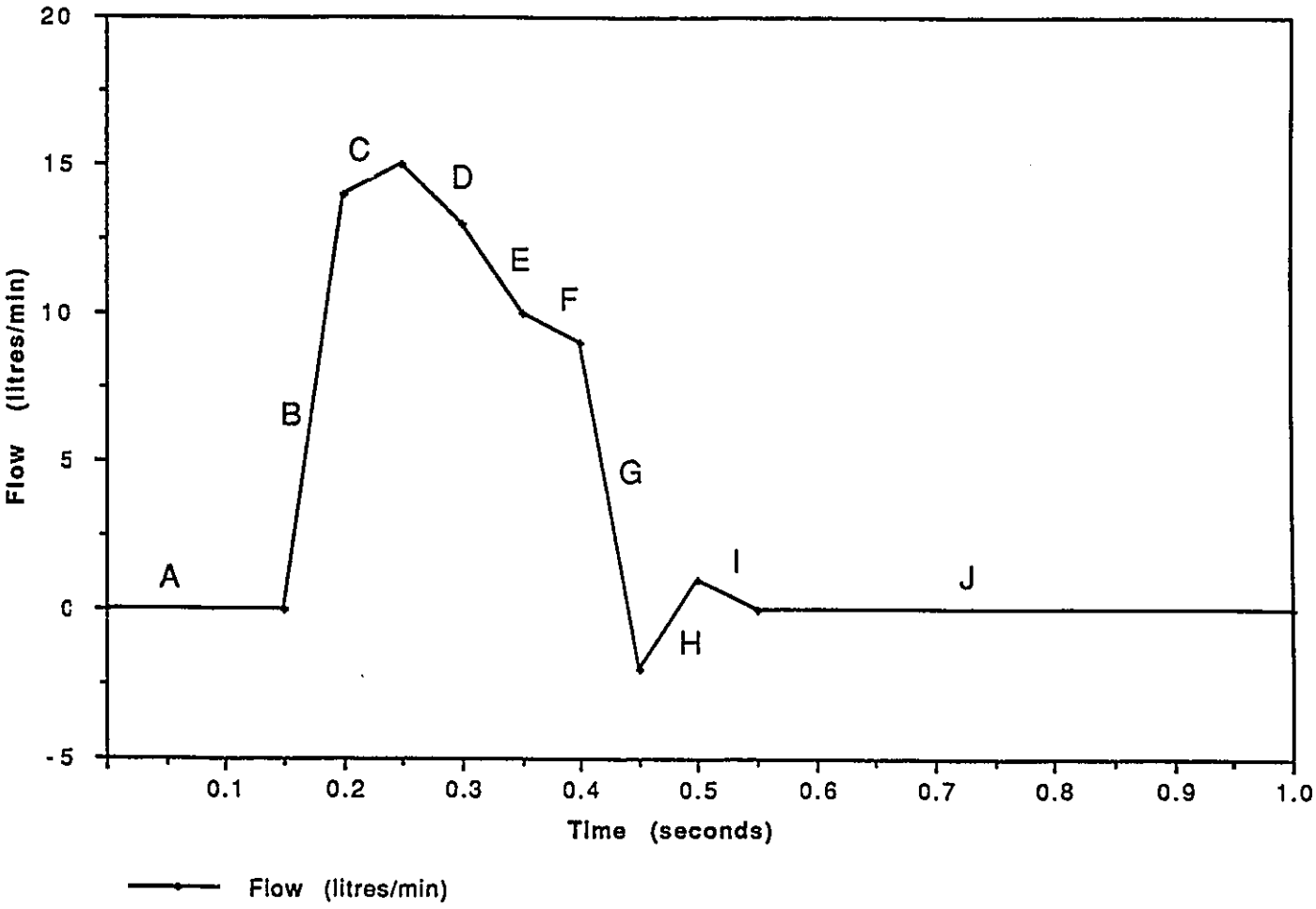

Table 3.1 - Example of Line Segment Slope, Intercept and Discontinuity Values for Aortic Flow Approximation

Line Segment	Slope, m (litres/min/s)	Intercept, b (litres/min)	Time of Discontinuity, D (seconds)
A	0.0	0.0	0.0
B	280.	-42.	0.15
C	20.	10.	0.2
D	-40.	25.	0.25
E	-80.	37.	0.3
F	-20.	17.	0.35
G	-200.	89.	0.4
H	60.	-29.	0.45
I	-20.	11.	0.5
J	0.0	0.0	0.55

The system is solved through Laplace transforms yielding,

$$P = (BPo + \dot{P}o)\left[k_1 e^{gt} + k_2 e^{ht}\right] + Po\left[k_3 e^{gt} + k_4 e^{ht}\right] + E\left[k_5 + k_6 e^{gt} + k_7 e^{ht}\right]$$
$$+F\sum_{i=1}^{n}\alpha(t-D_i)\left[HH_i(k_5 + k_6 e^{g(t-D_i)} + k_7 e^{h(t-D_i)})\right]$$
$$+G\sum_{i=1}^{n}\alpha(t-D_i)\left[\begin{array}{l} HH_i(D_i(k_5 + k_6 e^{g(t-D_i)} + k_7 e^{h(t-D_i)}) + k_5(t-D_i) + k_8 + k_9 e^{g(t-D_i)} + k_{10} e^{h(t-D_i)}) \\ +HHH_i(k_5 + k_6 e^{g(t-D_i)} + k_7 e^{h(t-D_i)}) \end{array}\right]. \quad (3.13)$$

This expression for aortic pressure, P, contains the independent variables, flow, Q, time, t, and inflow pressure, P_a. The expressions for flow are partially contained with the HH_i and HHH_i terms where,

$HH_i = m_i - m_{i-1}$ and $HHH_i = m_i - m_{i-1} + b_i - b_{i-1}$.

The inflow pressure, Pa, is contained within the expression, E, where

$$E = P_a/\phi C. \quad (3.14)$$

The expressions for B, D, F and G are defined as,

$$B = R/\phi \quad (3.15)$$

$$D = 1/\phi C \quad (3.16)$$

$$F = 1/C \text{ and} \quad (3.17)$$

$$G = R/\phi C \quad (3.18)$$

respectively. The lumped-parameter values of k_1 through k_{10} are defined as:

$$k_1 = \frac{1}{g-h},\ k_2 = \frac{1}{h-g},\ k_3 = \frac{g}{g-h},\ k_4 = \frac{h}{h-g},\ k_5 = \frac{1}{gh}$$

$$k_6 = \frac{1}{g(g-h)}, k_7 = \frac{1}{h(h-g)}, k_8 = \frac{g+h}{g^2h^2}, k_9 = \frac{1}{g^2(g-h)}, k_{10} = \frac{1}{h^2(h-g)},$$

where g and h are roots of the expression $s^2 + Bs + D$, a Laplace domain expression arising during the solution. Appendix A shows the detailed solution to the model.

4 - EXPERIMENTAL SET-UP AND DATA COLLECTION

4.1 - The Donovan Mock Circulation Unit

A Donovan mock circulation unit was used to obtain experimental results. It was obtained from the Institute for Biomedical Engineering at the University of Utah, Salt Lake City. Designed in 1974 by Dr. F. Donovan, the Donovan mock circulation unit (MCU) models the physiological circulatory elements of resistance, compliance and inertance for both the systemic and pulmonary sides of the human circulation system (4). The instrument consists of four sealed lexan® chambers each representing the inflow and outflow reservoirs of the natural circulation around the heart (Figure 4.1). The first chamber is the systemic high pressure element of the system corresponding to the afterload pressure on the left ventricle. Anatomically, it is intended to represent the pressure and compliance associated with the natural aorta and the systemic arterial system. The second chamber is the low pressure element corresponding to the preload pressure on the right ventricle. Anatomically, it represents the pressure and compliance associated with the systemic venous system and right atria. The two chambers are connected in series with a variable resistance element between them. The resistance element is intended to model the resistance associated with the arterial and venous capillary systems. Similarly, the third and fourth chambers represent the high and low pressure elements of the pulmonary circulation with their associated pressures and compliancies. The resistance element between these two chambers represents the resistance of the pulmonary capillary system.

Figure 4.1 - The Donovan Mock Circulation Unit

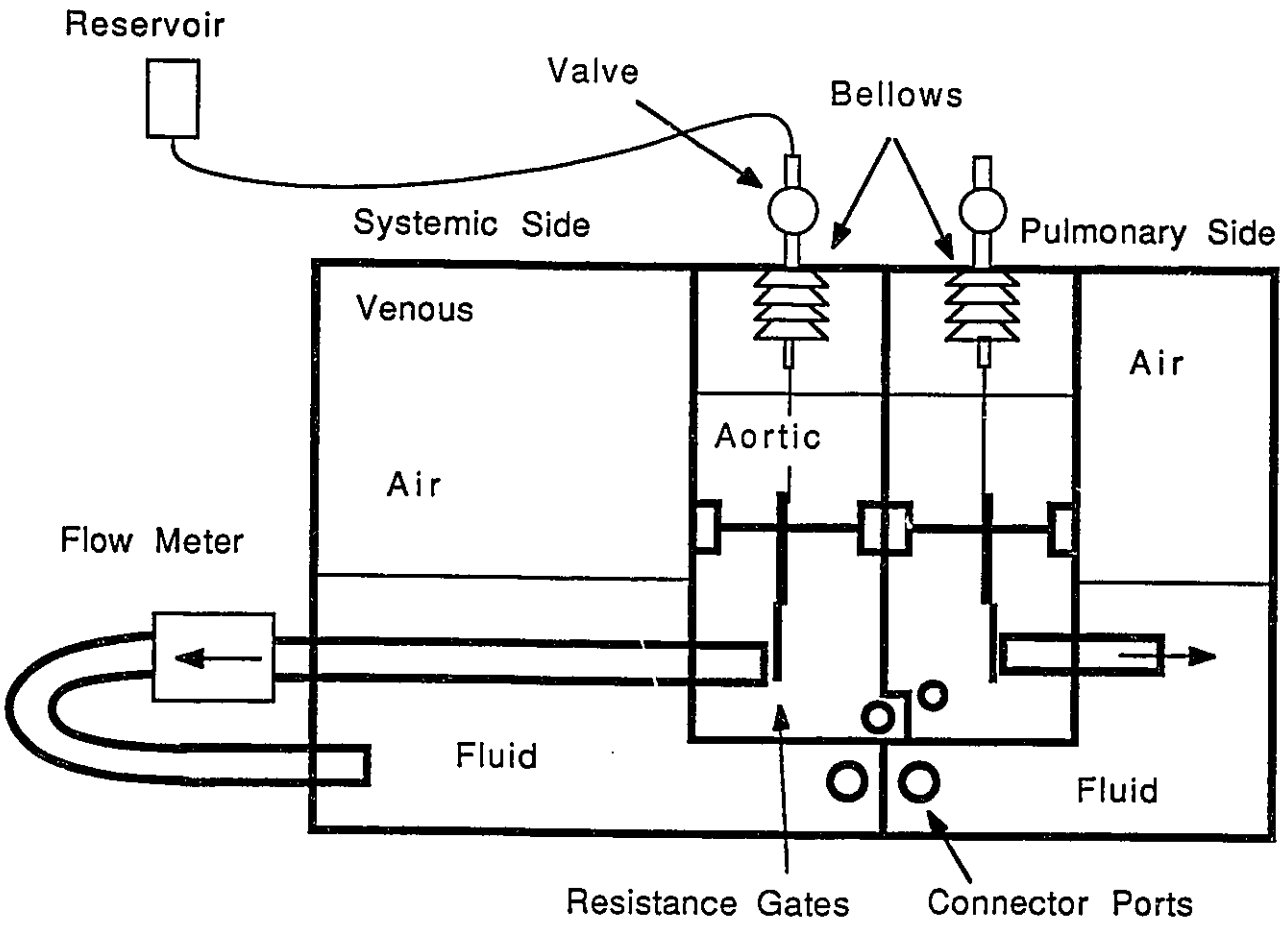

The size of each chamber and the fluid level associated with that chamber determines the compliance or distensibility of the vessels associated with that particular element. The chambers are closed against the atmosphere and therefore exist with a fixed volume of air above a fluid level. The level of fluid in the chamber and the physical dimensions of the chamber determines the compliance of that particular chamber. As the fluid level rises within the chamber, the air above the chamber is compressed and the compliance of the chamber decreases non-linearly with respect to the total volume according to

$$P_1V_1 = P_2V_2. \qquad (4.1)$$

For this reason, only small changes in volume will yield accurate pressure calculations. The arterial system of the human circulation has a smaller volume than the venous side and has a smaller compliance. The Donovan MCU reflects this difference by a smaller volume of liquid and smaller volume of air above the fluid surface. The compliance of the aortic chamber can be set to desired systolic/diastolic ratios by changing the fluid level within the chamber. By raising or lowering the water level, the volume of air above the fluid is reduced or increased, thereby decreasing or increasing the compliance.

The resistance element consists of a swinging gate arm across an orifice of fixed diameter. The arm is connected through a direct link to a variable volume bellows system. A change in the pressure within the bellows determines the resistance by causing the arm to move across the orifice, thereby increasing or decreasing the cross-sectional area to flow. The pressure within the bellows is altered by raising or lowering a fluid reservoir outside the tanks. As the reservoir is raised, the pressure inside the bellows is increased causing the bellows to expand, thereby moving

the position of the resistance gate to a more closed position. Similarly, a lowering of the reservoir will decrease the pressure inside the bellows which will then contract the bellows, reducing the fluid volume within and moving the gate to a more open position. Resistance is, therefore, increased by raising the reservoir and lowered by lowering the reservoir. After setting the resistance the external reservoir is closed to the bellows by means of a valve. During operation of the MCU, this valve can be set to remain open, resulting in a non-linearly varying resistance with respect to time. The valve was set to the closed position for this study, thereby enabling a non-varying resistance term to be utilized in the model.

This study was concerned with the development of an EVAD, where the natural heart is left in situ and the device is implanted in order to support the pumping of the left heart only. For this reason the pumping device was configured to the systemic side of the circulation only. Mathematically, the systemic and pulmonary sides of the MCU differ only in the parameters describing each individual side.

4.2 - Instrumentation of the Mock Circulation Unit and the Data Acquisition System

A Macintosh IIx computer was established as the data acquisition system (DAS) in conjunction with a Macadios II analog/digital convertor board (GW Instruments, Somerville, Massachusetts). Analog signals were conditioned to ±5 Volts DC. Data acquisition software was LabView (National Instruments, Austin, Texas). Acquisition software programs were written to obtain and process data from the MCU (Appendix C).

Data required from the MCU included instantaneous pressure from both the aortic and systemic sides, bulk flow or cardiac output, instantaneous aortic flow and heart rate. Aortic and systemic pressures were measured using Spectramed physiological pressure transducers (Model DTX) (Oxnard, California) mounted in the aortic and systemic chambers at the inflow and outflow levels of the VAD. These transducers operated under the principle of a pressure change eliciting a change in voltage across a Wheatstone bridge. The voltage signal (mV) was amplified before entering the data acquisition system and had ±1 mmHg accuracy. Pressure transducers were calibrated using a water manometer configured to the MCU. The voltage change with respect to pressure was linear across the entire operating range (-5 mmHg to 120 mmHg). Cardiac output was measured using a SRI-2 turbine flow meter (Flow Technologies Inc., Phoenix, Arizona) mounted in series between the aortic and systemic chambers downstream of the resistance element. An analog signal was input to the DAS. The flow meter was calibrated with a rotometer (Brooks Instruments, Markham, Ontario). Instantaneous aortic flow was measured using a T101 Ultrasonic Blood Flow Meter (Transonic Systems Inc., Ithaca, New York) with a RS-32 probe (Figure 4.2). The probe was calibrated against the turbine flow meter for each individual run. A 10 Hz low-pass filter was used to condition the analog signal prior to input to the DAS. This filter was a 2nd order Butterworth which corresponded to a 24 millisecond phase shift for the flow signal. The flow data from the MCU was, therefore, back-shifted by 24 milliseconds within the DAS to compensate for the filter. The probe was mounted around the ventricle outflow cannulae and acoustically coupled with ultrasonic jelly.

Figure 4.2 - Top View of Experimental Set-up

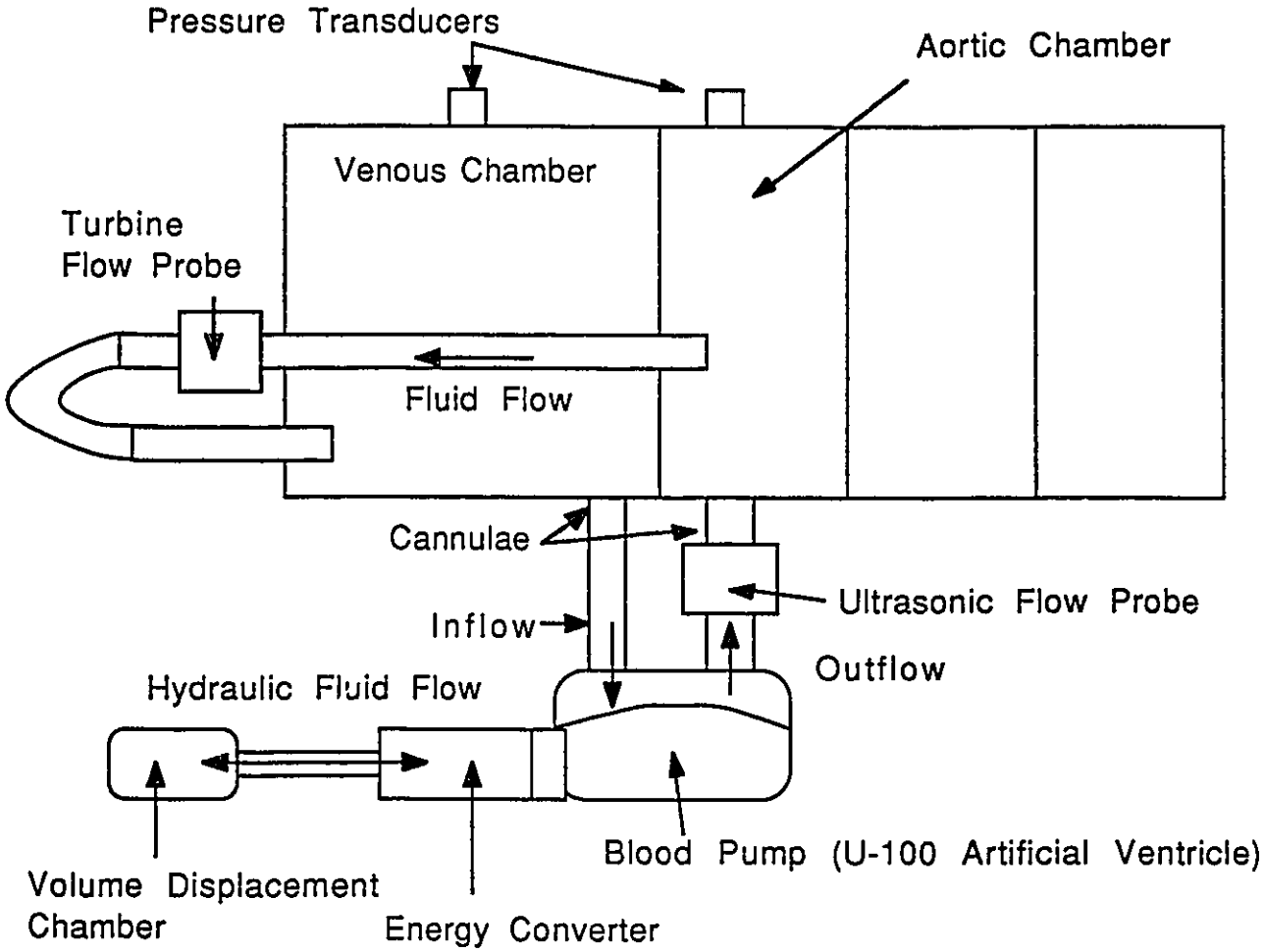

The pumping system consisted of blood pump, energy convertor, volume displacement chamber and physiological controller. The blood pump was a University of Utah U-100 ventricle with a 75 ml stroke volume with St. Jude Medical (St. Paul, MN) bileaflet valves. The energy convertor was a two phase, reversing brushless DC motor (Nu-Tech, Dayton, Ohio) with a 4 ounce-inch torque rating. The energy convertor included a four blade 8° impeller (8° refers to the eighth iteration in design that the impeller has undergone) developed at the Institute for Biomedical Engineering, Salt Lake City, Utah. The volume displacement chamber was a 235 ml custom-made Biomer chamber from the Institute of Biomedical Engineering, Salt Lake City, Utah. The blood pump, energy convertor and volume displacement chamber were connected in series with screw sleeves (Figure 4.2). The system hydraulic fluid was decamethyltetrasiloxane (Petrarch Systems, Bristol, Pennsylvania, Lot# 70177). The system contained approximately 300 ml of hydraulic fluid. A custom physiological controller (Institute for Biomedical Engineering, Salt Lake City, Utah) in conjunction with an IBM PC was used to drive the energy converter. In its manual mode of operation, systolic and diastolic pumping times could be set for the cardiac cycle, thus enabling a specific heart rate to be set.

The data acquisition software was designed to obtain 201 samples of aortic pressure, systemic pressure, cardiac output and instantaneous aortic flow over two complete cardiac cycles. The time between successive samples was therefore dependent on the heart rate utilized for a particular run.

The system was operated at ambient temperature (22° C) and at atmospheric pressure.

4.3 - Data Collection Procedure

An individual data set was obtained by setting the desired systolic/diastolic pressures, cardiac output and pre-load. Through manipulation of the systemic resistance, aortic compliance and systolic and diastolic energy convertor times, a steady-state condition would be established for the systolic/diastolic pressures, cardiac output and pre-load. When these conditions were set, the DAS was turned on to record two consecutive cardiac cycles. Table 4.1 indicates the conditions set for the data runs where the pre-load was varied from 0 to 15 mmHg, cardiac output was set approximately at 5 litres/min, and approximate systolic/diastolic pressures of 110/90 mmHg were utilized. Table 4.1 also indicates the operating conditions for the physiological data set.

Table 4.1- Summary of Operating Conditions for the Physiological and MCU Data

Physiological Data (O'Rourke, 1982)

Run Number	Systolic/Diastolic Pressure (mmHg)	Cardiac Output (litres/min)	Filling Pressure (P_a) (mmHg)	Heart Rate (bpm)
1	125/65	5.0	5	92

Mock Circulation Unit Data

Run Number	Systolic/Diastolic Pressure (mmHg)	Cardiac Output (litres/min)	Filling Pressure (P_a) (mmHg)	Heart Rate (bpm)
0	111/86	5.16	15	100
1	111/86	4.95	10	100
2	107/84	5.00	6	100
3	104/84	5.11	0	100

5 - ANALYSIS OF DATA

5.1 - MCU Data and Approximation of Aortic Flow

The operating conditions for the physiological data from O'Rourke (31) and data collected from the MCU over four runs are summarized in Table 4.1. Typical data from the MCU (Run zero) is shown in Figure 5.1. The physiological pressure and flow data is shown in Figure 5.2. Figure 5.1 shows 201 data points collected from the MCU over the scan time for both the aortic pressure and aortic flow rate. The MCU pressure data used in fitting the model for the four runs is summarized as follows: Every fifth data point from zero time to the scan time for the individual scan was selected and the pressure and time value recorded. This effectively reduced the number of data points from 201 per scan to 41. The result of this is shown in Figure 5.3 which compares the pressure data collected from the MCU as 201 data points to the data fit to the model as 41 data points. This was done in order to reduce the computer time required to fit the model during the minimization routines and to average the noise associated with the aortic pressure profile. With the aortic flow profile, the same averaging effect was not required as a result of a probe filter. The highly non-linear nature of the aortic flow profile was well approximated by 41 line segments over two cardiac cycles as shown in Figure 5.4. A larger number of data points merely increased computer time while a smaller number did not accurately reflect the measured profile.

Figure 5.1 - MCU Pressure and Flow Data

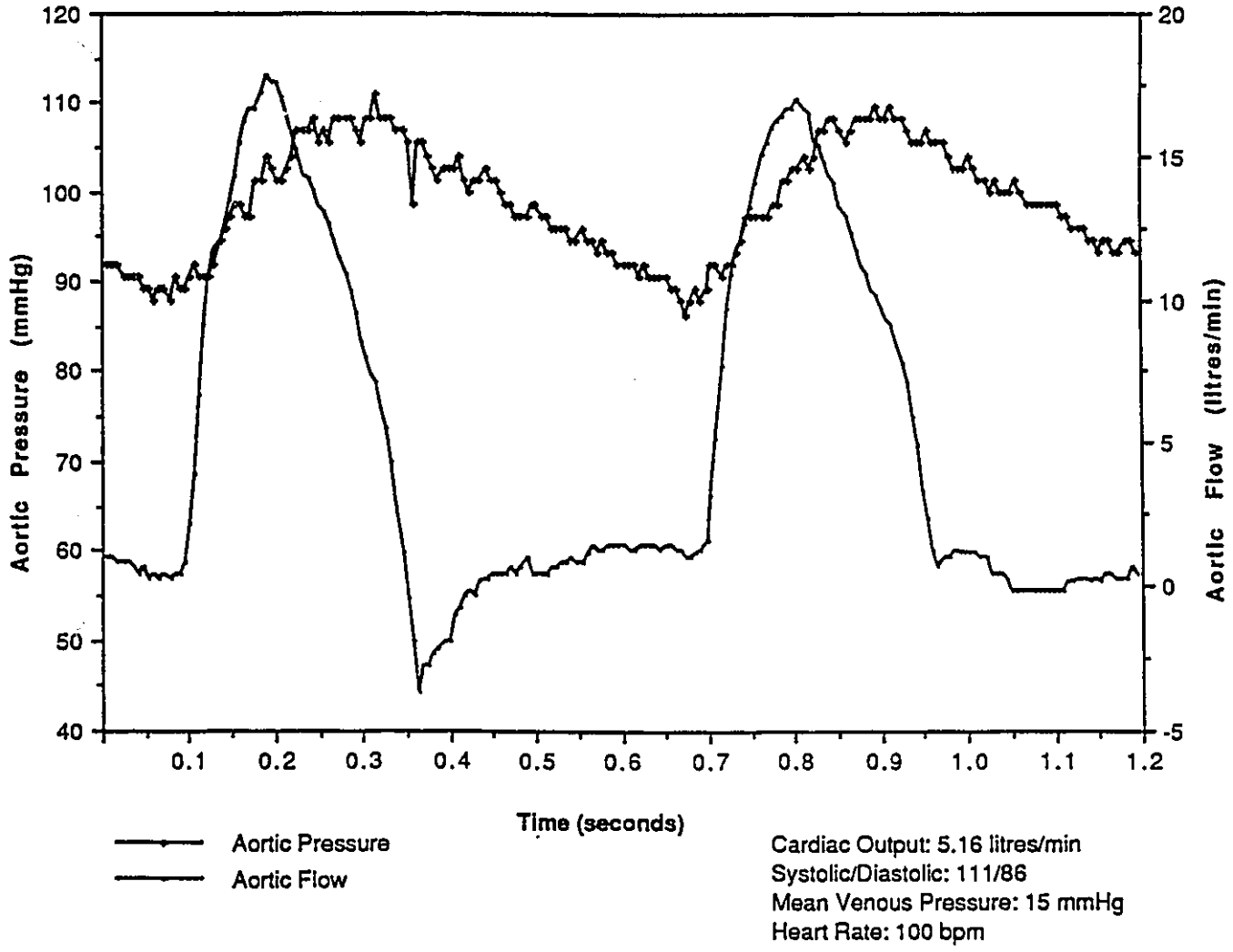

Figure 5.2 - Physiological Pressure and Flow Data

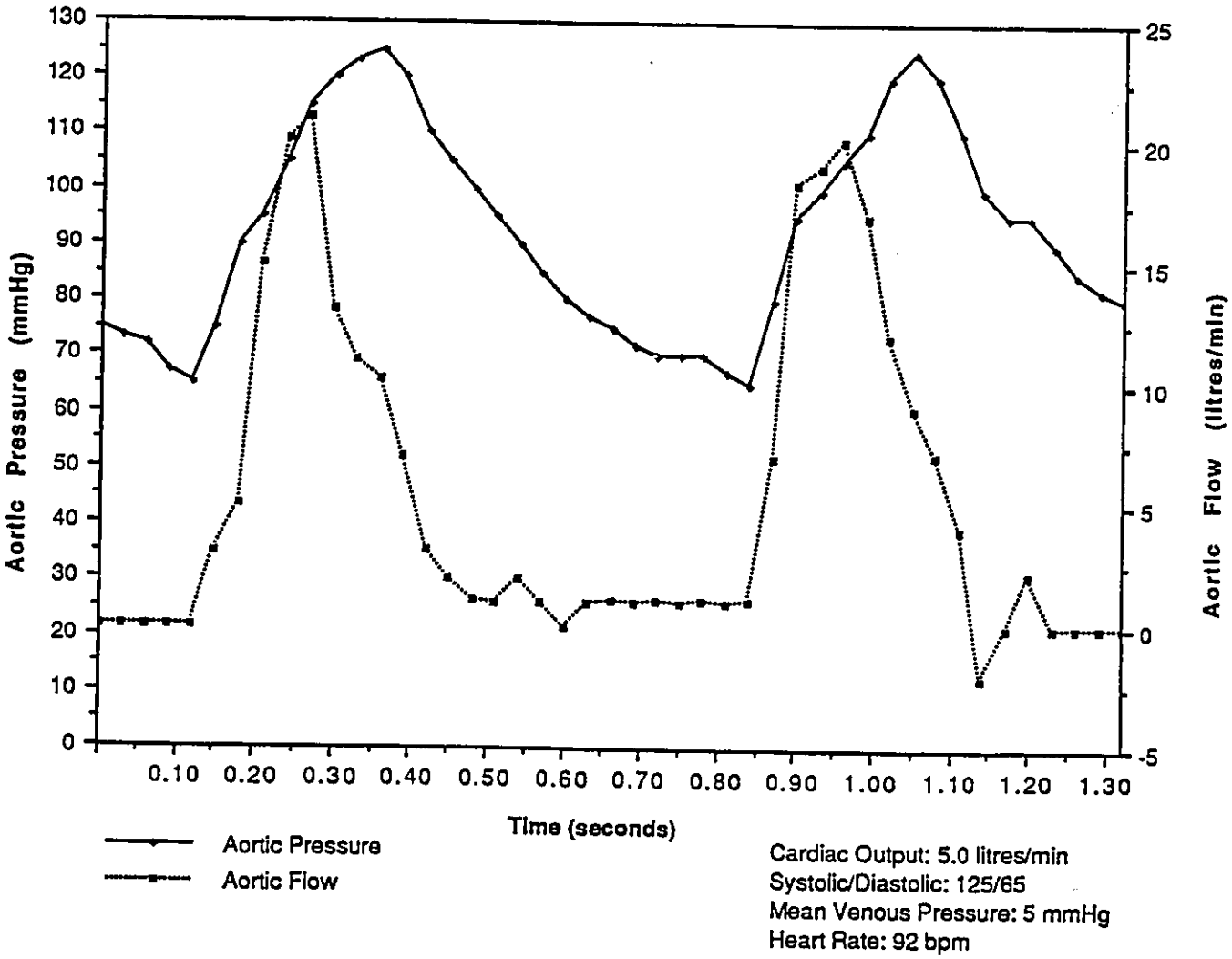

Figure 5.3 - Comparison of MCU Pressure Data to Model Fit Pressure Data

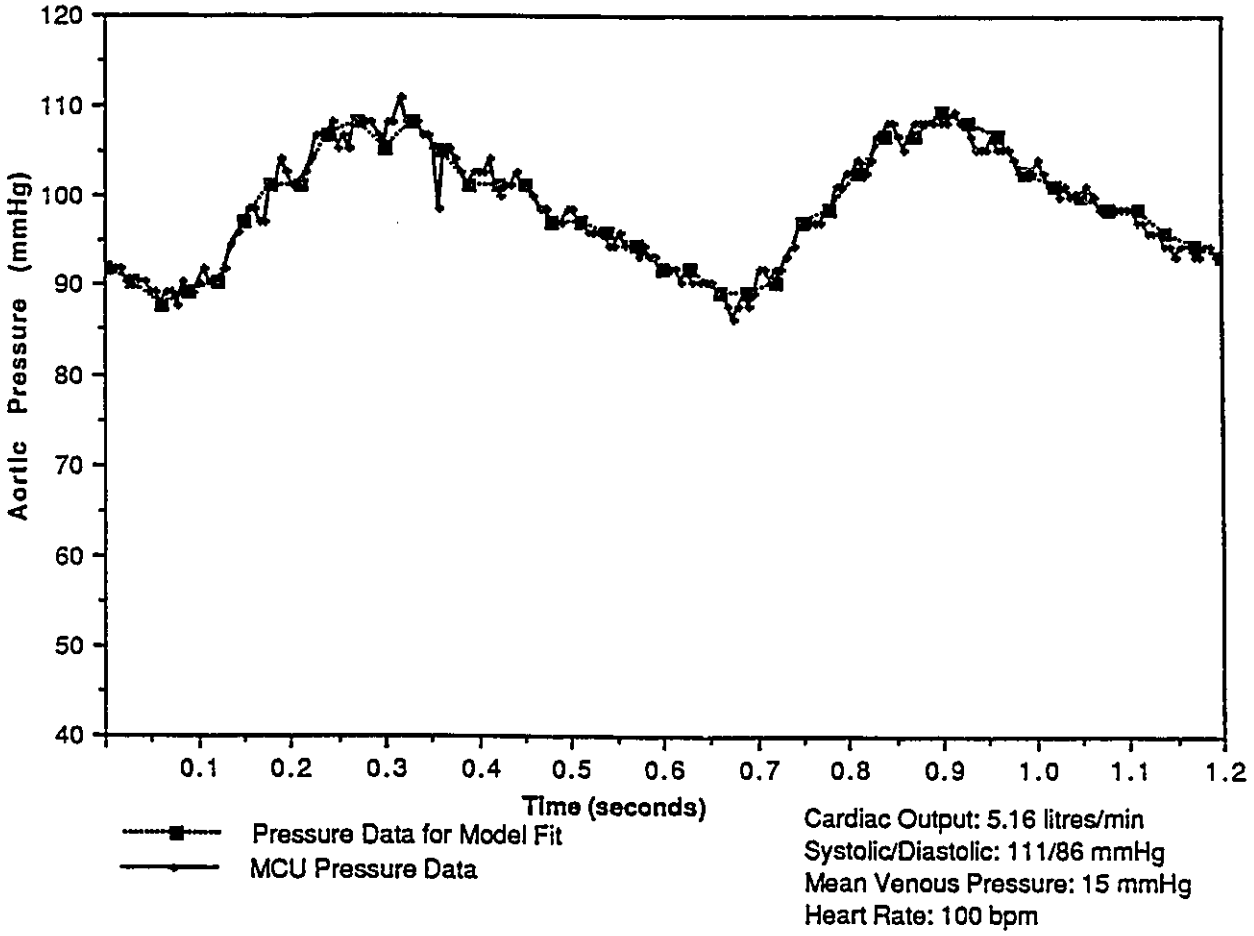

Figure 5.4 - Comparison of MCU Flow Data to Flow Data Input to Model

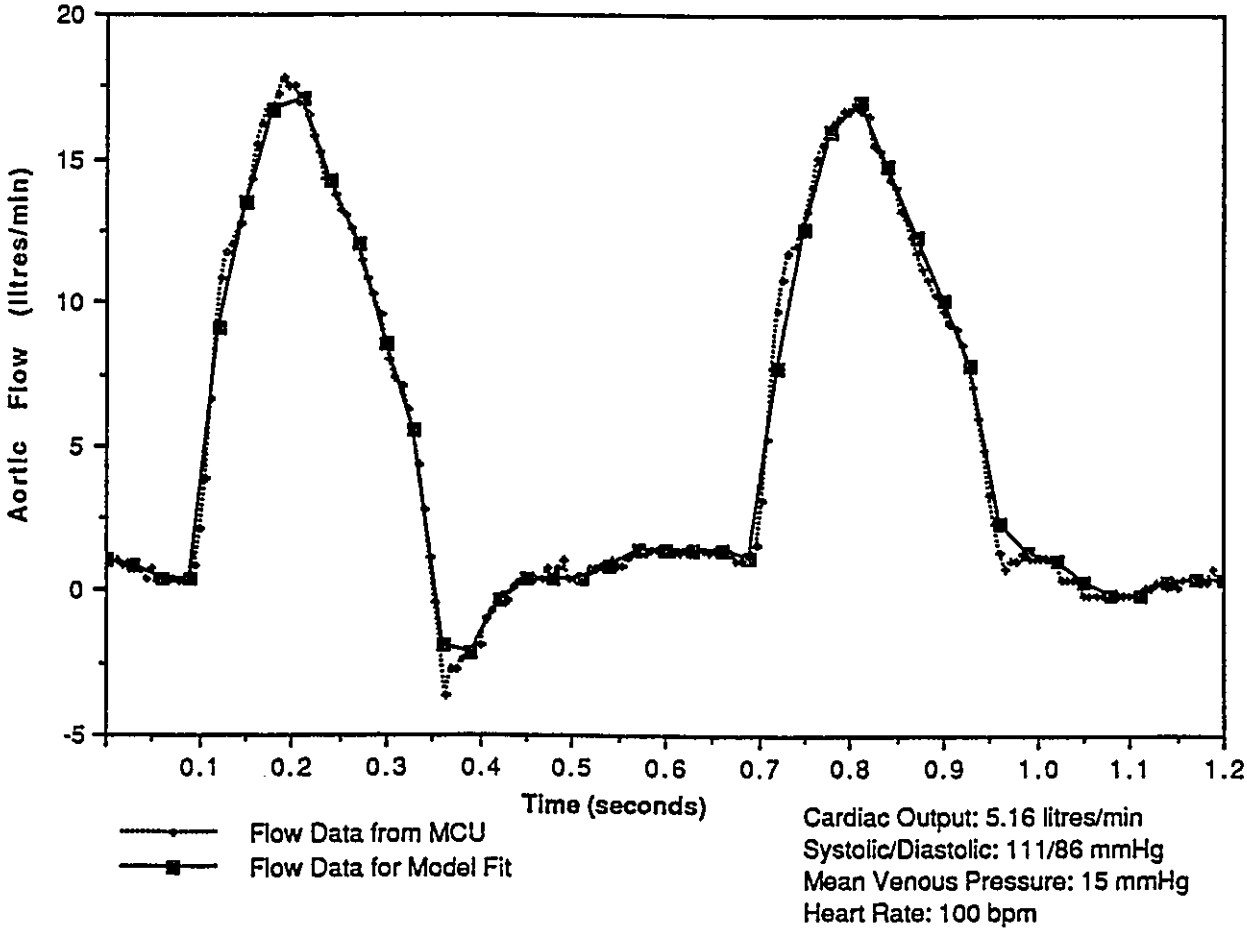

5.2 - Three-Parameter Model Fit

In order to obtain the best parameter estimates, that is, those minimizing the sum of squares of residuals of the expectation function, a Simplex algorithm (32) was used. Initial guesses for the three parameters were obtained from the analog computer estimates of Rosenberg et al, 1981 (2). The Simplex algorithm minimizes the sum of squares of residuals through successive reflections of an equilateral triangle across the sum of squares surface. By calculating $s(\underline{\theta})$, at the three corners of the triangle and comparing their values, a reflection is made where the corner with the greatest $s(\underline{\theta})$ value is reflected across the axis defined by the other two points. A new $s(\underline{\theta})$ is then calculated at the reflected position and again compared to the other two, whereupon a new direction of reflection is decided upon. As a minimum is approached the magnitude of the reflection is adjusted in order to ensure that the true minimum $s(\underline{\theta})$ value is determined to an appropriate tolerance level. This method of minimization is advantaged over others by not requiring first derivatives of the sum of squares function with respect to each parameter at each iteration but is disadvantaged by not supplying them. False minima on the sum of squares surface were detected. The global minimum was determined through calculating the sum of squares of residuals over a grid of parameter values and exploring the local minima to obtain a converged value. Local minima were compared to determine the global minima in conjunction with knowledge of the anticipated parameter values. The limits of the parameter values for the grid search were determined by the

values of the parameters which gave a real solution and by realistic parameter values.

After obtaining, least-squares parameter estimates for the data, the Hessian, $H(\hat{\theta})$, was calculated at the minimum using a finite difference algorithm. The selection of step size was important for this numerical procedure in order to obtain the best Hessian approximation. For a specific level of parameter precision, the minimum step size to maintain a positive definite Hessian had to be determined. This was done through an optimization scheme where a step size was chosen and the determinant of the Hessian compared with the determinant of a Hessian at a larger step size. If the determinant of the Hessian became negative, the step size was small for the precision of the parameter estimates. Once the best positive definite Hessian was obtained, the correlation matrix, standard error and marginal 95% confidence region for the parameter estimates could be determined.

The parameter estimates for the physiological data are summarized in Table 5.1 along with the sum of squares value, correlation matrix, standard error, and marginal 95% confidence region for the parameters. Table 5.2 indicates the same for each run of the MCU data. Figure 5.5 compares the MCU pressure data to the pressure predicted by the three-parameter model after the least squares parameter estimates were determined. Figure 5.6 shows the same for the physiological data. Inspection of this graph shows that the predicted pressure appears to be time-shifted to the right compared with the physiological data.

Table 5.1 - Summary of Physiological Data for Three-Parameter Model - Sum of Squares, Parameter Estimates, Correlation Matrices, Pure Error and Marginal 95% Confidence Regions for the Parameter Estimates

Run Number	1
Sum of Squares	1.67×10^{3}
Variance Estimate	39.8
Parameter Estimates	
Resistance	1.08×10^{3}
Compliance	6.47×10^{-4}
Inertance	3.06×10^{-3}
Correlation Matrix	
Resistance	1.0
Compliance	.65 1.0
Inertance	.94 .71 1.0
Degrees of Freedom	42
Standard Error	
Resistance	114.
Compliance	1.63×10^{-4}
Inertance	24.4
95% Marginal Confidence	
Resistance	±230.
Compliance	$\pm 3.29 \times 10^{-4}$
Inertance	±49.3

Units:

$$\text{Resistance} = \frac{\text{mmHg s}}{\text{litres}} \qquad \text{Compliance} = \frac{\text{litres}}{\text{mmHg}} \qquad \text{Inertance} = \frac{\text{mmHg s}^2}{\text{litres}}$$

Table 5.2 - Summary of MCU Data for Three-Parameter Model- Sum of Squares, Parameter Estimates, Correlation Matrices, Pure Error and Marginal 95% Confidence Regions for the Parameters

Run Number	0	1	2	3
Sum of Squares	91.8	36.6	125.	194.
Variance Estimate	2.42	2.15	6.94	10.8
Parameter Estimates				
Resistance	9.70×10^{2}	1.07×10^{3}	1.26×10^{3}	1.30×10^{3}
Compliance	1.59×10^{-3}	1.84×10^{-3}	1.96×10^{-3}	3.94×10^{-3}
Inertance	2.80×10^{-2}	2.31×10^{-2}	2.29×10^{-2}	2.71×10^{-2}
Correlation Matrix				
Resistance	1.0	1.0	1.0	1.0
Compliance	.19 1.0	.16 1.0	-.61 1.0	.19 1.0
Inertance	.35 .73 1.0	.32 .57 1.0	-.80 .78 1.0	.44 .29 1.0
Degrees of Freedom	38	18	18	18
Standard Error				
Resistance	9.92	9.67	32.3	42.6
Compliance	3.24×10^{-4}	2.82×10^{-4}	7.32×10^{-4}	9.62×10^{-4}
Inertance	32.6	15.4	54.7	68.4
95% Marginal Confidence				
Resistance	±20.0	±20.4	±67.9	±89.5
Compliance	$\pm 6.54 \times 10^{-4}$	$\pm 5.95 \times 10^{-4}$	$\pm 1.93 \times 10^{-4}$	$\pm 2.02 \times 10^{-3}$
Inertance	±65.8	±32.5	±115.	±144.

Units:

$$\text{Resistance} = \frac{\text{mmHg s}}{\text{litres}} \qquad \text{Compliance} = \frac{\text{litres}}{\text{mmHg}} \qquad \text{Inertance} = \frac{\text{mmHg s}^2}{\text{litres}}$$

Figure 5.5 - Comparison of MCU Pressure Data to Pressure Predicted by Model

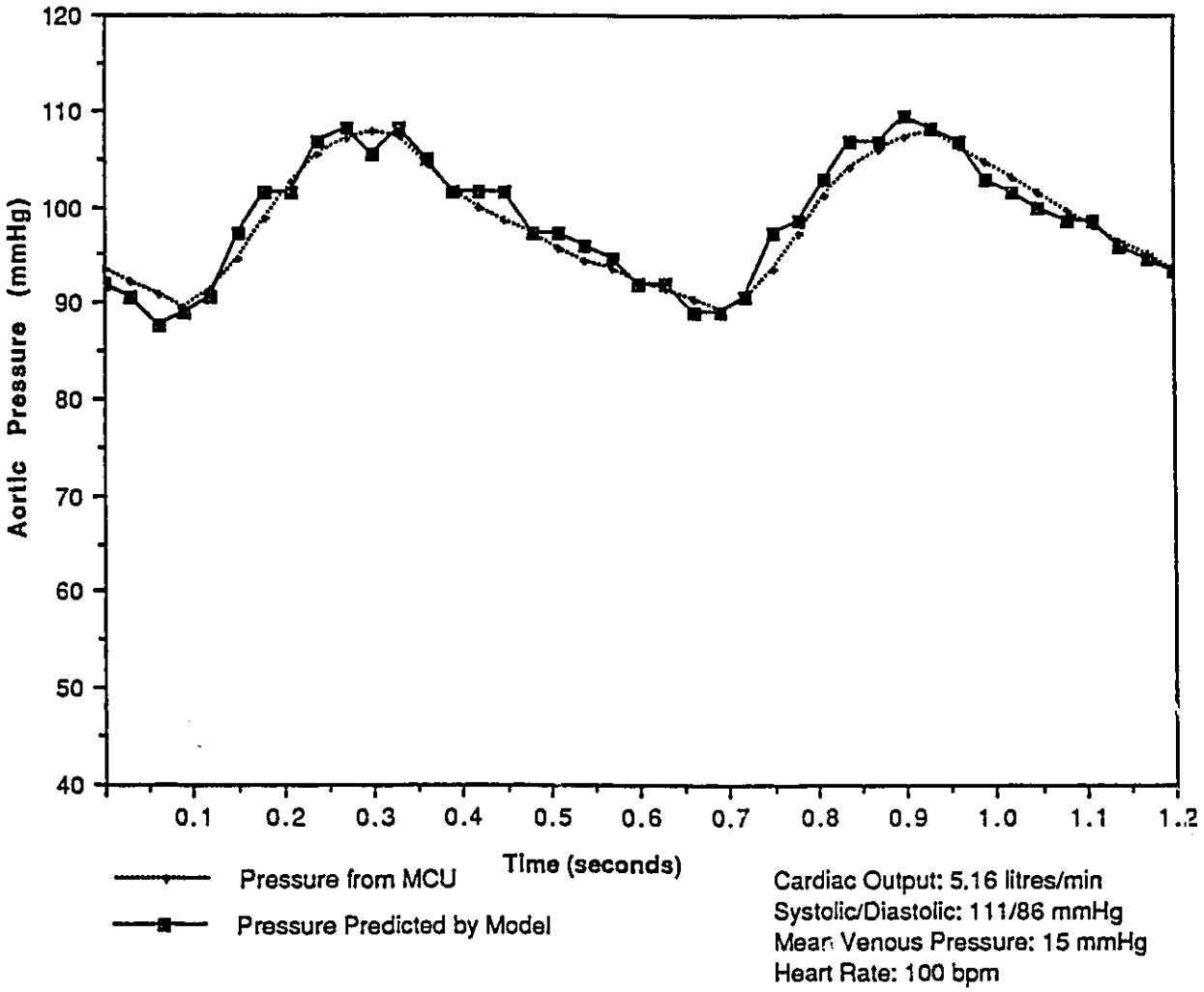

Figure 5.6 - Comparison of Physiological Pressure Data to Pressure Predicted by Model

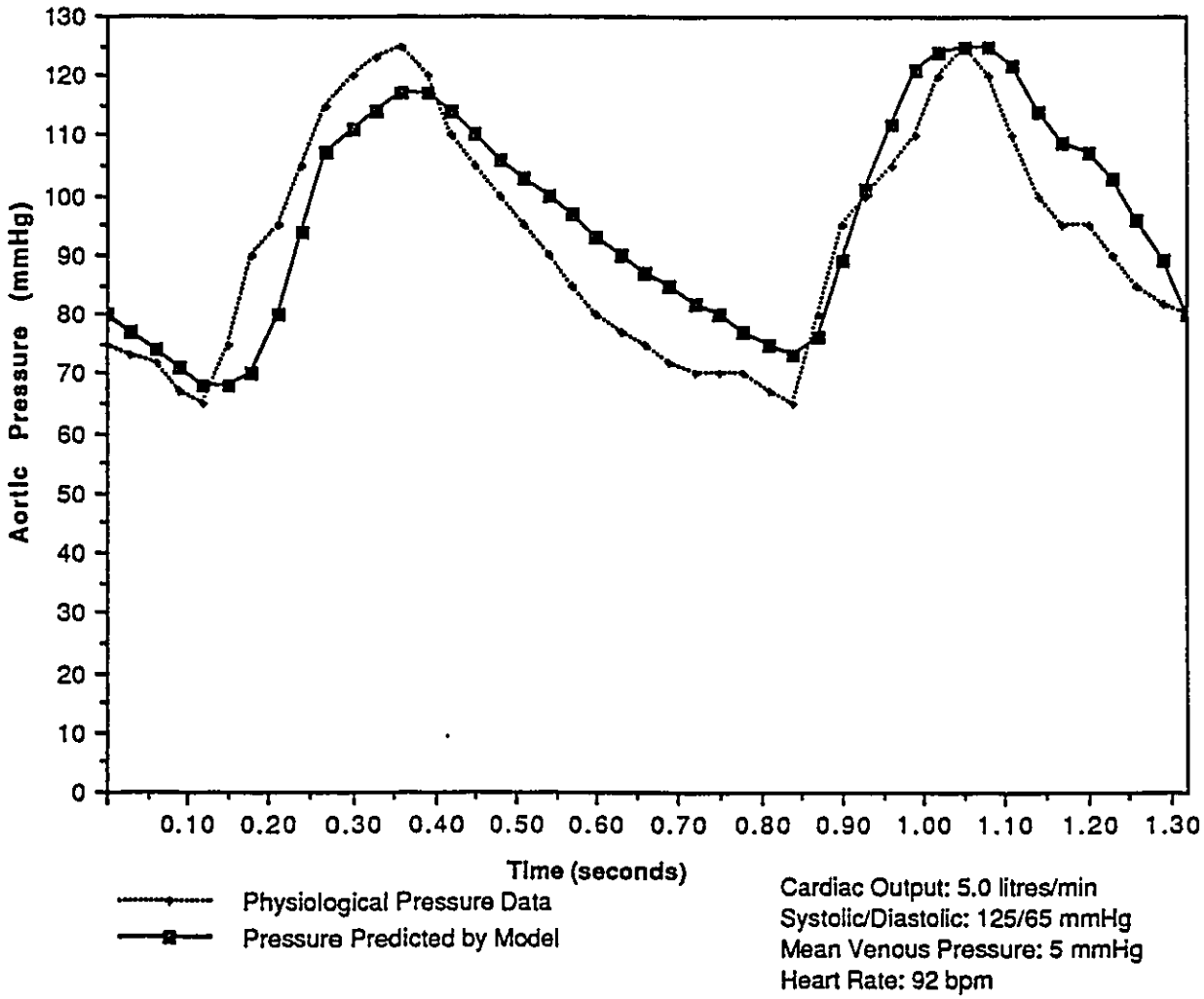

Table 5.7 compares parameters from the literature, estimates from the ideal fluid equations and the estimates derived from the MCU data.

5.3 - Tests for Adequacy of the Three-Parameter Model

Model adequacy or lack-of-fit tests can be performed through both qualitative and quantitative analysis. Qualititative lack-of-fit can be examined through examination of residual plots. Figure 5.7 shows residuals plotted against time for run zero of the MCU data. Examination of this plot indicates a random scatter of residuals around the expected value zero and shows that no time trends are apparent. Figure 5.8 shows residuals plotted against response and again indicates random scatter around the expected value of zero. Figure 5.9 shows residuals at time u plotted against residuals at time u-1. This plot, indicates that a correlation exists between successive residuals. This observation is in direct violation of assumption four for fitting of data via least squares as outlined in section 2.3.1. This trend suggests that the model must be modified to account for this correlation.

Quantitative lack-of-fit tests can provide useful information to the non-linear model and are performed when replicates are available from the data. This is achieved through comparing the pure error of the residuals with the error associated with model inadequacy with the appropriate number of degrees of freedom for each estimate. Table 5.3 shows a summary of the quantitative lack-of-fit tests for the three-parameter model with the summary of calculations shown in Appendix D.

Figure 5.7 - Residuals versus Time for Three-Parameter Model

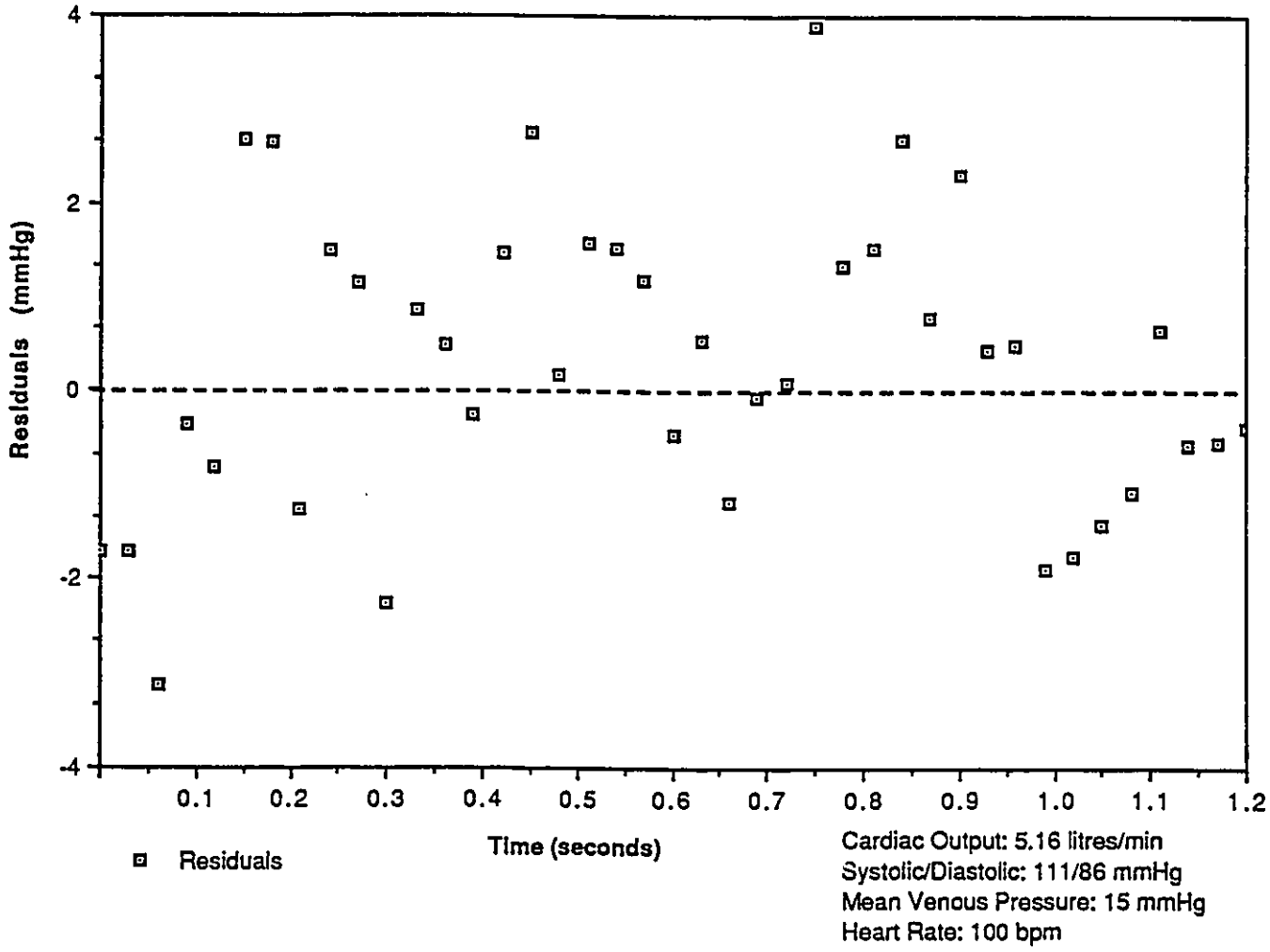

Figure 5.8 - Residuals versus Response for Three-Parameter Model

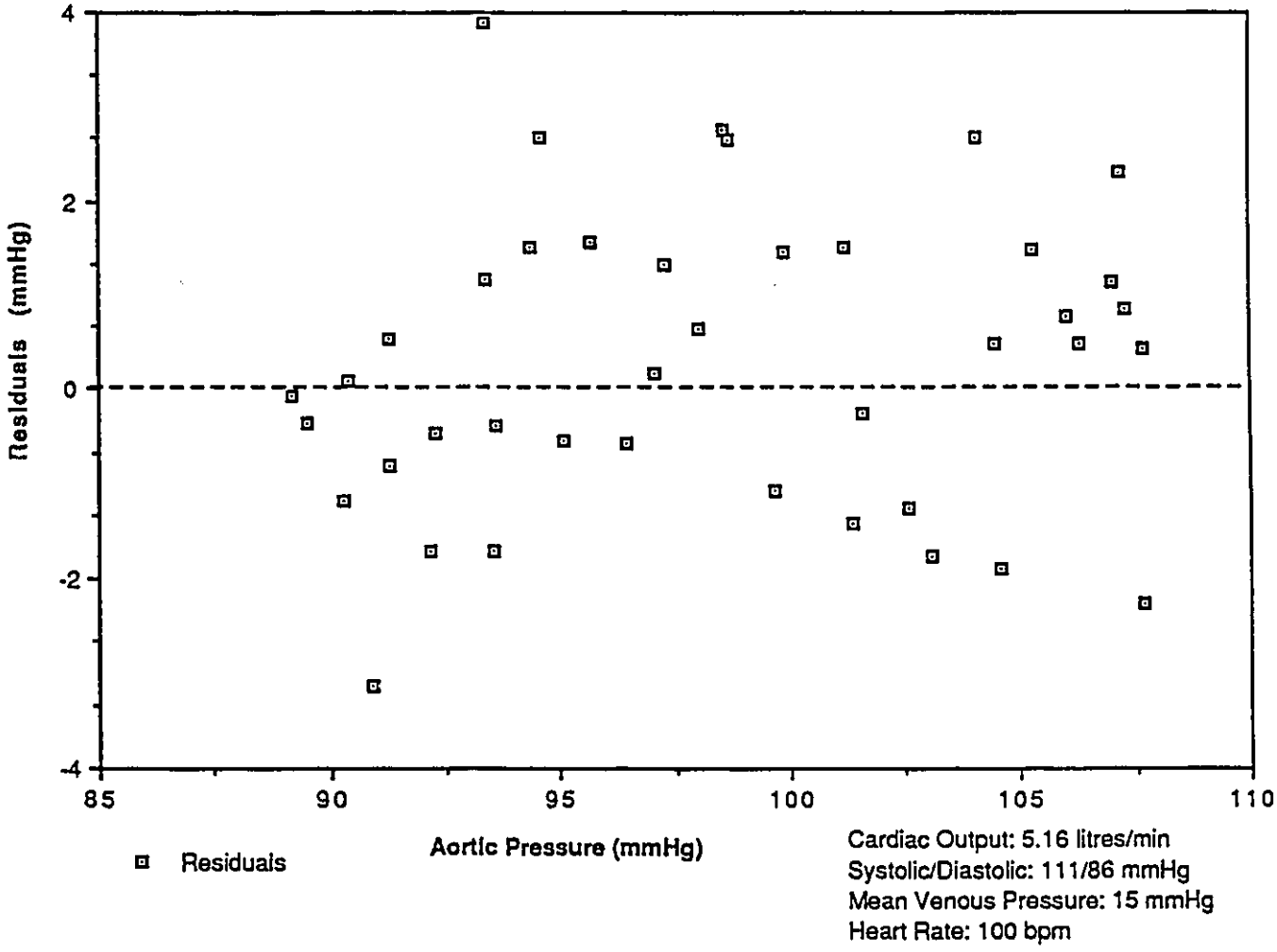

Figure 5.9 - Residuals at Time u versus Residuals at Time u-1 for Three-Parameter Model

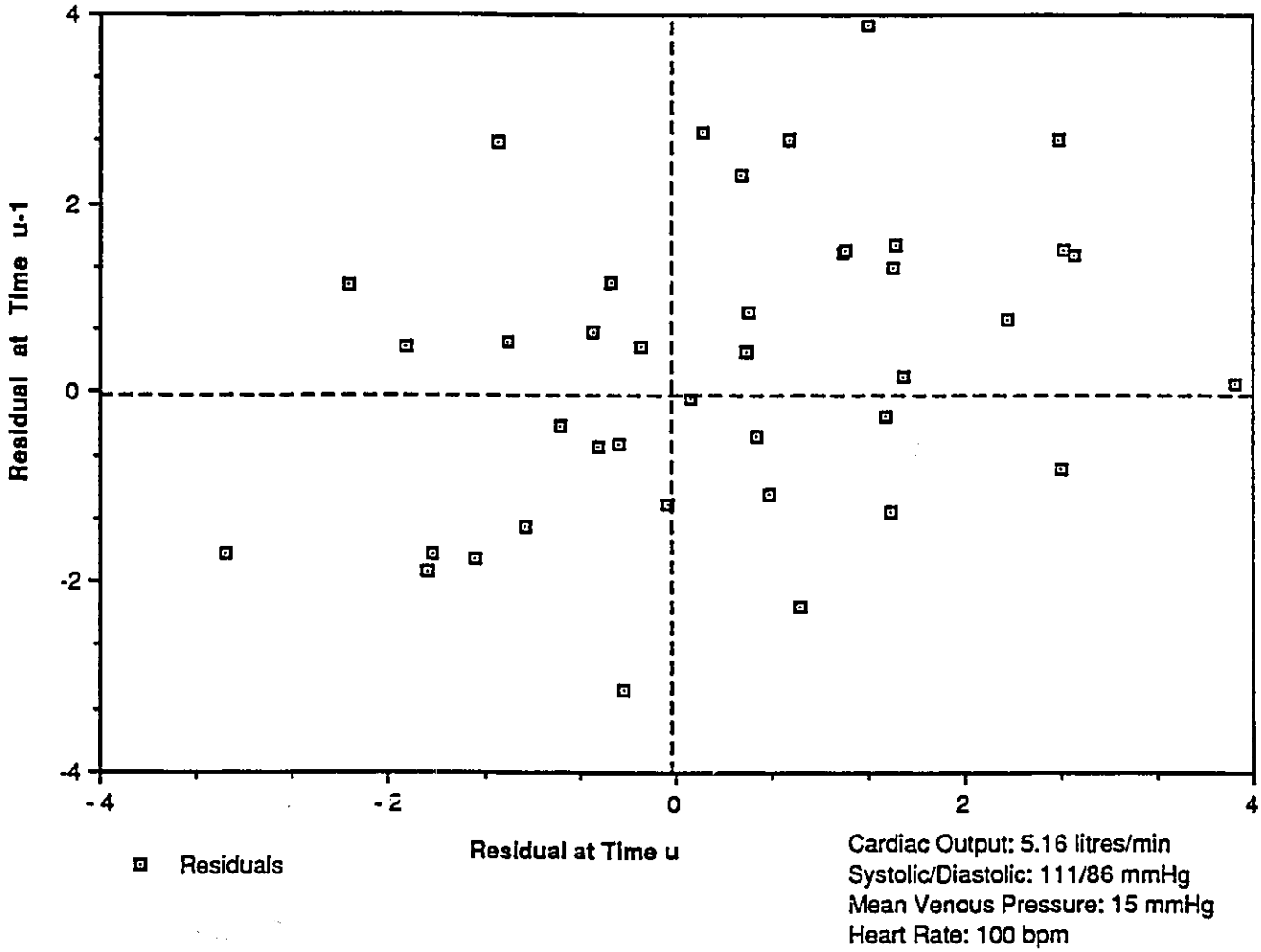

True replicates were not available from the data as a result of the complex relationship between the independent and dependent variables and the parameters and the difficulty in setting operating conditions to precisely the same settings in subsequent runs. However, approximate replicates exist by using information from the other data runs. Runs zero through three were considered to be similar enough to obtain an estimate of pure error variance (Figure 5.10). An approximation of pure error variance was obtained by averaging the pure error associated with the replicate data obtained at a specific time of the cardiac cycle across the entire cycle. Thus, at a specific time, there are four predicted pressure responses from which an estimate of pure error variance can be obtained for that specific time. The nature of the non-linear model is such that the variance of the response is proportional to the slope of the expectation function resulting in a different value of the response variance at different positions. If the pure error variance across the cardiac cycle does not change extensively, the pure error variance at each specific time can be averaged to provide a pooled estimate of variance for the four runs. Table 5.3 indicates that the lack-of-fit due to model inadequacy was significantly less than lack-of-fit due to experimental error.

5.4 - Autocorrelation and a Moving Average Model

As Figure 5.9 indicates that a correlation exists between residuals, the nature of the model suggests that the correlation could be explained through time series analysis.

Figure 5.10 - Approximate Replicates for Lack-of-Fit Test

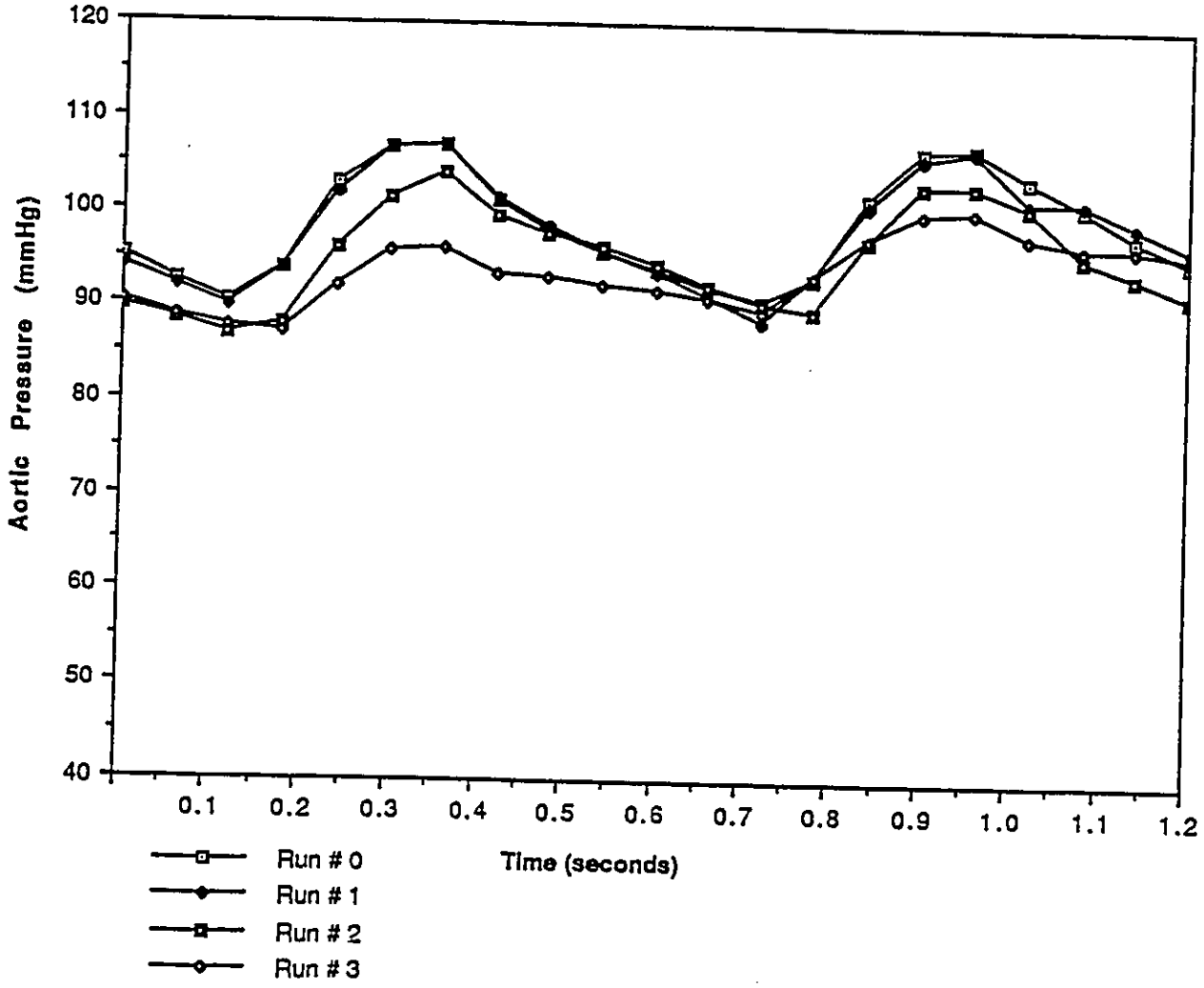

Table 5.3 - Summary of Quantitative Lack-of-Fit Tests for Three-Parameter Model

(See Appendix D for calculation procedure)

Replication Sum of Squares	8.79
Degrees of Freedom (ν_1)	35
lack-of-fit Sum of Squares	65.2
Degrees of Freedcm (ν_2)	3
Test Ratio	.21
$F(\nu_1, \nu_2; \gamma)$ γ=0.05	8.57
Significant lack-of-fit	No

Calculation of the autocorrelation function indicates whether the correlation between residuals at a specific lag is significant. The autocorrelation function versus lag for the three-parameter model is shown in Figure 5.11. The dotted lines indicate an interval in which 95% of the correlations would be expected to lie if the true correlation was zero. Examination of this plot indicates that at a lag of one, the correlation lies outside the expected region indicating a significant correlation between successive residuals. The autocorrelation function at lags greater than one lie within the expected region indicating no significant correlation between those residuals.

A moving average process of order one was implemented in an attempt to improve parameter estimates, reduce the sum of squares of residuals, the pure error and marginal confidence intervals for the parameter estimates as well as eliminating the correlation between successive residuals. The moving average model introduces an additional parameter, γ, which is a weight applied to the previously calculated residual according to,

$$Y_n = f(\underline{x}_n,\underline{\theta}) + \omega\varepsilon_{n-1} + \varepsilon_n \qquad (5.1)$$

where ε is the residual calculated as,

$$\varepsilon_n = Y_n - f(\underline{x}_n,\underline{\theta}) \qquad (5.2)$$

This moving average model was fitted. The sum of squares, parameter estimates, correlation matrix, pure error and marginal confidence regions of the parameter estimates for the physiological data are indicated in Table 5.4. Table 5.5 indicates the same summary for the MCU data.

Figure 5.11 - Autocorrelation Function versus Lag for Three-Parameter Model

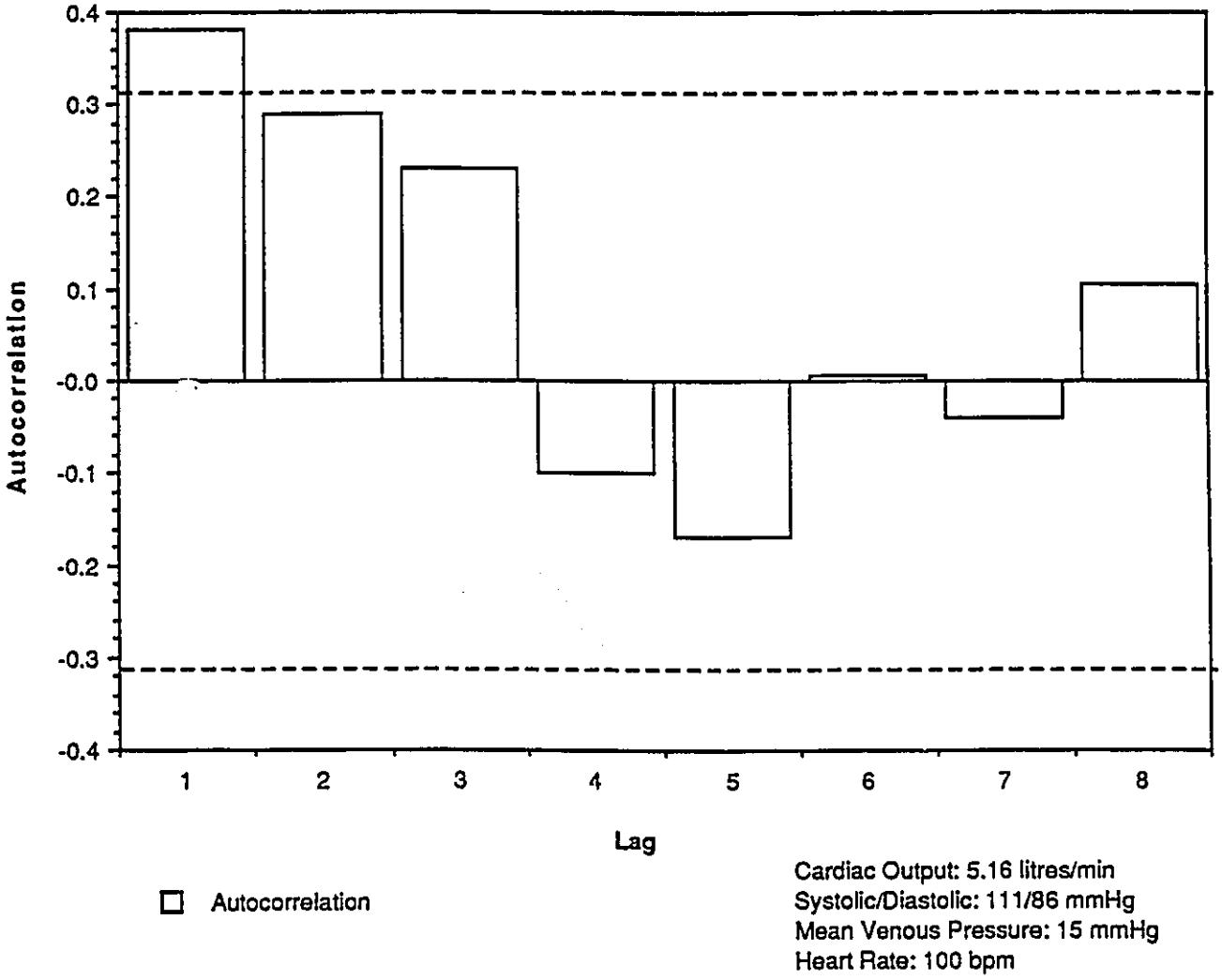

Table 5.4 - Summary of Physiological Data for Moving Average Model - Sum of Squares, Parameter Estimates, Correlation Matrices, Pure Error and Marginal 95% Confidence Regions for the Parameters

Run Number	1
Sum of Squares	919
Variance Estimate	21.9
Parameter Estimates	
Resistance	1.07×10^{3}
Compliance	6.47×10^{-4}
Inertance	4.49×10^{-3}
Fit Parameter	-.63
Correlation Matrix	
Resistance	1.0
Compliance	.28 1.0
Inertance	.86 .41 1.0
Fit Parameter	-.49 -.27 ..24 1.0
Degrees of Freedom	41
Standard Error	
Resistance	91.1
Compliance	1.60×10^{-4}
Inertance	19.7
Fit Parameter	.27
95% Marginal Confidence	
Resistance	±184.
Compliance	$\pm 3.23 \times 10^{-4}$
Inertance	±39.8
Fit Parameter	±.54

Units:

$$\text{Resistance} = \frac{\text{mmHg s}}{\text{litres}} \qquad \text{Compliance} = \frac{\text{litres}}{\text{mmHg}} \qquad \text{Inertance} = \frac{\text{mmHg s}^2}{\text{litres}}$$

Table 5.5 - Summary of MCU Data for Moving Average Model - Sum of Squares, Parameter Estimates, Correlation Matrices, Pure Error and Marginal 95% Confidence Regions for the Parameters

Run Number	0	1	2	3
Sum of Squares	90.0	36.2	88.8	124.
Variance Estimate	2.43	2.12	5.22	7.33
Parameter Estimates				
Resistance	9.70×10^{2}	1.07×10^{3}	1.26×10^{3}	1.30×10^{3}
Compliance	1.58×10^{-3}	1.85×10^{-3}	1.94×10^{-3}	3.87×10^{-3}
Inertance	2.90×10^{-2}	2.34×10^{-2}	5.60×10^{-2}	3.91×10^{-2}
Fit	-.10	-.12	-.53	-.60
Correlation Matrix				
Resistance	1.0	1.0	1.0	1.0
Compliance	.21 1.0	-.55 1.0	-.581.0	.78 1.0
Inertance	.36 .00 1.0	-.64 .88 1.0	.32 .78 1.0	.52 -.32 1.0
Fit	-.13 -.31 -.44 1.0	.43 .58 .65 1.0	-.14-.37 .34 1.0	.18 .74 -.42 1.0
Degrees of Freedom	37	17	17	17
Standard Error				
Resistance	10.9	13.3	25.3	34.2
Compliance	3.68×10^{-4}	5.31×10^{-4}	4.32×10^{-4}	6.27×10^{-4}
Inertance	38.4	42.4	42.7	59.9
Fit	.37	.68	.79	.94
95% Marginal Confidence				
Resistance	±21.9	±26.9	±53.15	±71.85
Compliance	$\pm 7.43 \times 10^{-4}$	$\pm 1.07 \times 10^{-3}$	$\pm 9.07 \times 10^{-4}$	$\pm 1.32 \times 10^{-3}$
Inertance	±77.6	±85.7	±89.7	±126.
Fit	±.75	±1.37	±1.65	±1.97

Units:

$$\text{Resistance} = \frac{\text{mmHg s}}{\text{litres}} \qquad \text{Compliance} = \frac{\text{litres}}{\text{mmHg}} \qquad \text{Inertance} = \frac{\text{mmHg s}^2}{\text{litres}}$$

Figure 5.12 compares the MCU pressure data with the pressure predicted by the moving average model. Figure 5.13 indicates the same for the physiological data. Examination of Figure 5.12, Figure 5.13 and Tables 5.4 and 5.5 indicate an improved fit over the three-parameter model. This is shown by an acceptable correlation matrix, reduced standard error and improved marginal 95% confidence regions for the parameter estimates. A lack-of-fit analysis is summarized in Table 5.6. Residual plots for the MCU data are shown in Figures 5.14, 5.15 and 5.16 as residuals versus time, residuals versus response and residuals at time u versus residuals at time u-1, respectively. In all three of these plots, no suspicious trends were observed indicating that the correlation between residuals observed in the three-parameter model is eliminated with the addition of the weighting parameter.

The autocorrelation function for the moving average model is shown in Figure 5.17. This plot shows that all the correlations lie within the band where 95% of the correlations would be expected to lie if the true correlation were zero.

The moving average model was deemed a better fit as determined by the qualitative analysis and the autocorrelation function.

Figure 5.12 - Comparison of MCU Pressure Data to Pressure Predicted by Moving Average Model

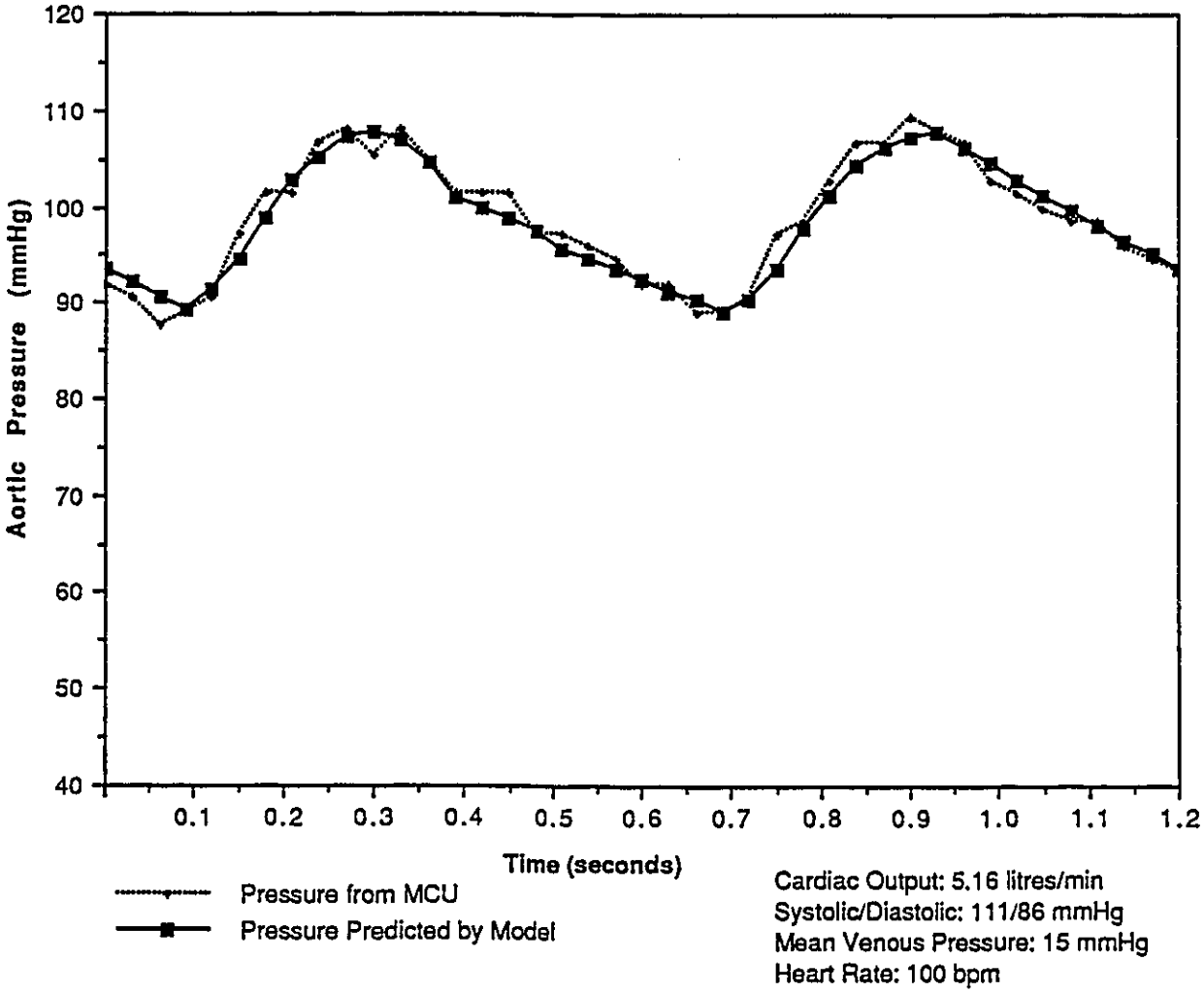

Figure 5.13 - Comparison of Physiological Pressure Data to Pressure Predicted by Moving Average Model

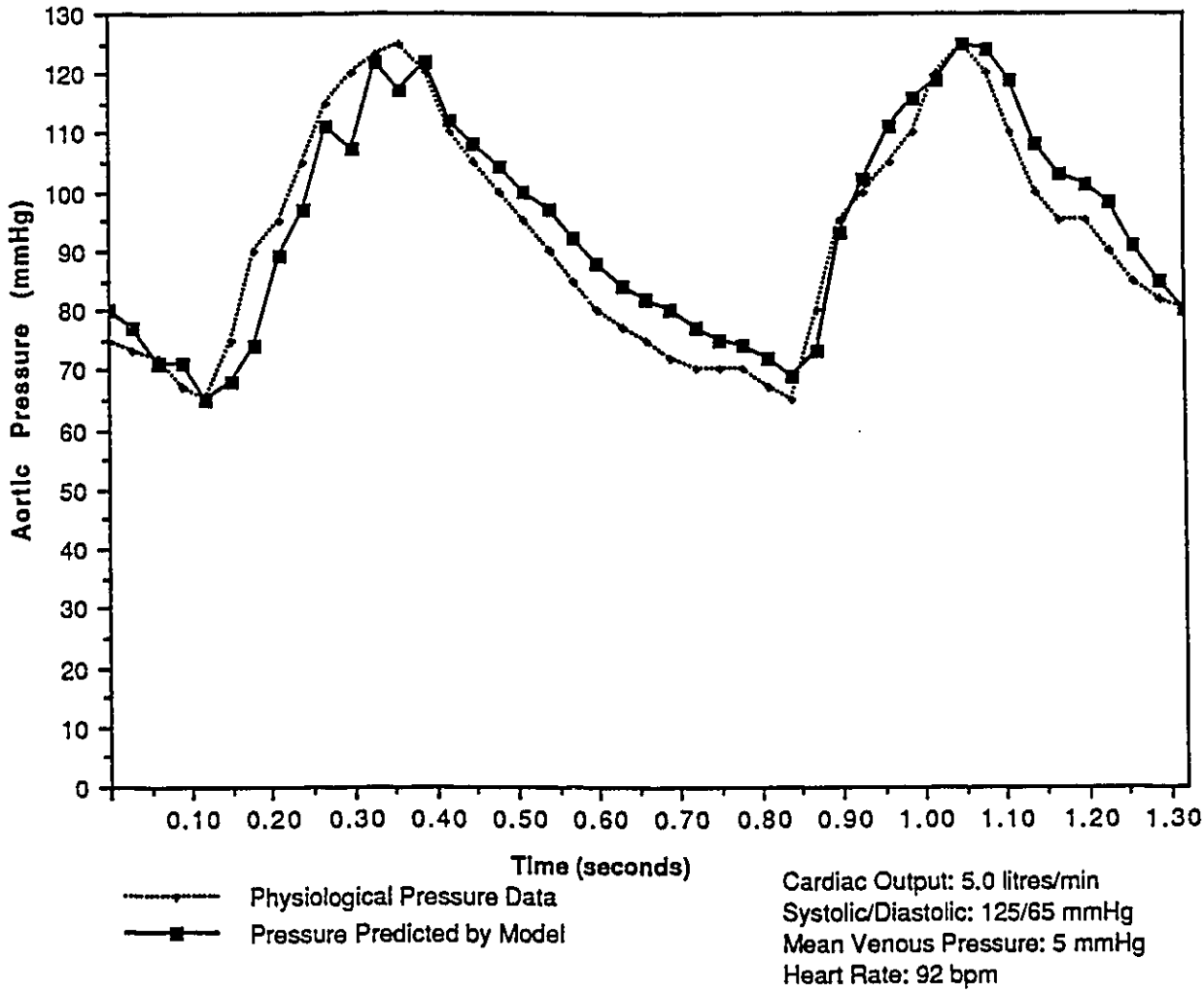

Table 5.6 - Summary of Quantitative Lack-of-Fit Tests for Moving Average Model

(See Appendix D for calculation procedure)

Replication Sum of Squares	8.81
Degrees of Freedom (v_1)	34
Lack-of-fit Sum of Squares	65.6
Degrees of Freedom (v_2)	3
Test Ratio	.22
$F(v_1, v_2; \gamma)$ $\gamma=0.05$	8.57
Significant lack-of-fit	No

Figure 5.14 - Residuals versus Time for Moving Average Model

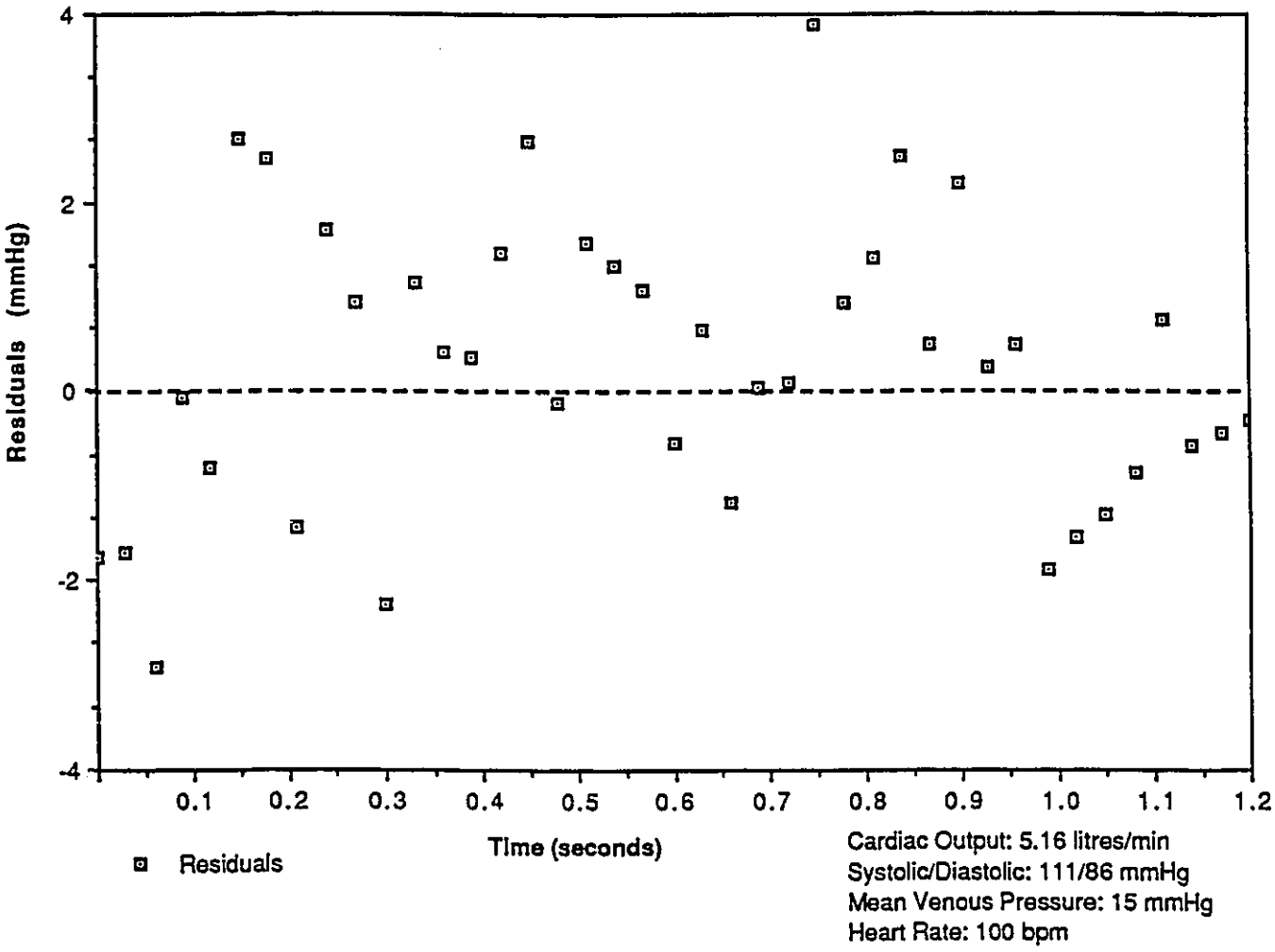

Figure 5.15 - Residuals versus Response for Moving Average Model

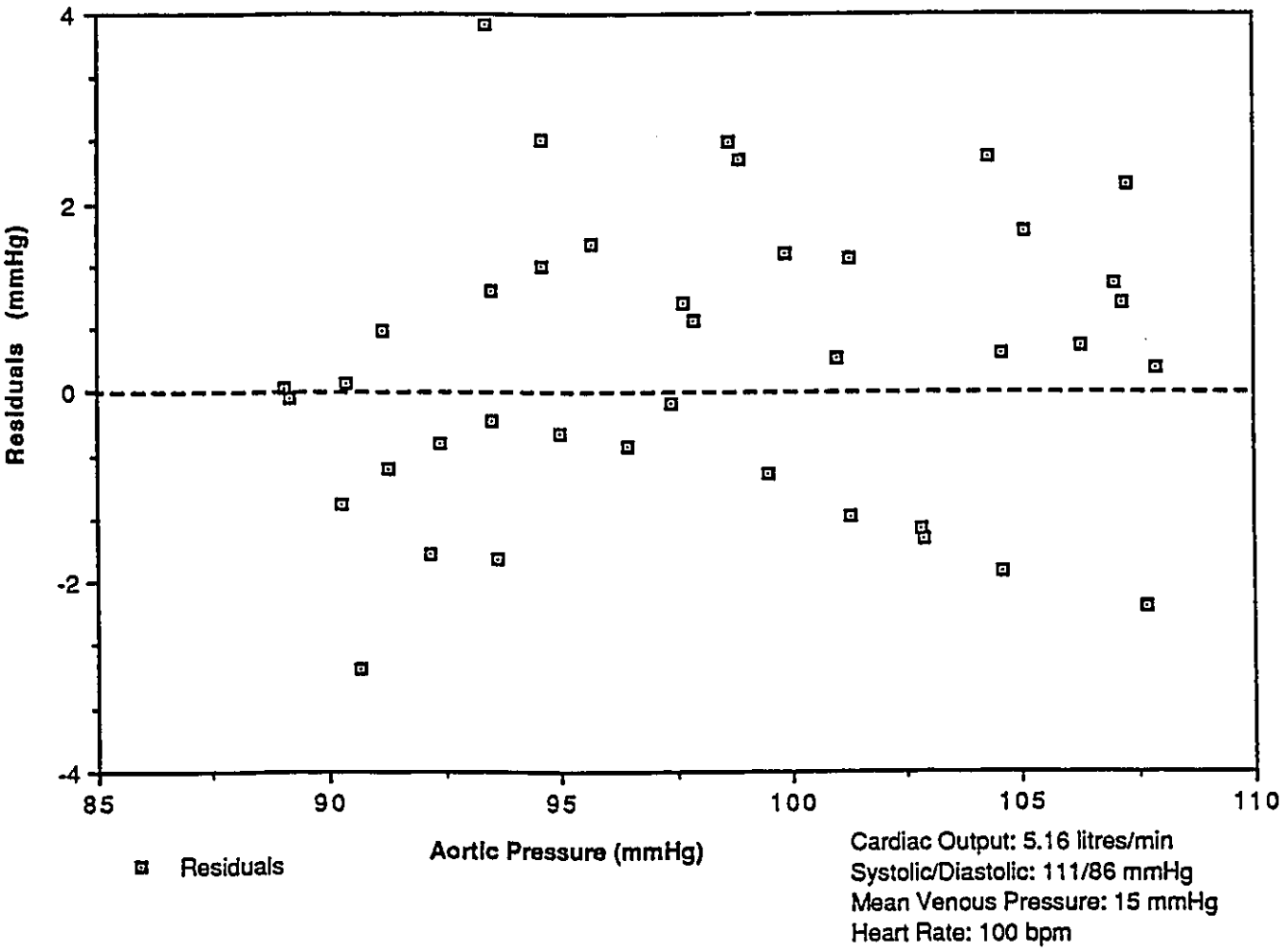

Figure 5.16 - Residuals at Time u versus Residuals at Time u-1 for Moving Average Model

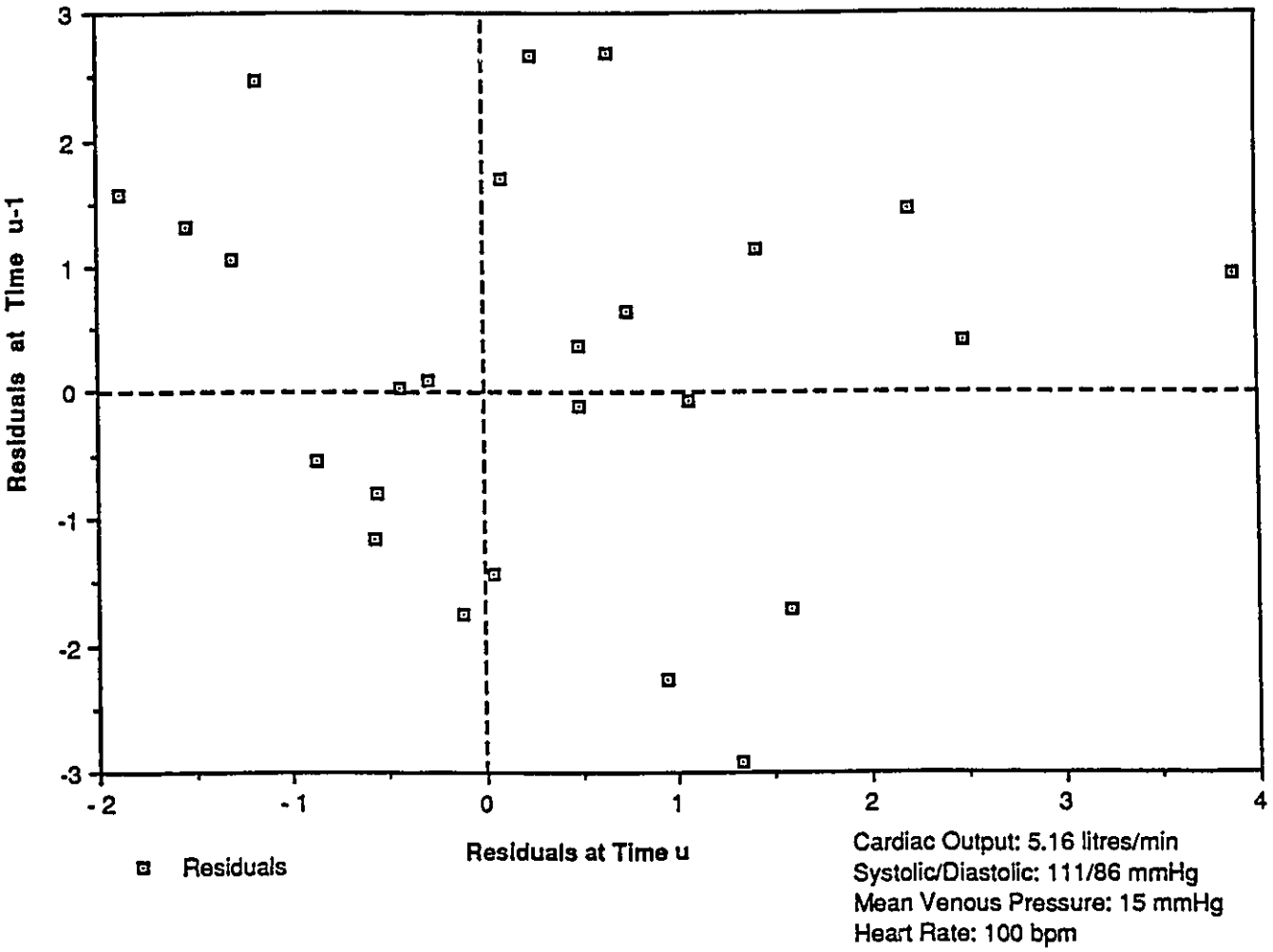

Figure 5.17 - Autocorrelation Function versus Lag for Moving Average Model

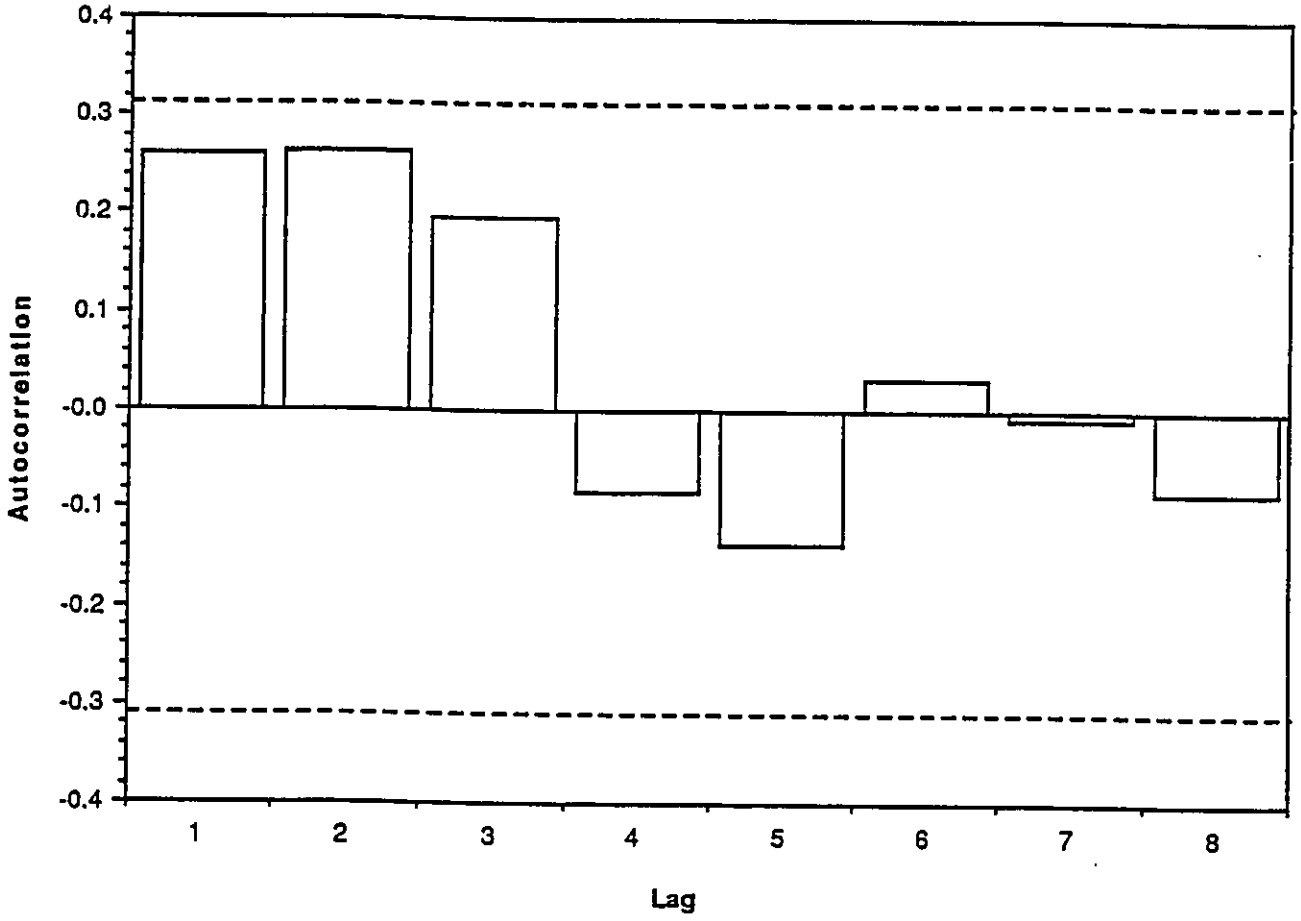

5.5 - Precision of the Predicted Response

The precision of the response is calculated through an approximation of the variance of the response at a particular time. Figure 5.18 indicates the approximate 95% inference band for the response for run zero of the MCU data. Figure 5.19 shows the same for the physiological data.

Figure 5.18 - Precision of the Response for the Moving Average Model for the MCU Data

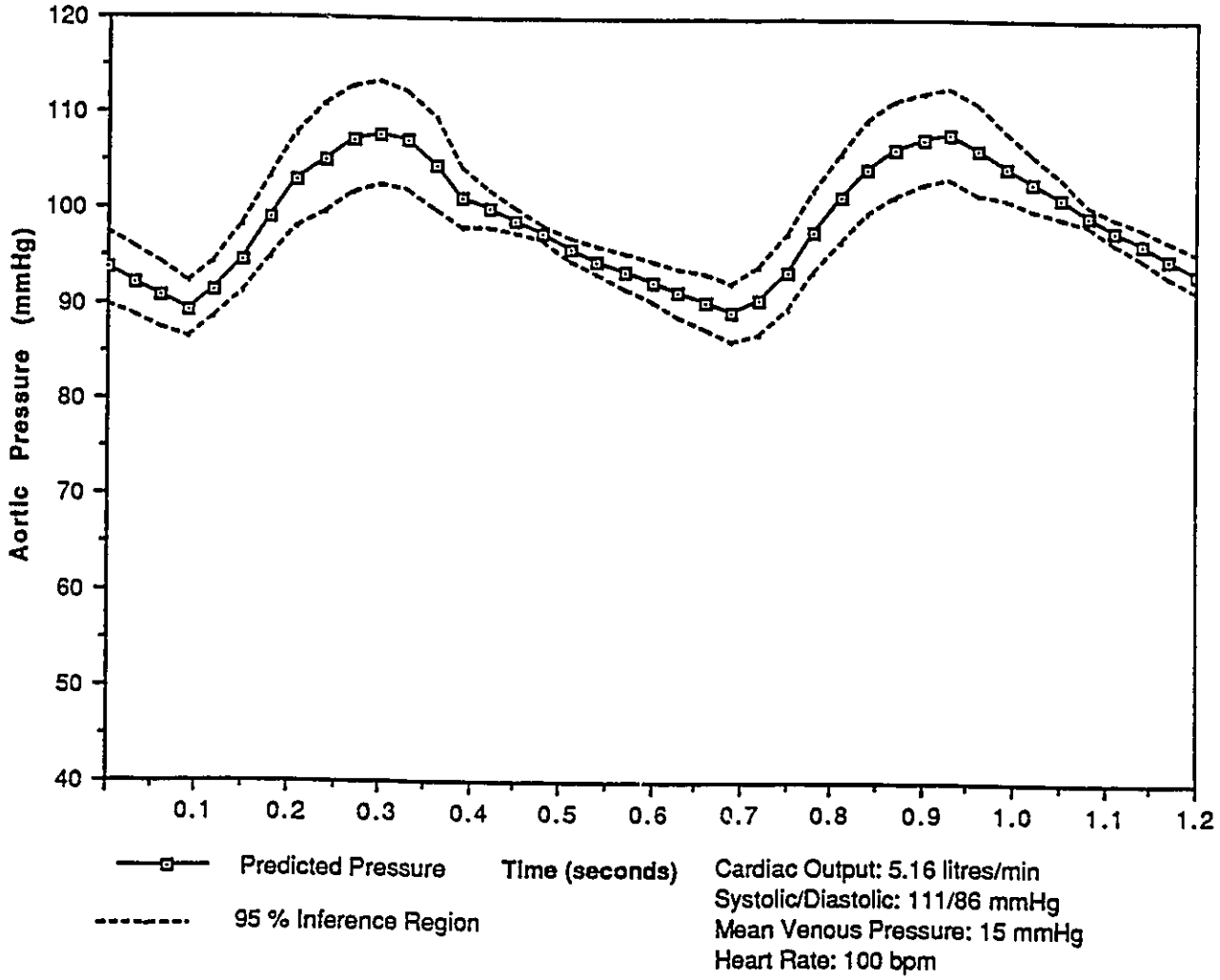

Figure 5.19 - Precision of the Response for the Moving Average Model for the Physiological Data

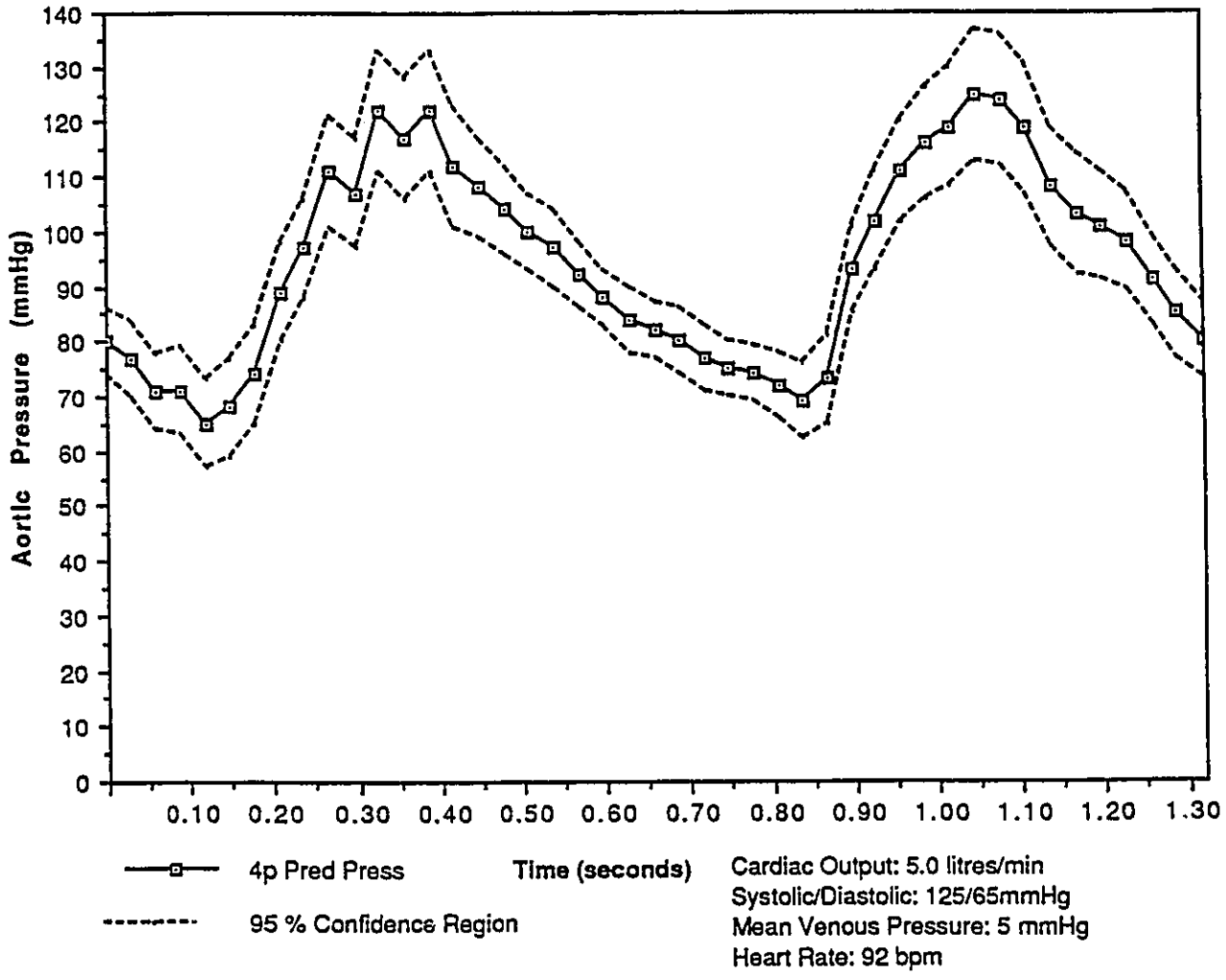

Table 5.7 - Parameters from Literature, Estimates from Ideal Fluid Equations and the MCU Data

Source	Parameter Resistance	Compliance	Inertance
Rosenberg et al (2)	1200.	1.56×10^{-3}	15.75
Sandquist et al (7)	860. (5.8 litres/min)	1.5×10^{-2}	-
	612. (10.1 litres/min)	1.6×10^{-3}	-
Guyton (27)	1200.	1.1×10^{-3}	-
Estimate from Ideal Fluid Equations	1200.	5.0×10^{-3}	1.1×10^{-3}
MCU Run 0	970. ± 21.9	$1.59 \times 10^{-3} \pm 7.43 \times 10^{-4}$	0.029 ± 77.6
MCU Run 1	$1.07 \times 10^{3} \pm 20.4$	$1.84 \times 10^{-3} \pm 5.95 \times 10^{-4}$	$2.31 \times 10^{-2} \pm 32.5$
MCU Run 2	$1.26 \times 10^{3} \pm 67.9$	$1.96 \times 10^{-3} \pm 1.93 \times 10^{-4}$	$2.29 \times 10^{-2} \pm 115.$
MCU Run 3	$1.30 \times 10^{3} \pm 89.5$	$3.94 \times 10^{-3} \pm 2.02 \times 10^{-3}$	$2.71 \times 10^{-2} \pm 144.$

Units:

$$\text{Resistance} = \frac{\text{mmHg s}}{\text{litres}} \qquad \text{Compliance} = \frac{\text{litres}}{\text{mmHg}} \qquad \text{Inertance} = \frac{\text{mmHg s}^2}{\text{litres}}$$

Notes:

(i) The values shown in this table for parameter estimates have been converted from their quoted units in the literature to the units indicated for ease of comparison.

(ii) The values of the parameters (unless otherwise indicated) are for an approximate cardiac output of 5 litres/min, a mean venous pressure of 5 mmHg and a mean arterial pressure of 100 mmHg.

6 - DISCUSSION OF RESULTS AND CONCLUSIONS

Results from the analysis of the moving average model of the human circulation indicate that both the Donovan mock circulation unit and human circulatory system are well described by this model. The model describes the Donovan mock circulation unit in terms of the independent variables of inflow pressure, cardiac cycle time and aortic flow, the parameters of systemic resistance, arterial compliance and venous inertance and the response variable, aortic pressure. In its mechanistic form, the model is represented by three parameters while the moving average model introduces an empirical fit parameter. The solution to the model using discontinuous line segments to approximate the complex aortic flow profile provides an effective means of introducing the instantaneous flow pattern of the aorta into the model.

Using non-linear least squares, the three-parameter model was fit to physiological aortic pressure and flow data and to data from the Donovan MCU. Parameter estimates were obtained that minimized the sum of squares of residuals. The correlation matrices for the data indicate an acceptable level of correlation between parameter estimates. An examination of the residual plots for the model prediction and MCU data indicate a correlation between successive residuals in violation of the assumption of uncorrelated residuals for fitting data through least squares. Quantitative lack-of-fit tests for the three-parameter model indicated no significant lack-of-fit.

As the data is a time-series, the significance and nature of the correlation could be determined through an examination of the autocorrelation function of the residuals. The autocorrelation function

suggested a significant correlation between successive residuals but an insignificant correlation at lags greater than one. This suggested that the data could be better fit to the model through a moving average process of order one. This involved the introduction of an additional weighting parameter applied to the previously calculated residual.

The moving average model was fit to the data and decreased the sum of squares of residuals for all data but did not consistently influence the standard error, the marginal 95% confidence regions for the parameter estimates or the 95% confidence band for the predicted response. Its main effect, therefore, was in eliminating the violation in the assumption of uncorrelated residuals for least squares fitting.

The residual plots for the moving average model did not indicate any suspicious trends and the correlation between successive residuals was eliminated. The autocorrelation function confirmed insignificant correlation between residuals. Quantitative lack-of-fit tests again confirmed no significant lack-of-fit.

Comparing data from different studies was difficult as the differences in experimental set-up can have major influences on the parameter values obtained. Rosenberg et al (2) used the same model as this study and obtained similar estimates for resistance and compliance but a much different estimate of inertance. During the minimization routine, the estimates of Rosenberg et al (2) were used as initial estimates. A false minima was detected in the region of their quoted value for inertance. This value did, however, lie within the 95% confidence region calculated by this study. The parameter values quoted by Sandquist et al (7) are for cardiac outputs greater than those utilized in this study but are comparable to the values obtained by this study by extrapolation.

For example, as cardiac output is increased, systemic resistance must drop as indicated by the estimates for resistance at different cardiac outputs. The inertance parameter was not used in their study. Guyton (27) indicated comparable parameter estimates but revealed few details about their development. None of these studies developed inference regions for the parameter estimates. The parameters of resistance, compliance and inertance quoted in the literature (2,7,27) do not provide information concerning marginal confidence regions and, hence, are of little use for prediction.

Comparison of the physiological data to the predictions indicated a small time shift which was reduced through the addition of the fit parameter. This time-shift could possibly be explained by a phase shift in the relationship of the aortic pressure wave to the aortic flow profile with respect to time. It had been determined with the MCU data that the model was sensitive to this phase shift as a similar time shift was observed with the MCU data prior to the discovery of the low pass filter within the Transonic flowmeter. It was, therefore, suggested that the physiological data might be better fit to the model if an accurate determination of the position of the pressure and flow profiles relative to one another was determined. This information was not provided with the data from O'Rourke (31).

The change in parameter estimates with respect to operating conditions are reasonable. As the mean venous pressure is increased, the estimate of systemic resistance is decreased as would be expected in the natural circulation. The estimate of arterial compliance was shown to decrease as the systolic/diastolic ratio increased and the change in venous inertance was affected by mean venous pressure, increasing with a

corresponding decrease in mean venous pressure. These observations are in agreement with the definitions of resistance, compliance and inertance as detailed in section 3.2.

The use of an approximate Hessian in the development of confidence levels is justifiable as the response function does not undergo exponential changes across its operating region making the approximations good. The model does, however, become more non-linear as the systolic/diastolic pressure ratio is increased. The effect of this was indicated in the sum of squares of residuals for the physiological data where the sum of squares value was significantly higher than those for MCU data with smaller ratios. While the model was still adequate for an increased systolic/diastolic ratio, extrapolation beyond normal physiological pressure limits, would likely see the breakdown of the model in terms of the precision of the predicted response.

In the context of the EVAD project, the model has shown that the MCU provides an accurate description of the aortic pressure and flow characteristics of the natural circulation as the model is well fitted to both data sets at a 95% confidence level. The MCU will provide an acceptable analogue for testing prototype devices as it responds to an input pressure and flow in a similar manner to the natural circulation.

As a potential control mechanism for the EVAD, the model could be utilized as a predictor of instantaneous power output of the VAD. By monitoring mean venous pressure, aortic flow rate and cardiac cycle time, the model could predict the hydraulic power output of the VAD to the circulation. Instantaneous power output information could be useful to the energy management circuit in determining charging/discharging regimes for the internal batteries.

Further work with the model should include development of a real time prediction of pressure after which the dynamic behaviour of MCU data and human physiological data could be studied.

7 - REFERENCES

1. Hawiger, J., "Chairman's Report", Thrombosis News, Spring 1989, 11-14 (1989).

2. Rosenberg, G., Phillips, W., Landis, D., Pierce, W., "Design and Evaluation of the Pennsylvania State University Mock Circulatory System", ASAIO, 4 (2), 41-49, (1981).

3. Arabia, M., Akutsu, T., "A New Test Circulatory System for Research in Cardiovascular Engineering", Annals of Biomedical Engineering, 12, 29-48, (1984).

4. Donovan, F., "Design of a Hydraulic Analog of the Circulatory System for Evaluation Artificial Hearts", Biomater Med Devices Artif Organs, 3, 439 - 449, (1975).

5. Nardi, G., Cicconardi, S., Dario, P., De Rossi, D., "Modular Hydropneumatic Mock Circulatory System for the Evaluation of Cardiovascular Prostheses", ASAIO, 4 (2), 139-148, (1981).

6. High, K., Brighton, J., Brickman, A., Pierce, W., "Analysis of an Artificial Ventricle and Mock Circulatory System", Journal of Biomedical Engineering, November 1977, 184-188 (1977).

7. Sandquist, G., Olsen, D., Kolff, W., "A Comprehensive Elementary Model of the Mammalian Circulatory System", Annals of Biomedical Engineering, 10, 1-33, (1982).

8. Martin, J., Schneider, A., Mandel, J., Prutow, R., Smith, R., "A New Cardiovascular Model for Real-Time Applications", Transactions of the Society for Computer Simulation, 3, 31-65, (1986).

9. Moller, D., Tsuchiya, K., "Mathematical and Mechanical Circulatory Simulators Applied to Heart Replacement Systems", In: Assisted Circulation Vol. II, Berlin, (1984).

10. Dinnar, U., "Cardiovascular Fluid Dynamics", CRC Press, 139-159, (1974).

11. ter Kevrs, H., Tyberg, J. (editors), "Mechanics of the Circulation", Martinus Nijhoff Publishers, (1987).

12. Geselowitz, D., Miller, G., Phillips, W., "Dynamic Model of a Sac-Type Pneumatically Driven Artificial Ventricle", Journal of Biomechanical Engineering, 99, 14-19, (1977).

13. Attinger, E., "Analysis of Pulsatile Blood Flow", University of Pennsylvannia, (1969).

14. Swanson, W., Clark, R., "Cardiovascular System Requirements", Journal of Bioengineering, 1, 121-133, (1976).

15. Swanson, W., Clark, R., "A Simple Cardiovascular System Simulator: Design and Performance", Journal of Bioengineering, 1, 135-145, (1977).

16. Bates, D., Watts, D., "Non-Linear Regression Analysis and its Applications", John Wiley and Sons, New York, (1988).

17. Guskov, I., Zatiuriukin, A., Kuznetsov, E., Khanin, M., Antropov, V., Bukharov, I., "Automatic Control Systems of the Artificial Heart and Ventricular Assist Device", Artificial Organs, 11(1) ,47-51, (1987).

18. Harvey, W., "The Circulation of the Blood and other Writings", (Franklin, K., Translator), J.M. Dent and Sons, London, (1963).

19. Moeller, D., Popovic, D., Thiele, G., "Modeling, Simulation and Parameter Estimation of the Human Cardiovascular System", Friedr. Vieweg and Sohn, (1983).

20. Lutz, R. J., Hsu, L., Menawat, A., Zrubek, J., Edwards, K., "Comparison of Steady and Pulsatile Flow in a Double Branching Arterial Model", J. Biomechanics, 16(9), 753-766, (1983).

21. Cho, Y., Back, L., Crawford, D., Cuffel, R., "Experimental Study of Pulsatile and Steady Flow through a Smooth Tube and an Atherosclerotic Coronary Artery Casting of Man", J. Biomechanics, 16 (11), 993-946, (1983).

22. Sarwal, S., Marble, A., Kinley, C., "A Mathematical Assessment of Suture Line Stress in the End-to-Side Anastomosis-11. Pulsatile Flow", J. Biomechanics, 13, 449-454, (1980).

23. Swanson, W., "Relative Performance of Prosthetic Heart Valves based on Power Measurements, Medical Instrumentation", 18(6), 318-325, (1984).

24. Hasenkam, J.M. Westphal, D., Nygaard, H., Nygaard, H., Reul, H., Giersiepen, M., Stodkilde-Jorgensen, H., "In vitro Stress Measurements in the Vicinity of Six Mechanical Aortic Valves using Hot-Film Anemometry in Steady Flow", J. Biomechanics, 21(3), 235-247, (1988).

25. Stacy, G. Jacobs, G., Yozu, R., Shimomitsu, T., Watanabe, T., Smith, W., Navarro, R., Nose, Y., "A Mathematical Model to Predict the Optimal Control Mode for a Pusher-Plate Total Artificial Heart (TAH)", Trans Am Soc Artif Intern Organs, 31,216-223, (1985).

26. "Mock Circulatory System", Hydrospace Research Corp, Rockville, MD, Report # 152, (1967).

27. Guyton, A., "Human Physiology and Mechanisms of Disease", 3rd Edition, WB Saunders Company, (1982).

28. Ahmed, S., Giddens, D., "Flow Disturbance Measurements through a Constricted Tube at Moderate Reynolds Numbers", J. Biomechanics, 16 (12), 955-963, (1983).

29. Box, G., Jenkins, G., "Time Series Analysis- Forecasting and Control", Holden-Day, (1970).

30. Wolf, L., Clinch, J., "Mock Circulatory System for Intra-Aortic Balloon Testing", IEEE Transactions on Biomedical Engineering, January 1972, 38-46, (1972).

31. O'Rourke, M.F., "Arterial Function in Health and Disease", Churchill Livingston, (1982).

32. Press, H., Flannery, B.,Teukolsky, S., Vetterling, W., "Numerical Recipes- The Art of Scientific Computing", Cambridge University Press, (1986).

33. Bacon, D., "Collection and Interpretation of Industrial Data", Department of Chemical Engineering, Queen's University, Kingston, Section 26, (1984).

34. Fogiel, M., (Director), " Handbook of Mathematical, Scientific and Engineering Formulas, Tables, Functions, Graphs, Transforms", Research and Education Association, (1984).

Appendix A - Solution to Model

$$P = \phi\frac{dQ}{dt} - \phi C\frac{d^2P}{dt^2} + RQ - RC\frac{dP}{dt} + P_a$$

General Form:

$$\phi C\frac{d^2P}{dt^2} + RC\frac{dP}{dt} + P = P_a + \phi\frac{dQ}{dt} + RQ$$

$$\frac{d^2P}{dt^2} + \frac{R}{\phi}\frac{dP}{dt} + \frac{P}{\phi C} = \frac{P_a}{\phi C} + \frac{1}{C}\frac{dQ}{dt} + \frac{R}{\phi C}Q$$

$$\frac{d^2P}{dt^2} + B\frac{dP}{dt} + DP = E + F\frac{dQ}{dt} + GQ$$

where $B = \frac{R}{\phi}$, $D = \frac{1}{\phi C}$, $E = \frac{P_a}{\phi C}$, $F = \frac{1}{C}$, $G = \frac{R}{\phi C}$

An expression for Q can be developed using line segments and the unit step function:

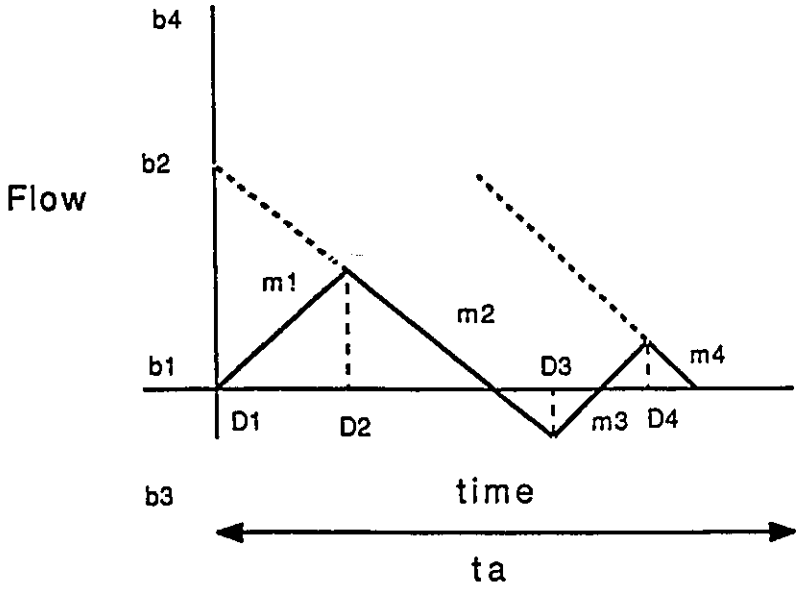

i	Di	mi	bi
1	D1	m1	b1
2	D2	m2	b2
3	D3	m3	b3
4	D4	m4	b4
⋮	⋮	⋮	⋮
n	Dn	mn	bn

A General Form of Flow, Q, can be written as,

$$Q(t) = \sum_{i=1}^{n} \alpha(t-D_i)\,(m_i t - m_{i-1} t + b_i - b_{i-1})$$

$$\frac{dQ}{dt} = \sum_{i=1}^{n} \alpha(t-D_i)\,(m_i - m_{i-1})$$

where,

$$\alpha(x) = 0.0 \text{ if } x < 0.0$$

$$1.0 \text{ if } x \geq 0.0$$

$\therefore$ the total expression is,

$$\frac{d^2P}{dt^2} + B\frac{dP}{dt} + DP = E + F\sum_{i=1}^{n} \alpha(t-D_i)\,(m_i - m_{i-1}) + G\sum_{i=1}^{n} \alpha(t-D_i)\,(m_i t - m_{i-1} t + b_i - b_{i-1})$$

Boundary Conditions:

a) $\frac{dP}{dt}(t=0) = \frac{dP}{dt}(t=t_a)$

b) $P(t=0) = P(t=t_a)$

Taking Laplace Transforms:

$$L\,[L.S.] = (s^2\bar{P} - sP_0 - \dot{P}_0) + B(s\bar{P} - P_0) + D\bar{P})$$

$$= \bar{P}(s^2 + Bs + D) - sP_0 - \dot{P}_0 - BP_0$$

$$L[R.S.] \quad = \frac{E}{s} + F\sum_{i=1}^{n} e^{-D_i s}\,(m_i - m_{i-1})\frac{1}{s}$$

$$+ G\sum_{i=1}^{n} e^{-D_i s}\left[(m_i - m_{i-1})\left(\frac{D_i}{s}+\frac{1}{s^2}\right)+(b_i-b_{i-1})\frac{1}{s}\right]$$

$$\therefore \quad \bar{P} = \frac{BP_0 + \dot{P}_0}{\theta} + \frac{sP_0}{\theta} + \frac{E}{s\theta} + F\sum_{i=1}^{n} e^{-D_i s}\,(m_i - m_{i-1})\frac{1}{s\theta}$$

$$+ G\sum_{i=1}^{n} e^{-D_i s}\left[(m_i - m_{i-1})\left(\frac{D_i}{s\theta} + \frac{1}{s^2\theta}\right) + (b_i - b_{i-1})\frac{1}{s\theta}\right]$$

where,

$$\theta = s^2 + Bs + D$$

Develop partial fractions to simplify:

$$\therefore \quad \bar{P} = (BP_0 + \dot{P}_0)\left(\frac{k_1}{s-g}+\frac{k_2}{s-h}\right) + P_0\left(\frac{k_3}{s-g} + \frac{k_4}{s-h}\right) + E\left(\frac{k_5}{s}+\frac{k_6}{s-g}+\frac{k_7}{s-h}\right)$$

$$+ F\sum_{i=1}^{n} e^{-D_i s}\left[HH_i\left(\frac{k_5}{s}+\frac{k_6}{s-g}+\frac{k_7}{s-h}\right)\right]$$

$$+ G\sum_{i=1}^{n} e^{-D_i s}\left[HH_i\left(D_i\left(\frac{k_5}{s}+\frac{k_6}{s-g}+\frac{k_7}{s-h}\right) + \frac{k_5}{s^2} + \frac{k_8}{s} + \frac{k_9}{s-g} + \frac{k_{10}}{s-h}\right)\right.$$

$$\left. + HHH_i\left(\frac{k_5}{s}+\frac{k_6}{s-g}+\frac{k_7}{s-h}\right)\right]$$

where,

$$k_1 = \frac{1}{g-h},\ k_2 = \frac{1}{h-g},\ k_3 = \frac{g}{g-h},\ k_4 = \frac{h}{h-g},\ k_5 = \frac{1}{gh},\ k_6 = \frac{1}{g(g-h)}$$

$$k_7 = \frac{1}{h(h-g)},\ k_8 = \frac{g+h}{g^2h^2},\ k_9 = \frac{1}{g^2(g-h)},\ k_{10} = \frac{1}{h^2(h-g)}$$

and,

$$HH_i = m_i - m_{i-1},\ HHH_i = b_i - b_{i-1}$$

Invert to time domain:

$$P = (BP_0 + \dot{P}_0)[k_1 e^{gt} + k_2 e^{ht}] + P_0[k_3 e^{gt} + k_4 e^{ht}] + E[k_5 + k_6 e^{gt} + k_7 e^{ht}]$$

$$+ F\sum_{i=1}^{n} \alpha(t-D_i)[HH_i(k_5 + k_6 e^{g(t-D_i)} + k_7 e^{h(t-D_i)})]$$

$$+ G\sum_{i=1}^{n} \alpha(t-D_i)[HH_i(D_i(k_5 + k_6 e^{g(t-D_i)} + k_7 e^{h(t-D_i)}) + k_5(t-D_i) + k_8$$

$$+ k_9 e^{g(t-D_i)} + k_{10} e^{h(t-D_i)} + HHH_i(k_5 + k_6 e^{g(t-D_i)} + k_7 e^{h(t-D_i)})]$$

(eqn A:1)

Evaluate the Boundary Conditions:

Simplify Eqn A:1

$$P = P_0 f_A(t) + \dot{P}_0 f_B(t) + f_C(t)$$

and take its derivative

$$\dot{P} = P_0 \dot{f}_A(t) + \dot{P}_0 \dot{f}_B(t) + \dot{f}_C(t)$$

where,

$$f_A(t) = Bk_1e^{gt} + Bk_2e^{ht} + k_3e^{gt} + k_4e^{ht}$$

$$f_B(t) = k_1e^{gt} + k_2e^{ht}$$

$$f_C(t) = E[k_5 + k_6e^{gt} + k_7e^{ht}]$$

$$+ F\sum_{i=1}^{n}\alpha(t-D_i)[HH_i(k_5 + k_6e^{g(t-D_i)} + k_7e^{h(t-D_i)})]$$

$$+ G\sum_{i=1}^{n}\alpha(t-D_i)\,(HH_i(D_i(k_5 + k_6e^{g(t-D_i)} + k_7e^{h(t-D_i)}) + k_5(t-D_i) + k_8$$

$$+ k_9e^{g(t-D_i)} + k_{10}e^{h(t-D_i)} + HHH_i(k_5 + k_6e^{g(t-D_i)} + k_7e^{h(t-D_i)})]$$

$$\dot{f}_A(t) = Bk_1ge^{gt} + Bk_2he^{ht} + k_3ge^{gt} + k_4he^{ht}$$

$$\dot{f}_B(t) = k_1ge^{gt} + k_2he^{ht}$$

$$\dot{f}_C(t) = E[k_6ge^{gt} + k_7he^{ht}]$$

$$+ F\sum_{i=1}^{n}\alpha(t-D_i)[HH_i(k_6ge^{g(t-D_i)} + k_7he^{h(t-D_i)})]$$

$$+ G\sum_{i=1}^{n}\alpha(t-D_i)[HH_i(D_i(k_6ge^{g(t-D_i)} + k_7he^{h(t-D_i)}) + k_5(t) + k_8$$

$$+ k_9ge^{g(t-D_i)} + k_{10}he^{h(t-D_i)} + HHH_i(k_6ge^{g(t-D_i)} + k_7he^{h(t-D_i)})]$$

Boundary Conditions are:

At $t=t_a$,

$$(1)\ P_{ta} = P_0$$

and,

$$(2)\ \dot{P}_{ta} = \dot{P}_0$$

$$\therefore \quad P_0 = P_0 f_A(t_a) + \dot{P}_0 f_B(t_a) + f_C(t_a)$$

and,

$$\dot{P}_0 = P_0 \dot{f}_A(t_a) + \dot{P}_0 \dot{f}_B(t_a) + \dot{f}_C(t_a)$$

Solve for P_0 and $\dot{P}_0$:

$$P_0 = \frac{\dot{P}_0 f_B(t_a) + f_C(t_a)}{1 - f_A(t_a)}$$

$$\dot{P}_0 = \frac{\dfrac{f_C(t_a)\dot{f}_A(t_a)}{1 - f_A(t_a)} + \dot{f}_C(t_a)}{1 - \dot{f}_B(t_a) - \left(\dfrac{f_B(t_a)\dot{f}_A(t_a)}{1 - f_A(t_a)} \right)}$$

which can then be substituted into equation A:1 giving an expression for Aortic Pressure,P, in terms of Aortic Flow, Q, Mean Venous Pressure or Pre–Load, Systemic Resistance, R, Arterial Compliance,C, Venous Inertance, I and Cardiac Cycle Time, t_a.

Appendix B - Fortran Program of Model Solution

```
C*************************************************************************NEW00010
C PREDICTED VALUE OF AORTIC PRESSURE                                      NEW00020
C*************************************************************************NEW00030
      IMPLICIT REAL*8(A-H,O-Z)                                            NEW00040
      PARAMETER(N=9,M=3,K=2)                                              NEW00050
      DIMENSION DATA(N,K),HESSN(10),XGUESS(3),                            NEW00060
     +HH(0:N),HHH(0:N),XSCALE(4),FSCALE(21),IPARAM(6)                     NEW00070
     +,RPARAM(7),FLOW(N,M),X(3),TT(21)                                    NEW00080
C                                                                         NEW00090
      COMMON/BK1/AMI(0:9),BI(0:9),DI(0:9),TA,PA                           NEW00100
      COMMON/BK2/Y(100),T(100),ND                                         NEW00110
      EXTERNAL FUNC,FUNC2                                                 NEW00120
      CHARACTER*72 TITLE                                                  NEW00130
      ND=21                                                               NEW00140
      NP=3                                                                NEW00150
C*************************************************************************NEW00160
C INPUT THE VALUES OF THE FORCING FUNCTION,AMI(I),BI(I),DI(I)             NEW00170
C AND THE MEASURED DATA                                                   NEW00180
C*************************************************************************NEW00190
      READ(15,99) TITLE                                                   NEW00200
      WRITE(16,114)                                                       NEW00210
         DO 10 I=1,N                                                      NEW00220
         READ(15,109) (FLOW(I,J),J=1,M)                                   NEW00230
         WRITE(16,109)(FLOW(I,J),J=1,M)                                   NEW00240
         AMI(I)=FLOW(I,1)*0.00001667                                      NEW00250
         BI(I)=FLOW(I,2)*0.00001667                                       NEW00260
         DI(I)=FLOW(I,3)                                                  NEW00270
 10   CONTINUE                                                            NEW00280
C                                                                         NEW00290
      DO 20 I=1,N                                                         NEW00300
         WRITE(16,110)I,AMI(I),BI(I),DI(I)                                NEW00310
 20   CONTINUE                                                            NEW00320
C                                                                         NEW00330
      READ(15,99) TITLE                                                   NEW00340
      READ(15,109) TA,PA                                                  NEW00350
      WRITE(16,119)TA,PA                                                  NEW00360
      PA=PA*133.3                                                         NEW00370
      READ(15,99) TITLE                                                   NEW00380
      DO 21 I=1,NP                                                        NEW00390
         READ(15,109) X(I)                                                NEW00400
         WRITE(16,113) X(I)                                               NEW00410
 21   CONTINUE                                                            NEW00420
C                                                                         NEW00430
      READ(15,99) TITLE                                                   NEW00440
         READ(15,115)XSCALE(1),XSCALE(2),XSCALE(3),XSCALE(4)              NEW00450
         WRITE(16,115)XSCALE(1),XSCALE(2),XSCALE(3),XSCALE(4)             NEW00460
C                                                                         NEW00470
      READ(15,99) TITLE                                                   NEW00480
      DO 22 I=1,ND                                                        NEW00490
         READ(15,113)(DATA(I,JJ),JJ=1,K)                                  NEW00500
         WRITE(16,113)(DATA(I,JJ),JJ=1,K)                                 NEW00510
         Y(I)=DATA(I,1)                                                   NEW00520
         T(I)=DATA(I,2)                                                   NEW00530
 22   CONTINUE                                                            NEW00540
C                                                                         NEW00550
```

```
C                                                                       NEW00560
C     X(1)=X(1)+XSCALE(1)                                               NEW00570
C     X(2)=X(2)+XSCALE(2)                                               NEW00580
C     X(3)=X(3)+XSCALE(3)                                               NEW00590
                                                                        NEW00600
      WRITE(16,*)X(1),X(2),X(3)                                         NEW00610
      XGUESS(1)=X(1)                                                    NEW00620
      XGUESS(2)=X(2)                                                    NEW00630
      XGUESS(3)=X(3)                                                    NEW00640
C                                                                       NEW00650
      FTOL=1D-8                                                         NEW00660
      CALL AMOEBA(XGUESS,XSCALE,NP,F,FTOL,FUNC,ITER)                    NEW00670
C     CALL AMOEBA(XGUESS,XSCALE,NP,F,FTOL,FUNC2,ITER)                   NEW00680
C     CALL HESS(FUNC,XGUESS,XSCALE,HESSN,NP)                            NEW00690
      T(1)=0.0                                                          NEW00700
      DO 77 I=1,ND                                                      NEW00710
         WW=PRED(T(I),X)                                                NEW00720
         WRITE(16,199)I,WW,T(I)                                         NEW00730
         T(I+1)=T(I)+0.05                                               NEW00740
 77   CONTINUE                                                          NEW00750
 199  FORMAT(1X,I3,1X,2E15.7)                                           NEW00760
C                                                                       NEW00770
C***********************************************************************NEW00780
C FORMAT STATEMENTS                                                     NEW00790
C***********************************************************************NEW00800
 99   FORMAT(A72)                                                       NEW00810
 109  FORMAT(5E15.7)                                                    NEW00820
 110  FORMAT(1X,I3,1X,3E15.7)                                           NEW00830
 113  FORMAT(4E15.5)                                                    NEW00840
 114  FORMAT('          MI(I)          BI(I)          DI(I)')           NEW00850
 115  FORMAT(4E16.8)                                                    NEW00860
 119  FORMAT(/,1X,'TA=',E10.3,1X,'PA=',E10.3)                           NEW00870
 129  FORMAT(1X,3E15.7)                                                 NEW00880
C                                                                       NEW00890
      STOP                                                              NEW00900
      END                                                               NEW00910
C                                                                       NEW00920
      FUNCTION PRED(T,X)                                                NEW00930
      IMPLICIT REAL*8(A-H,O-Z)                                          NEW00940
      PARAMETER(N=9,NP=3)                                               NEW00950
      DIMENSION HH(0:9),HHH(0:9),X(3)                                   NEW00960
C                                                                       NEW00970
      COMMON/BK1/AMI(0:9),BI(0:9),DI(0:9),TA,PA                         NEW00980
C***********************************************************************NEW00990
C CALCULATE BB,DD,EE,FF,GG,G,H,AK1,AK2,AK3,AK4,AK5,AK6,AK7,AK8,AK9,AK10 NEW01000
C HH(I),HHH(I)                                                          NEW01010
C***********************************************************************NEW01020
      BB=X(1)/X(3)                                                      NEW01030
      DD=1./(X(3)*X(2))                                                 NEW01040
      EE=PA/(X(3)*X(2))                                                 NEW01050
      FF=1./(X(2))                                                      NEW01060
      GG=X(1)/(X(3)*X(2))                                               NEW01070
      G=(-BB+SQRT(BB**2-4.*DD))/2.                                      NEW01080
      H=(-BB-SQRT(BB**2-4.*DD))/2.                                      NEW01090
                                                                        NEW01100
```

```
      AK1=1./(G-H)                                                          NEW01110
      AK2=1./(H-G)                                                          NEW01120
      AK3=G/(G-H)                                                           NEW01130
      AK4=H/(H-G)                                                           NEW01140
      AK5=1./(G*H)                                                          NEW01150
      AK6=1./(G*(G-H))                                                      NEW01160
      AK7=1./(H*(H-G))                                                      NEW01170
      AK8=(G+H)/(G*G*H*H)                                                   NEW01180
      AK9=1./(G*G*(G-H))                                                    NEW01190
      AK10=1./(H*H*(H-G))                                                   NEW01200
C     CC=EE/(G*H)                                                           NEW01210
C                                                                           NEW01220
      DI(0)=0.0                                                             NEW01230
      AMI(0)=0.0                                                            NEW01240
      BI(0)=0.0                                                             NEW01250
      HH(0)=0.0                                                             NEW01260
      HHH(0)=0.0                                                            NEW01270
      DO 499 I=1,N                                                          NEW01280
           HH(I)=(AMI(I)-AMI(I-1))                                          NEW01290
           HHH(I)=(BI(I)-BI(I-1))                                           NEW01300
 499  CONTINUE                                                              NEW01310
C                                                                           NEW01320
C***************************************************************************NEW01330
C CALCULATE FATA,FBTA,FCTA,DFATA,DFBTA,DFCTA                                NEW01340
C***************************************************************************NEW01350
C                                                                           NEW01360
      FATA=BB*AK1*EXP(G*TA)+BB*AK2*EXP(H*TA)+AK3*EXP(TA*G)+AK4*EXP(H*TA)    NEW01370
C                                                                           NEW01380
      FBTA=AK1*EXP(G*TA)+AK2*EXP(H*TA)                                      NEW01390
C                                                                           NEW01400
      DFATA=BB*G*AK1*EXP(G*TA)+BB*H*AK2*EXP(H*TA)+G*AK3*EXP(G*TA)+H*AK4*    NEW01410
     +EXP(H*TA)                                                             NEW01420
C                                                                           NEW01430
      DFBTA=AK1*G*EXP(G*TA)+AK2*H*EXP(H*TA)                                 NEW01440
C                                                                           NEW01450
      ETERM=EE*(AK5+AK6*EXP(G*TA)+AK7*EXP(H*TA))                            NEW01460
      DETERM=EE*(G*AK6*EXP(G*TA)+H*AK7*EXP(H*TA))                           NEW01470
C                                                                           NEW01480
      TEMP1=0.0                                                             NEW01490
      TEMP1A=0.0                                                            NEW01500
      TEMP2=0.0                                                             NEW01510
      TEMP2A=0.0                                                            NEW01520
C                                                                           NEW01530
      DO 1000 I=1,N                                                         NEW01540
           XX=(TA-DI(I))                                                    NEW01550
           IF (XX.LT.0.0)THEN                                               NEW01560
           XX=0.0                                                           NEW01570
           ELSE                                                             NEW01580
           XX=1.0                                                           NEW01590
           ENDIF                                                            NEW01600
C                                                                           NEW01610
C                                                                           NEW01620
      SUM1=HH(I)*XX*(AK5+AK6*EXP(G*(TA-DI(I)))+AK7*EXP(H*(TA-DI(I))))       NEW01630
                                                                            NEW01640
                                                                            NEW01650
```

```
      SUM1A=XX*(HH(I)*(DI(I)*(AK5+AK6*EXP(G*(TA-DI(I)))+AK7*EXP(H*      NEW01660
     +(TA-DI(I))))                                                      NEW01670
     ++AK5*(TA-DI(I))+AK8+AK9*EXP(G*(TA-DI(I)))+AK10*EXP(H*(TA-DI(I)))) NEW01680
     ++HHH(I)*(AK5+AK6*EXP(G*(TA-DI(I)))+AK7*EXP(H*(TA-DI(I)))))       NEW01690
C                                                                       NEW01700
      SUM2=XX*HH(I)*(AK6*G*EXP(TA-DI(I))+AK7*H*EXP(H*(TA-DI(I))))       NEW01710
C                                                                       NEW01720
      SUM2A=XX*(HH(I)*(DI(I)*(AK6*G*EXP(G*(TA-DI(I)))+AK7*H             NEW01730
     +*EXP(H*(TA-DI(I))))                                               NEW01740
     ++AK5*TA+AK9*G*EXP(G*(TA-DI(I)))+AK10*H*EXP(H*(TA-DI(I))))         NEW01750
     ++HHH(I)*(AK6*G*EXP(G*(TA-DI(I)))+AK7*H*EXP(H*(TA-DI(I)))))       NEW01760
C                                                                       NEW01770
      TEMP1=TEMP1+SUM1                                                  NEW01780
      TEMP1A=TEMP1A+SUM1A                                               NEW01790
      TEMP2=TEMP2+SUM2                                                  NEW01800
      TEMP2A=TEMP2A+SUM2A                                               NEW01810
                                                                        NEW01820
 1000 CONTINUE                                                          NEW01830
C                                                                       NEW01840
      FCTA=FF*TEMP1+GG*TEMP1A+ETERM                                     NEW01850
      DFCTA=FF*TEMP2+GG*TEMP2A+DETERM                                   NEW01860
C                                                                       NEW01870
C***********************************************************************NEW01880
C CALCULATE VALUES OF PO AND DPO AT TA                                  NEW01890
C***********************************************************************NEW01900
      DPO=((FCTA*DFATA)/(1.-FATA)+DFCTA)/((1.-DFBTA)-(FBTA*DFATA)       NEW01910
     +/(1.-FATA))                                                       NEW01920
C                                                                       NEW01930
      PO=(DPO*FBTA+FCTA)/(1.-FATA)                                      NEW01940
C                                                                       NEW01950
C***********************************************************************NEW01960
C STEP FUNCTION SUMMATIONS FOR G AND F AT ANY TIME                      NEW01970
C***********************************************************************NEW01980
C                                                                       NEW01990
      TEMP3=0.0                                                         NEW02000
      TEMP3A=0.0                                                        NEW02010
      SUM3=0.0                                                          NEW02020
      SUM3A=0.0                                                         NEW02030
C                                                                       NEW02040
      DO 2000 I=1,N                                                     NEW02050
      XX=(T-DI(I))                                                      NEW02060
      IF (XX.LT.0.0)THEN                                                NEW02070
      XX=0.0                                                            NEW02080
      ELSE                                                              NEW02090
      XX=1.0                                                            NEW02100
      ENDIF                                                             NEW02110
C                                                                       NEW02120
      SUM3=HH(I)*XX*(AK5+AK6*EXP(G*(T-DI(I)))+AK7*EXP(H*(T-             NEW02130
     +DI(I))))                                                          NEW02140
C                                                                       NEW02150
      SUM3A=XX*(HH(I)*(DI(I)*(AK5+AK6*EXP(G*(T-DI(I)))+AK7*EXP(         NEW02160
     +H*(T-DI(I))))                                                     NEW02170
     ++AK5*(T-DI(I))+AK8+AK9*EXP(G*(T-DI(I)))+AK10*EXP(H*(T-            NEW02180
     +DI(I))))                                                          NEW02190
     ++HHH(I)*(AK5+AK6*EXP(G*(T-DI(I)))+AK7*EXP(H*(T-DI(I)))))         NEW02200
```

```
C                                                                       NEW02210
      TEMP3=TEMP3+SUM3                                                  NEW02220
      TEMP3A=TEMP3A+SUM3A                                               NEW02230
 2000 CONTINUE                                                          NEW02240
C                                                                       NEW02250
      FCT=FF*TEMP3+GG*TEMP3A+EE*(AK5+AK6*EXP(G*T)+AK7*EXP(H*T))         NEW02260
C                                                                       NEW02270
C*********************************************************************  NEW02280
C CALCULATE PRED                                                        NEW02290
C*********************************************************************  NEW02300
      PRED=(((BB*P0+DP0)*(AK1*EXP(G*T)+AK2*EXP(H*T))+P0*(AK3*EXP(       NEW02310
     +G*T)+AK4*EXP(H*T))+FCT)-666.5)                                    NEW02320
C                                                                       NEW02330
      RETURN                                                            NEW02340
      END                                                               NEW02350
C                                                                       NEW02360
      FUNCTION FUNC(X)                                                  NEW02370
      IMPLICIT REAL*8(A-H,O-Z)                                          NEW02380
      DIMENSION F(100),X(3)                                             NEW02390
      COMMON/BK2/T(100),Y(100),ND                                       NEW02400
      FUNC=0D0                                                          NEW02410
      DO 1 I=1,21                                                       NEW02420
C        WRITE(6,*)I,Y(I),F(I)                                          NEW02430
         F(I)=Y(I)-PRED(T(I),X)                                         NEW02440
         FUNC=FUNC+F(I)**2                                              NEW02450
  1   CONTINUE                                                          NEW02460
      WRITE(16,*)FUNC                                                   NEW02470
      RETURN                                                            NEW02480
      END                                                               NEW02490
C                                                                       NEW02500
      END                                                               NEW02510
```

Appendix C - LabView MCU Data Acquisition Program

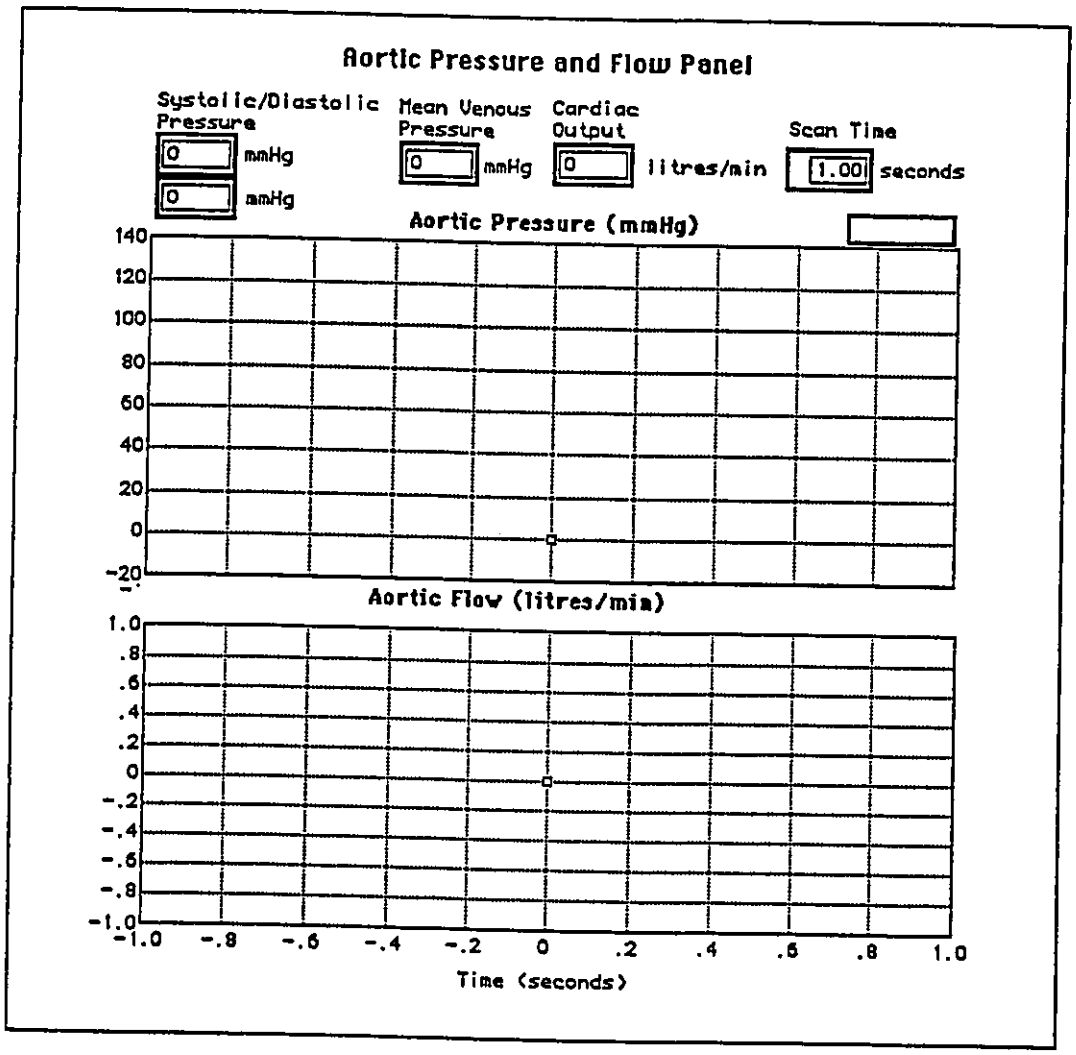

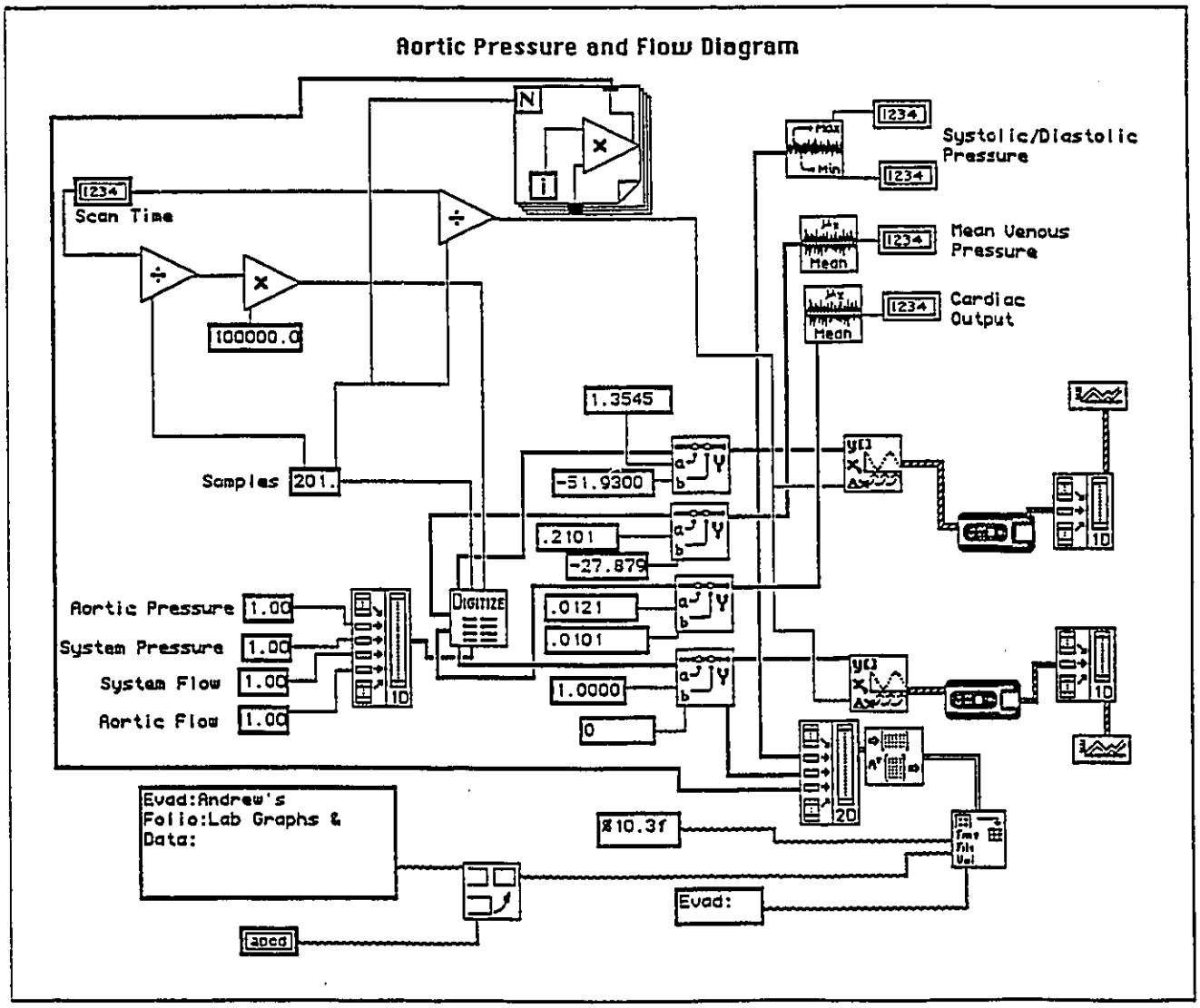
Aortic Pressure and Flow Diagram
Scan Time
100000.0
Samples
201.
1.3545
-51.9300
.2101
-27.879
.0121
.0101
1.0000
0
Digitize
Aortic Pressure
System Pressure
System Flow
Aortic Flow
1.00
Systolic/Diastolic Pressure
Mean Venous Pressure
Cardiac Output
Mean
Evad:Andrew's Folio:Lab Graphs & Data:
%10.3f
Evad:
aaaa

Appendix D - Quantitative Lack-of-Fit Test

For the non-linear model, no rigorous means of obtaining variance exists. However, we can develop an estimate of the variance based on the linear model.

Assuming that runs zero to three are replicate sets of data, that is, the operating conditions were similar for each of these runs, we have 4 x 41 or 164 data points, collected at 0.03 sec intervals. At each time interval, u, a mean pressure response can be calculated from M replicate points where,

$$\bar{Y}_u = \sum_{i=1}^{M} \frac{Y_i}{M}.$$

From these values of $\bar{Y}_u$, a variance estimate at each interval is determined by,

$$\hat{\sigma}_u^2 = \sum_{i=1}^{M} \frac{(Y_i - \bar{Y}_i)^2}{(M-1)}$$

These variance estimates are pooled as

$$\hat{\sigma}_p^2 = \sum_{u=1}^{J} \frac{\hat{\sigma}_u^2}{J}$$

where J is the number of time intervals. A test ratio compares the lack-of-fit sum of squares with the replicate sum of squares with the appropriate degrees of freedom and probability level where,

$$R = \frac{\dfrac{s(\hat{\underline{\theta}}) - \hat{\sigma}_p^2 \sum_{i=1}^{j} (M_j - 1)}{J - P - \sum_{i=1}^{j} (M_j - 1)}}{\hat{\sigma}_p^2}$$

where j is the number of different operating conditions the replicates were collected at, M_j is the number of data points collected at one time interval and P is number of parameters being estimated.

This is compared with an $F(\nu_1,\nu_2;\gamma)$ value to determine whether lack-of-fit due to experimental error is more significant than lack-of-fit due to model inadequacy.

From the data, a pooled variance estimate is 8.79 from 41 individual estimates of variance at each time interval. A test ratio, R, is calculated as 0.21 from the $s(\underline{\theta})$ value of 91.8, the estimate of variance, j = 1 operating conditions, m = 4 replicates, I = 41 data points and p = 3 parameters. This is compared with the F(35,3; 0.05) value of 8.57. As 0.21 is smaller than 8.57, it can then be concluded that lack-of-fit due to experimental error is significantly greater than lack-of-fit due to model inadequacy.